

SUPPRESSION OF INTENTION TREMOR BY
MECHANICAL LOADING

by

DAVID EDWARD DUNFEE

B.S. University of New Hampshire
(1974)

SUBMITTED IN PARTIAL FULFILLMENT
OF THE REQUIREMENTS FOR THE
DEGREE OF

MASTER OF SCIENCE

at the

MASSACHUSETTS INSTITUTE OF TECHNOLOGY

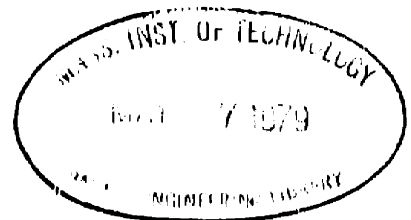
(FEBRUARY 1979)

Signature of Author.....*[Handwritten Signature]*.....
Department of Mechanical Engineering, February 1979

Certified by.....*[Handwritten Signature]*.....
Thesis Supervisor

Accepted by.....
Chairman, Department Committee

Eng.
MASSACHUSETTS INSTITUTE
OF TECHNOLOGY
MAR 21 1979
LIBRARIES



SUPPRESSION OF INTENTION TREMOR
BY MECHANICAL LOADING

by

DAVID EDWARD DUNFEE

Submitted to the Department of Mechanical Engineering
on February 2, 1979 in partial fulfillment of the requirements
for the Degree of Master of Science.

ABSTRACT

A Transduction and Loading Device (TLD) has been built to investigate the utility of suppressing intention tremor in human subjects through the application of viscous damping. The device restrains the forearm while allowing the hand, fastened to a handle, to rotate freely about the wrist. As the subject performs a tracking task requiring position control of the hand, a magnetic particle brake applies across the wrist a selectable passive torque which is proportional to the velocity of the hand. The damping constants developed by the TLD are in the 0.0 to 4.0 in-lbf/(rad/sec) range.

Three subjects were tested with the TLD; two with intention tremor and one normal. For the subjects with intention tremor, reduction in levels of tremor significant at better than the .05 level (based on a paired Student's t test) were realized through the application of viscous damping. One subject's tremor was reduced in specific cases by a factor of 10, approaching the levels of tremor witnessed in the normal. Viscous damping across the wrist maintained or improved the average intended response.

Dr. M. J. Rosen, Director
Rehabilitation Engineering
Center
Massachusetts Institute of
Technology

TABLE OF CONTENTS

	3
List of Figures	5
List of Tables	7
Chapter 1 - Introduction	8
1.1 What, Why, and How? The Purpose, Extent, and Approach	8
1.2 What is AIM? The Disorders Studied	9
1.3 How Has AIM Been Controlled? Reported Techniques of Tremor Management	9
1.4 What Causes Tremor? Muscle/Load System Models	11
1.5 How Do We Proceed From Here?	13
Chapter 2 - System Description	
2.1 Introduction	15
2.2 Definition of Equipment Needs	15
2.3 Transduction and Loading Device	16
2.3.1 Mechanical and Electromechanical Components	20
2.3.2 Instrumentation and Electronics	22
2.4 Dynamic Response Characteristics	25
2.4.1 Differentiator and Gain Stage	25
2.4.2 Magnetic Particle Brake	29
2.4.3 Current Stage	32
2.4.4 Torque Transducer and Amplifier	36
2.4.5 Simple Brake Model	37
2.4.6 Rectifier	42
2.4.7 Combined Current Stage, Brake, and Torque Transducer Response	42
2.4.8 Brake Subsystem Model	46
2.4.9 TLD System Response	52

Chapter 3 - Methods	
3.1 Introduction	58
3.2 Selection of Subjects	58
3.3 Experimental Procedures	59
3.4 Data Analysis	63
3.4.1 Evaluating Intended Response	64
3.4.2 Evaluating Abnormal Movement	66
3.4.3 Spectral Analysis of Response	69
Chapter 4 - Results	
4.1 Introduction	72
4.2 Intended Response	72
4.3 Tremor Attenuation	80
4.4 Frequency Content	88
4.5 Discussion	89
Chapter 5 - Conclusion	98
Appendix I - SUBJECTS	100
Appendix II - COMPUTER PROGRAMS	105
Bibliography	117

LIST OF FIGURES

<u>Figure Number</u>	<u>Title</u>	<u>Page</u>
2-1	Transduction and Loading Device	17
2-2	Photographs of TLD and Experimental Set-up	18
2-3	Instrumentation Block Diagram	24
2-4	Differentiator and Gain Stage	26
2-5	Differentiator and Gain Stage Frequency Response	28
2-6	Static Response of Magnetic Particle Brake	30
2-7	Response of M and i_b to Step Input in Voltage	31
2-8	Current Stage	33
2-9	Effect of Power Transistor Supply Voltage, V_s , on i_b Response Time	35
2-10	Torque Transducer Amplifier Circuit	38
2-11	Instrumentation Amp Output vs Applied Torque	39
2-12	Simple Magnetic Particle Brake Model and its Response to Various Inputs i_b	41
2-13	Full Wave Rectifier	43
2-14	Frequency Response of Current Stage, Torque Transducer, and Brake	45
2-15	Magnetic Particle Brake Model	47
2-16	$\text{Sgn}(d(\theta_w)/dt)$ Function	48
2-17	Magnetic Particle Brake Model Response	50
2-18	Observed Response of M During Direction Reversals	51
2-19	Frequency Response of TLD	53
2-20	Current Stage, Brake, and Torque Transducer Frequency Response as Measured in Complete TLD System	55
2-21	Equivalent Damping Constant vs Pot Setting	57

<u>Figure Number</u>	<u>Title</u>	<u>Page</u>
3-1	Unfiltered Ensemble Averaged Response	65
3-2	Filtered Ensemble Averaged Response	68
3-3	Analog Data Processing Setup for Determining Tremor	68
4-1	Normalized Averaged Intended Response vs Pot Setting Subject JF	73
4-2	Normalized Averaged Intended Response vs Pot Setting Subject FS	74
4-3	Normalized Averaged Intended Response vs Pot Setting Subject ED	75
4-4	Phase Lag of Average Intended Response vs Pot Setting Subject JF	76
4-5	Phase Lag of Average Intended Response vs Pot Setting Subject FS	77
4-6	Phase Lag of Average Intended Response vs Pot Setting Subject ED	78
4-7	RMS Tremor vs Pot Setting Subject JF	81
4-8	RMS Tremor vs Pot Setting Subject FS	82
4-9	RMS Tremor vs Pot Setting Subject ED	83
4-10	RMS Tremor vs Target Frequency for All Subjects Tested (No Damping)	90
4-11	Response Power Spectra Subject JF D = 0	91
4-12	Response Power Spectra Subject JF D = 4	92
4-13	Response Power Spectra Subject JF D = 8	93
4-14	Power Spectra of Processing System Noise	94
4-15	Power Spectra of Response Minus Contribution of Processing Noise	95
4-16	Response of Subject JF For Target Frequency = 1/4 Hz	96

LIST OF TABLES

<u>Table Number</u>	<u>Title</u>	<u>Page</u>
2-1	Definition of Variables	19
2-2	1b Rise Time for Various Current Stage Supply Voltages	34
4-1	Statistical Significance of Reduction in Abnormal Population RMS Tremor	85
4-2	Statistical Significance of the Difference in RMS Tremor Between Abnormal Subjects With Damping and Undamped Normal	85
4-3	RMS Tremor Data	86

CHAPTER 1

INTRODUCTION

1.1 What, Why, and How? The Purpose, Extent, and Approach

Abnormal Involuntary Movement (AIM) can be a significant barrier to individual independence. The severity of this handicap can range from a minor inconvenience to a more moderate level where the individual is unable to use an otherwise normal limb in everyday life. In extreme cases, individuals must be restrained to protect themselves and others from their violent but involuntary movements. If some means of minimizing this abnormal movement could be developed, these people, particularly those with a moderate level of AIM, could benefit from the resulting increased functional independence.

This thesis addresses the feasibility of suppressing AIM through the application of viscous damping. The equipment built to conduct this evaluation is presented in detail. In this evaluation, subjects attempt to keep two lines displayed on an oscilloscope aligned. The target line moves up and down sinusoidally while the other line is controlled by the position of the subject's hand relative to his/her forearm. During the tracking task, various viscous damping loads are applied between the restrained forearm and moving hand by a magnetic particle brake. The effect of this external damping element is monitored by comparing the target and response variables recorded on an FM tape recorder.

1.2 What is AIM? The Disorders Studied

Abnormal involuntary movement is a "recurring pattern of motion of any part of the body which is both unintended and purposeless."¹² This definition distinguishes AIM from normal involuntary movements such as withdrawal reflexes or shivering; from behavior abnormalities of emotional disorders; and from pathological quantitative changes in voluntary motion.

The AIM studied in this thesis was restricted to intention tremor which is characterized by oscillatory patterns of motion in the 3 to 12 Hz (hertz) range. Intention or "action" tremor is initiated during the act of making an intended movement and, unlike "resting" tremor, is absent in the relaxed limb. In light of this definition, intention tremor can severely limit the use of the afflicted limb even when useful levels of strength and average position control are present. Consequently, individuals with this type of neurological disorder would obtain considerable return of function if the unintended oscillations could be minimized.

1.3 How Has AIM Been Controlled? Reported Techniques of Tremor Management

Intention tremor is a difficult therapeutic problem since most conventional techniques for tremor management have been unsuccessful in treating it. Drug therapy with such drugs as amantadine and L-dopa have been of little help in reducing intention tremor despite the effectiveness of these drugs in the treatment of Parkinsonism.⁵ The reported success of surgical techniques such as thalamic surgery has been

inconsistent and seems to depend upon the etiology of the tremor.

Pursuing a different approach, several individuals have studied the effect of attaching weights to the wrist as a means of reducing upper extremity tremor. In two separate studies, Morgan, Hewer, and Cooper observed appreciable reductions in tremor in 58% and 64% of the subjects tested.^{3,7} Chase et al found the application of a constant force to the finger in the direction of extension (upward direction for a pronated hand) attenuated finger movement during tracking tasks for subjects with cerebellar system lesions as well as normals. Applying a constant force in the direction of flexion resulted in a marked increase in the tremor amplitude.²

Despite a recognized need for a "simple mechanical damping device", little work has been reported on the use of viscous damping as a means of suppressing AIM. Rosen and Gesink tested the feasibility of this approach on a single subject with upper extremity intention tremor.¹² In these tests, a lightweight hinged brace was fitted to the subject's forearm and hand. This brace incorporated a linear pneumatic dashpot with a damping constant of 4 in lbf/(rad/sec). The subject performed a sinusoidal tracking task similar to the tasks used in this work. In these trials, tremor was reduced anywhere from .92 to .14 times the undamped value. In addition, more accurate tracking was reported in 12 out of 16 trials. Simoes et al at the Ranchos Los Amigos Hospital tested orthotic braces incorporating viscous damping as a means of controlling athetosis.¹⁴ This AIM is characterized by a complex writhing

motion of lower frequency than the "action" tremors studied in this paper. These researchers found that the performance of the athetoid cerebral-palsy or brain damaged patients wearing these braces showed little or no consistent improvement.

1.4 What Causes Tremor? Muscle-Load System Models

The above approaches to tremor management are justified since the application of forces to a limb will ultimately change the muscle-load system dynamics. Stiles showed that under conditions of constant muscle stiffness, k , in normals, the addition of mass with moment of inertia I to the hand lowered the frequency ω of the spectral peak of normal hand tremor consistent with the relationship $\omega^2 \propto k/I$, where I is the moment of inertia of the hand and added mass about the wrist.¹¹ Joyce and Rack also showed that the frequency of elbow tremor in normals could be adjusted in a consistent fashion by selecting the appropriate combination of spring and mass loads.⁵

Such results have lead several researchers to develop models of the muscle-load system in an attempt to explain the onset and existence of tremor, both normal and physiological. Two models have received considerable attention in the literature. The reflex oscillator hypothesis proposes that tremor reflects an instability in the reflex servo loop primarily due to delays in neural transmission and excitation contraction coupling. On the other hand, the mechanical resonance hypothesis assumes that the muscle-load system is an underdamped second order system subjected to broad frequency band forcing in the form

of asynchronous muscle fiber contraction. Mathematical models of both these concepts were developed by Stein and Oguztoreli.¹⁰ These math models indicate that both mechanisms for tremor could result in oscillations in response to impulse inputs, hence establishing a theoretical basis for both conceptual models.

Considerable support exists in the literature for both of the above mentioned hypotheses. Lippold, in support of the reflex oscillator hypothesis, points out that tremor was not present in deafferented limbs, that the frequency of tremor decreased when the limb was cooled, and that bursts of muscle action potential coincided with the frequency of tremor. Stiles also observed amplitude modulation of EMG at the same frequency as hand tremor during large (>100 μ meters) displacements.¹⁷ The mechanical resonance hypothesis is supported by evidence of increased tremor frequency with increased muscle tension, decreased frequency with added mass, and the existence of tremor oscillations in neurally isolated limbs. Other workers have shown that the forearm and hand muscle-load system is in fact underdamped having a damping ratio of 0.1 to 0.2.¹⁷ To complicate matters more, recent work by Stiles indicates that the mechanism for normal hand tremor with RMS magnitudes in excess of 100 μ meters involves a combination of mechanical resonance and neural feedback factors.¹⁷ In addition, Stiles suggests that the mechanism for Parkinsonian hand tremor is similar to that for normal hand tremor of large displacements, indicating that physiological tremor may just

be an exaggeration of normal tremor!¹⁷ In fact, Thorner is referenced by Stiles to have hypothesized that Parkinsonian tremor results from the loss of damping in the neuromuscular system.

1.5 How Do We Proceed From Here? A Brief Overview

It is evident that the muscle-load system is a dynamic system albeit not completely understood. Consequently, it may be possible to alter the parameters of the system and hence the response in such a way as to ~~attenuate~~ abnormal movements. This thesis investigates this hypothesis as it relates to the suppression of intention tremor through the addition of an external damping element. The design of this element is described in detail in Chapter 2. Three subjects have been tested using this equipment; one with rubral-like intention tremor, and another with essential intention tremor, and a normal to provide a basis for comparison. The methods used to evaluate the results of these tests are presented in Chapter 3, and the results themselves are discussed in Chapter 4.

It may be said that the effect of viscous damping will vary from subject to subject. Hence a large test population is necessary if one intends to draw conclusions from these tests which could be applied to a general patient population. Only three subjects were tested in this work; therefore no such conclusions could honestly be made. However, the work reported here does identify statistically significant trends evident as a result of applying viscous damping, and thus

highlights the need for continued evaluation of this approach to tremor management.

CHAPTER 2

SYSTEM DESCRIPTION2.1 Introduction

The emphasis of this thesis was two fold. The first objective was to fabricate the equipment needed for the experiments required to assess the utility of the proposed method of tremor management. With this task complete, the next objective was to conduct a few initial trials with human subjects using this apparatus. This chapter documents the results of the first task; the equipment. The procedures and results of the second task are discussed in Chapters 3 and 4.

2.2 Definition of Equipment Needs

Tests conducted by Rosen and Gesink¹² in Miami suggest the feasibility of suppressing intention tremor by mechanical loading. In these tests, thermo-plastic cuffs were fitted to the subject's forearm and hand. These cuffs were coupled together and hinged at the wrist. When conducting tests with a larger subject population, such customizing would be inefficient. Further, a linear pneumatic dashpot was positioned between the hand and forearm cuffs to provide viscous damping. Fluctuations in damping constants could be expected with this dashpot due to changes in air properties such as temperature. In addition, the compressibility of the air results in the dashpot acting more like a damper and spring in series rather than a damper alone.

These drawbacks helped to define specific functional

requirements for the equipment developed for this thesis.

These requirements were:

- Versatility - Fit a large subject population with minimal "customizing."
- Repeatability - Provide accurate control of viscous damping constant.
- Provide "pure" viscous damping

The above functional requirements had to be satisfied by any apparatus developed in order for the proposed experiments to be significant. In addition to these requirements, certain design constraints were also specified. They were:

- Provide a means for measuring the level of torque applied across the wrist
- Provide a means for securing the forearm
- Provide the capability to align the subject's wrist with the axis of rotation of the apparatus
- Make the apparatus safe and comfortable for the subjects
- Make the apparatus portable

2.3 Transduction and Loading Device

The transduction and loading device (TLD) developed to satisfy the above requirements and constraints is shown in Figure 2-1. It consists of a rigid base to which the subject's forearm is securely attached. Mounted on this base is a magnetic particle brake whose output torque, m , is controlled by the input current i_b . See Table 2-1 for definition of all variables included in this thesis. This brake is coupled via a torque transducer and shaft to a handle which rotates about the same axis as the wrist. The subject's hand is strapped to this handle. The rotational position of the handle θ_w is

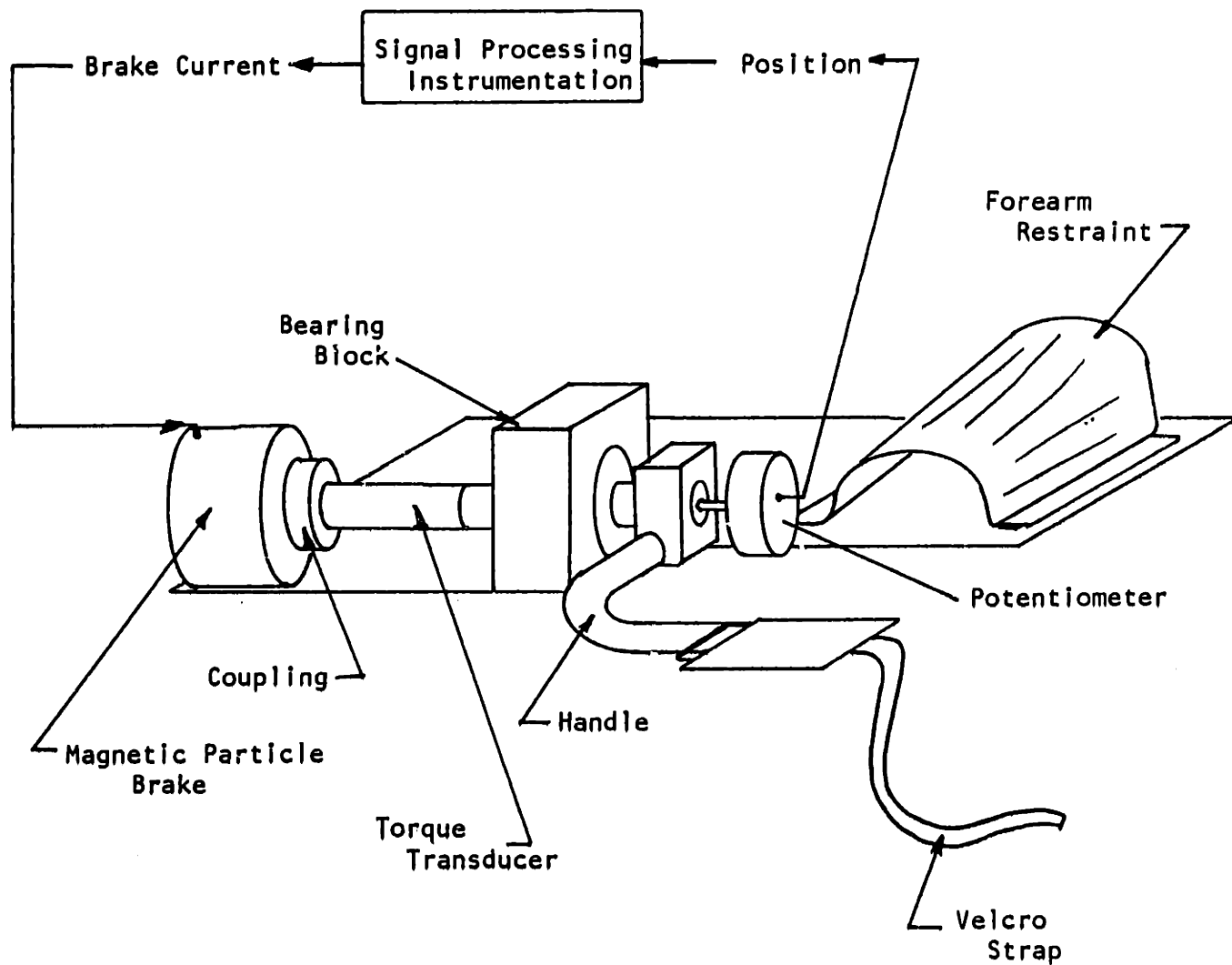


Figure 2-1 Transduction And Loading Device (TLD)

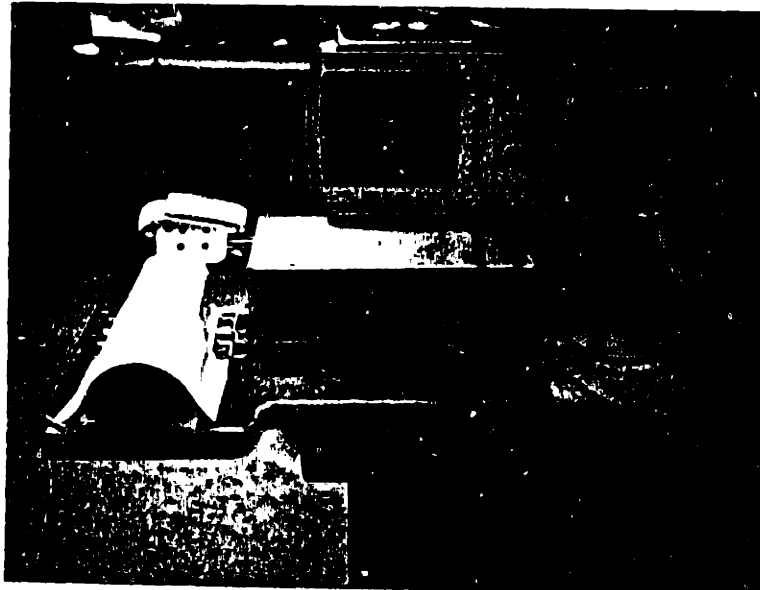


Figure 2-2a) TLD Forearm Restraint, Brake Enclosure, and Oscilloscope Display

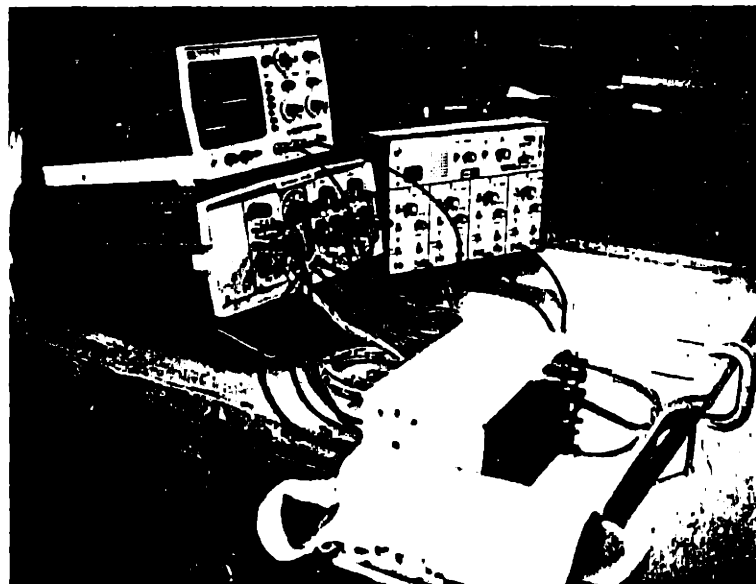


Figure 2-2 b) Experimental Setup Showing TLD, Display, Power Supplies/Signal Processing Modules, and Four Channel FM Tape Recorder

Table 2-1

Definition of Variables

B	System damping constant, in-lbf/(rad/sec)
cm	Centimeter
D	Gain stage pot setting
f_r	Frequency of input to the differentiator
Hz	Hertz
i_b	Brake current
in-lbf	inch-pounds force
k_d	Differentiator gain, volts/volt
k_g	Gain stage gain, volts/volt
k_p	Position potentiometer, gain mV/degree
k_{wb}	Display gain, volts/volt
m	Torque output of brake, in-lbf
M	Torque Transducer system output, volts
M'	Torque output of Brake dynamics in model
mA	milliamperes
mV	millivolts
θ_w	Rotational position of TLD handle, degrees
rad	Radian
, rad/sec	Radian/second .
R	Response (or position) voltage, volts
T	Target voltage, volts

detected by a precision potentiometer, and differentiated to generate a signal proportional to the velocity of the handle. This signal is gain adjusted, rectified, and then used to generate brake current i_b ; thus producing electronically controlled viscous damping. A more detailed description of these components and their response characteristics follows. Figure 2-2a and b are polaroid photographs of the complete experimental set-up.

2.3.1 Mechanical and Electro-Mechanical Components

The TLD consists of the following mechanical and electro-mechanical components:

- A 3/4 inch plywood base sized to rest across the arms of a wheelchair or arm chair. During an experiment this base is clamped to the chair the subject is sitting upright in.
 - A 1/4 inch aluminum plate bolted to the plywood base. This plate is the foundation onto which all other TLD components are mounted. This allows the TLD to be positioned under either the left or right forearm without having to move the plywood base.
 - A thermo-plastic cuff fitted to each subject's forearm. The process of forming this cuff was the only "customizing" required by this design.
- Spring clamps and velcro strap for securing the forearm cuff to the TLD foundation. This configuration provided a means of quickly aligning the wrist by positioning the forearm. The velcro strap can be used to secure the subject's elbow if necessary to

prevent any violent proximal movements from damaging the forearm restraints.

- A Force Limited (of Santa Monica, California) Model B215F3-2 magnetic particle brake. This brake has a maximum output of 40 inlbf for an input current of 400 mA.
- A flexible coupling (Metal Bellows Model R3-C56). This coupling compensates for any parallel, angular, or end-to-end misalignment while exhibiting very low windup ($1/3^\circ$ at 24 inlbf).
- A stainless steel torque transducer for measuring the torque applied to the handle by the magnetic particle brake.
- A 1.0 inch thick bearing block with two $3/8$ inch flanged and double shielded bearings, one mounted on each side. This arrangement results in the bearings carrying all loads applied to the handle, including any bending moments. Any bending moment applied to the handle is transformed into a couple acting at the bearings in the plane of the applied moment. This prevents any bending loads from being carried by the torque transducer and ultimately the bushings in the magnetic particle brake.
- An aluminum coupling, handle, and a section of thermo-plastic material with a strip of velcro fitted to the handle. The subject's palm rests on the thermo-plastic pad and the velcro strip provides a means of

securing the hand to the handle. The coupling, handle, pad and velcro strip have a combined moment of inertia about the axis of rotation of $0.006 \text{ in-lbf/sec}^2$, based on the handle having a radius of 2.72 inches. For an average male, this moment of inertia is approximately 15% of the moment of inertia of the hand about the wrist.³

- A precision potentiometer (New England Instruments $5k\Omega$ Econopot) used to sense the rotational position of the handle. This potentiometer incorporates a continuous plastic conductive resistance element rather than conventional wound wire. Consequently, the resolution is better than 1.0 mV or 0.072° . It has a gain, k_p , of 13.9 mV/degree of rotation and the RMS noise level is minimal (measured, using a HP 3004A RMS Voltmeter, to be less than 1.0 mV).

2.3.2 Instrumentation and Electronics

The following commercial and custom built electronics were used to provide the necessary power, display, controls, and outputs for the experiments: See Figure 2-3

- A display oscilloscope (HP 3310A) for presenting the target and subject response as the vertical position of half-screen line segments.
- A portable power module/main frame (Tektronix TM505) containing;
 - + Two power supplies (tektronix PS501) capable of being connected with a common ground in order to provide ± 40 volts DC across the

output terminals.

- + One function generator (Tektronix FG501) to provide amplitude and frequency adjustable inputs for the target signal.
- + One custom built signal processing plug-in.
- Custom signal processing circuits packaged in a TM500 plug-in module. Included in this module were;
 - + Adisplay driver circuit.
 - + ± 15 volt DC and +5 volt DC regulators.
 - + A practical differintiator for generating a voltage proportional to the angular velocity of the handle.
 - + A gain control circuit for regulating the damping constant of the system.
 - + A rectifying circuit to generate a uni-directional signal for driving the magnetic particle brake.
- A voltage controlled current source for controlling the brake current i_b .
- An instrumentation amplifier (Burr Brown 3626AP) for amplifying the low level torque transducer signals close to the transducer. This minimizes the contamination of the low-level output of the transducer strain gages prior to amplification.
- A 4 channel FM tape recorder (Tandberg Instrumentation Model 100) for recording target, wrist angle, and torque signals.

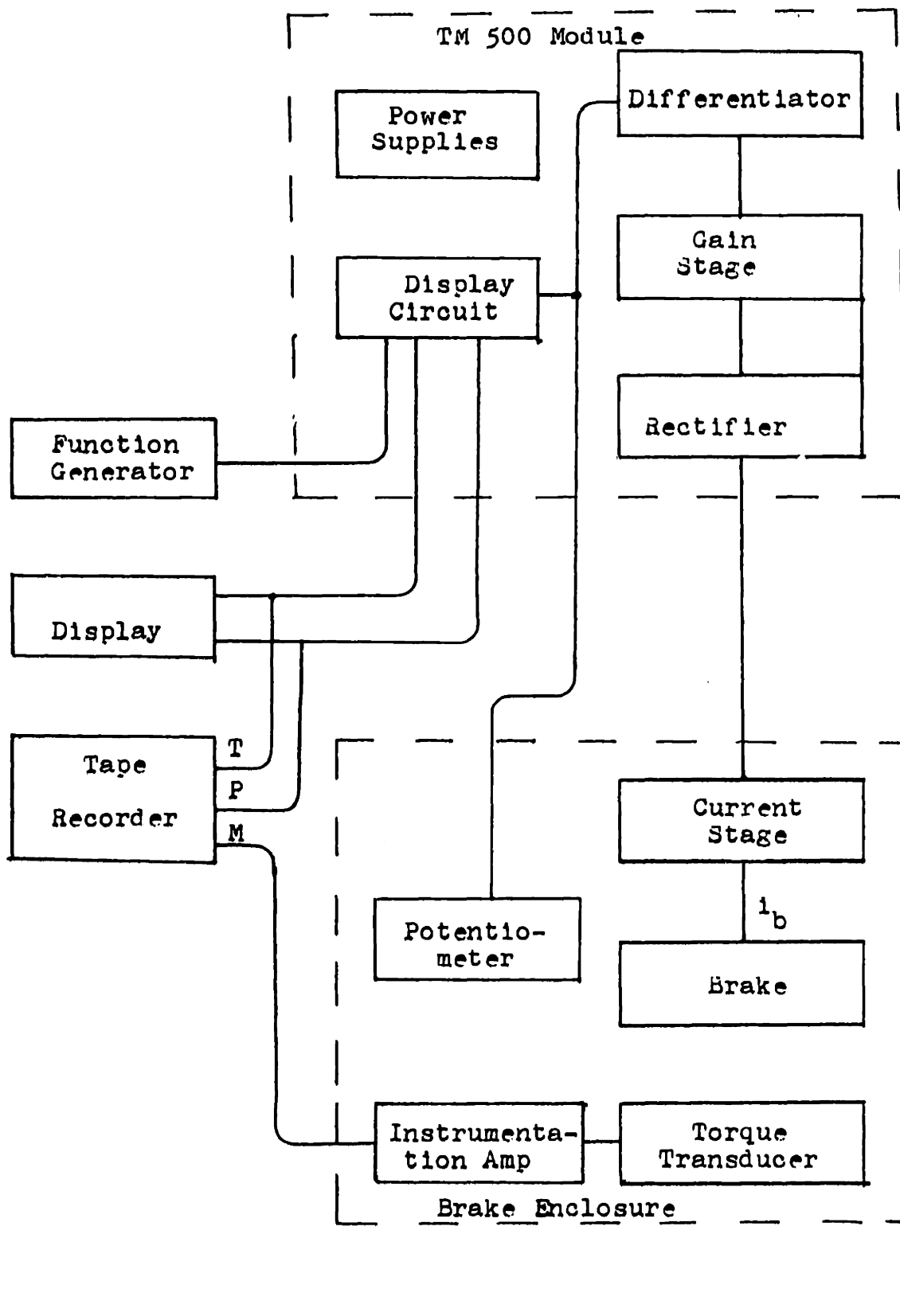


Figure 2-3 TLD Instrumentation Block Diagram

2.4 Dynamic Response Characteristics

The electrical and electro-mechanical response characteristics of the TLD will dictate how effective this device will be in performing its assigned task. This section discusses the design and response characteristics of the dynamic elements of the TLD. From the individual component responses, the total system response can be better understood and predicted. The nomenclature used in the following sections is defined in Table 2-2.

2.4.1 Differentiator and Gain Stage

An operational amplifier differentiation circuit is used to generate a voltage proportional to $d(\theta_w)/dt$. This signal is used to control the magnetic particle brake and thus provide viscous damping. The gain stage provides a means of adjusting the damping constant by modifying the output of the differentiator.

The differentiator circuit shown in Figure 2-4 was used rather than a tachometer because the rotation of the handle was small and reversing. Tachometers are not well suited for this type of application. Rosen and Gesink observed hand tremor amplitudes of $\pm 20^\circ$ at 3 to 4 Hz. Tachometers generally do not operate well when shaft rotations are less than one complete revolution and include direction reversals. Gearing to obtain greater shaft rotations was considered infeasible since it would increase the inertia of the rotating portion of the TLD. It would also be difficult to eliminate backlash in the

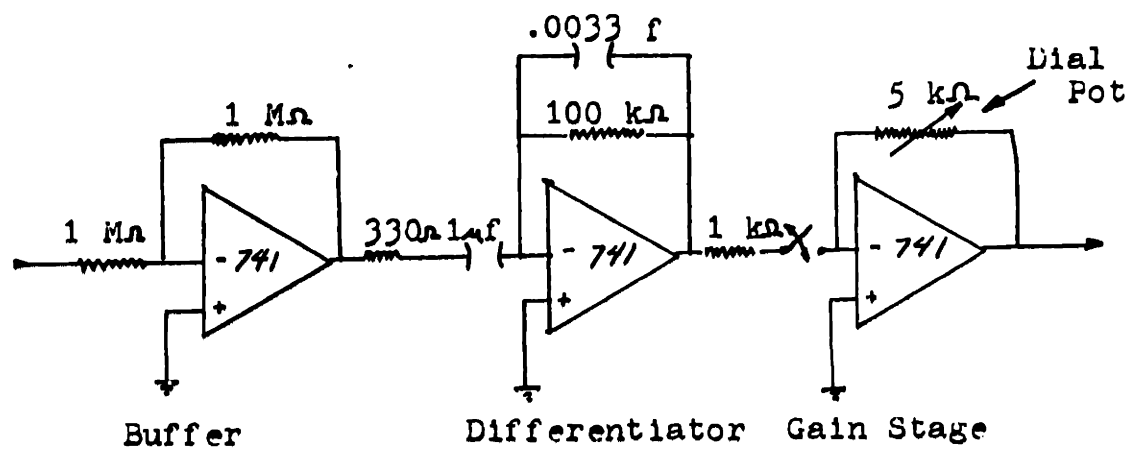


Figure 2-4 Differentiator and Gain Stage

gearing.

Electronic differentiation is not without its problems. It is well known that electronic differentiation amplifies any noise or high frequency components in a signal, thus degrading the signal to noise ratio. To minimize this problem, a "practical" differentiator for low frequency signals was used. This circuit acts as a differentiator for low frequency signals and converts to an integrator when the signal frequency exceeds a limit whose value is dependent upon the circuit component values. The corner frequency for this work is 330 Hz, and the corresponding component values result in a differentiator gain of 0.1.

The gain stage, also included in Figure 2-4, is a standard inverting op amp configuration whose gain, k_g , is proportional to the ratio of the feedback resistance to the input resistance. The feedback resistance can be adjusted by a dial potentiometer provided on the front of the signal processing box. As fabricated, this stage can provide gains between zero and five.

The Bode plot for the differentiation and gain stages combined is shown in Figure 2-5. It is evident from this plot that this subsystem behaves as a differentiator up to approximately 300 Hz since the slope of the plot in this region is +20 db/decade.⁹ This plot corresponds well with the calculated response of $k_d k_g 2\pi f_r$ where f_r is the frequency in Hz of the input signal and k_d the differentiator

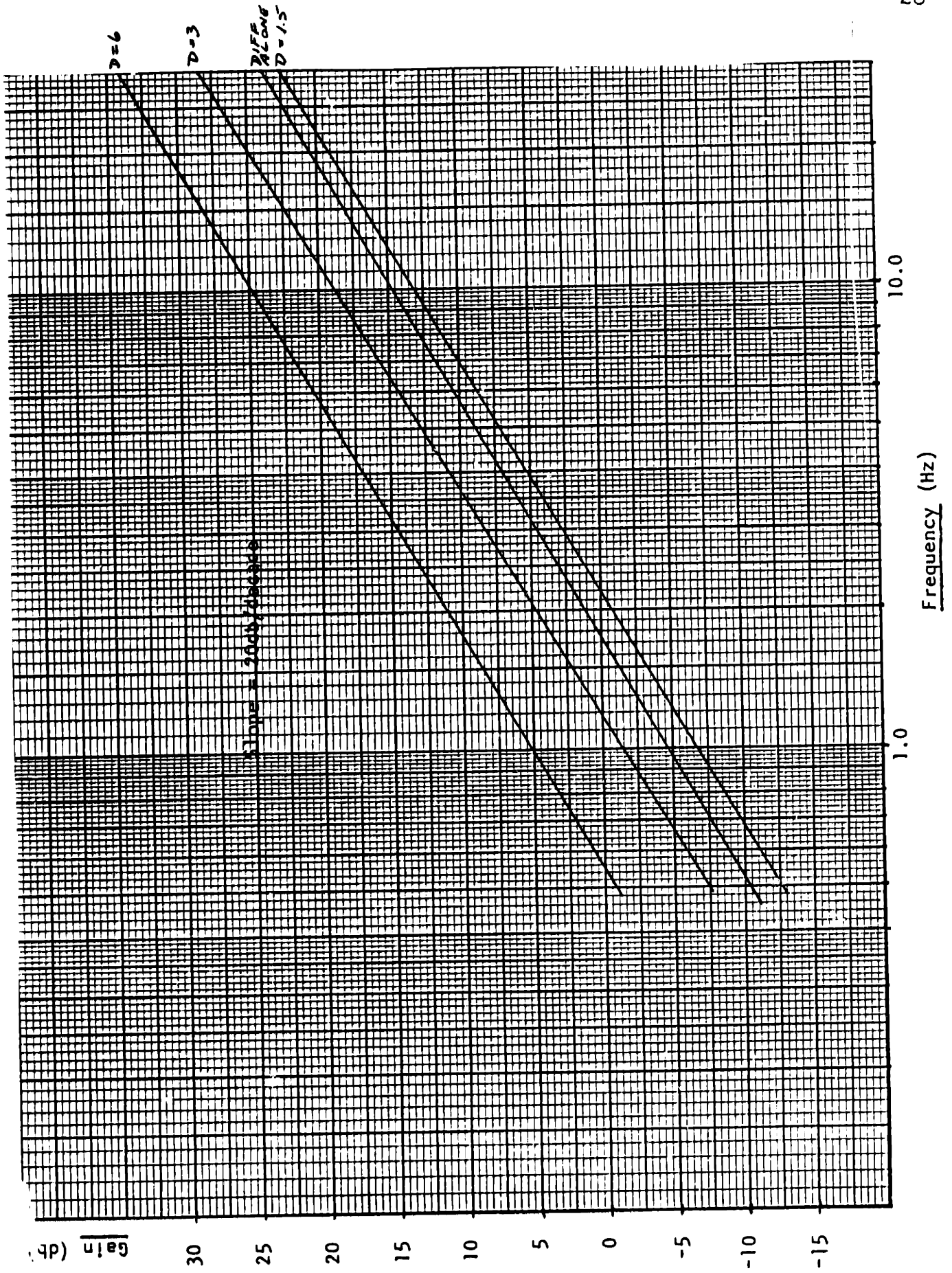


Figure 2-5 Differentiator and Gain Stage Frequency Response

gain. The phase of the response is $+90^\circ$ (i.e. lead) in the .1 to 4.0 Hz range, decreasing to $+85^\circ$ at 10.0 Hz.

2.4.2 Magnetic Particle Brake

A magnetic particle brake was selected to provide viscous damping based on its successful performance in a similar role in prosthetic knee simulators developed at M.I.T.⁶ The brake selected for this project was a Force Limited Model B215F3-2 which has a maximum output torque of 40 in-lbf. The brake current may range between 0 and 400 mA. However, the range of incrementally proportional response is 50 to 160 mA. Figure 2-6 shows the measured DC torque versus DC current characteristics of the brake.

The brake consists of two disks, one fixed and one rotating, inside a housing. Surrounding these disks is an inductive coil and the gap between the disks is filled with magnetic particles (iron filings). Brake current, i_b , flowing through the coil produces a magnetic field across the gap causing the metal filings to line up perpendicular to the disks. When one disk begins to rotate relative to the other, the filings shear in the middle of the gap. The force required to shear the particles (the torque output m) is proportional to the strength of the magnetic field and consequently i_b .

The response of i_b to a step change in voltage across the brake consists of two portions, as shown in Figure 2-7. The first is a steep rise lasting 5 msec. This portion is indicative of a time constant of 40 msec determined

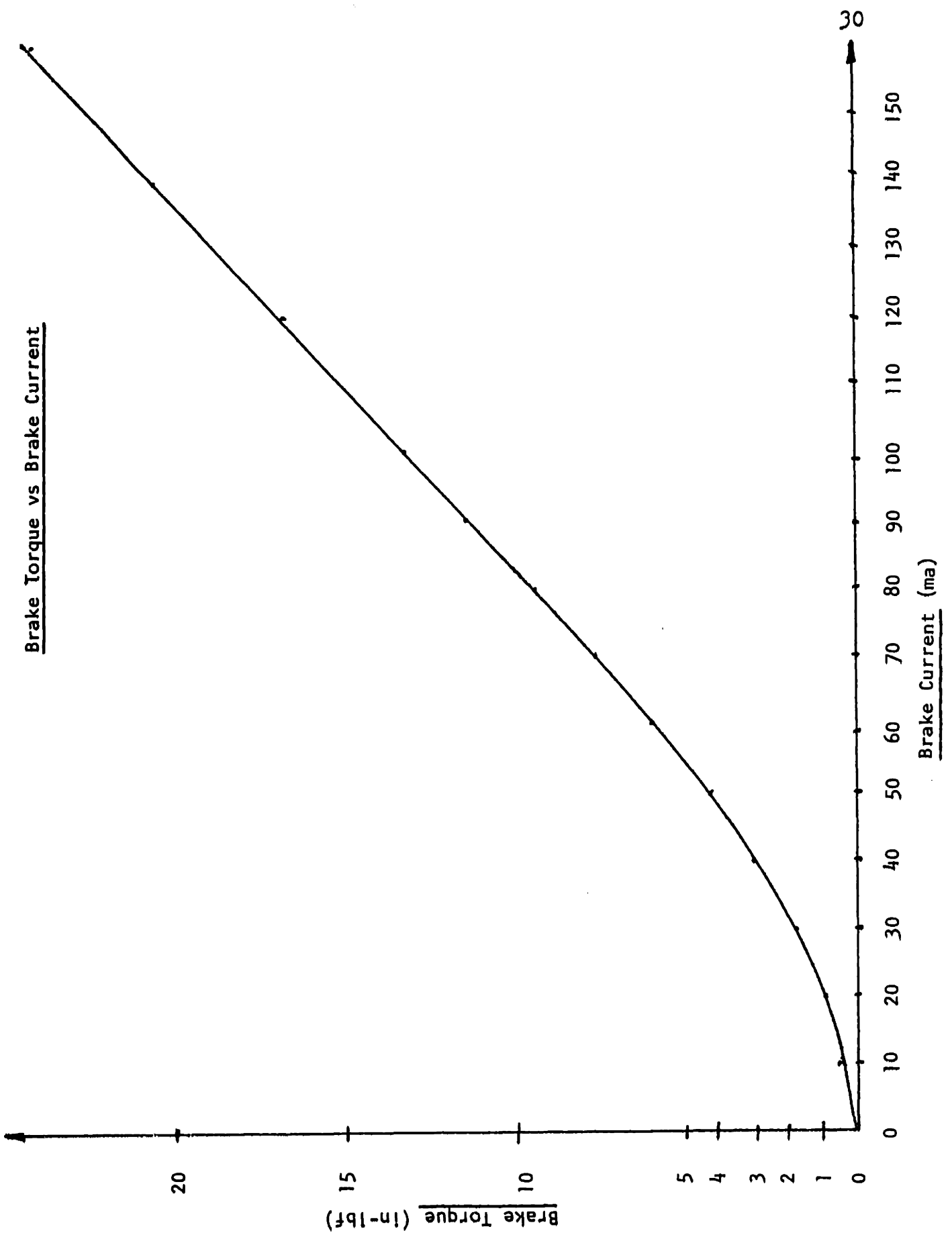


Figure 2-6 Static Response of Magnetic Particle Brake

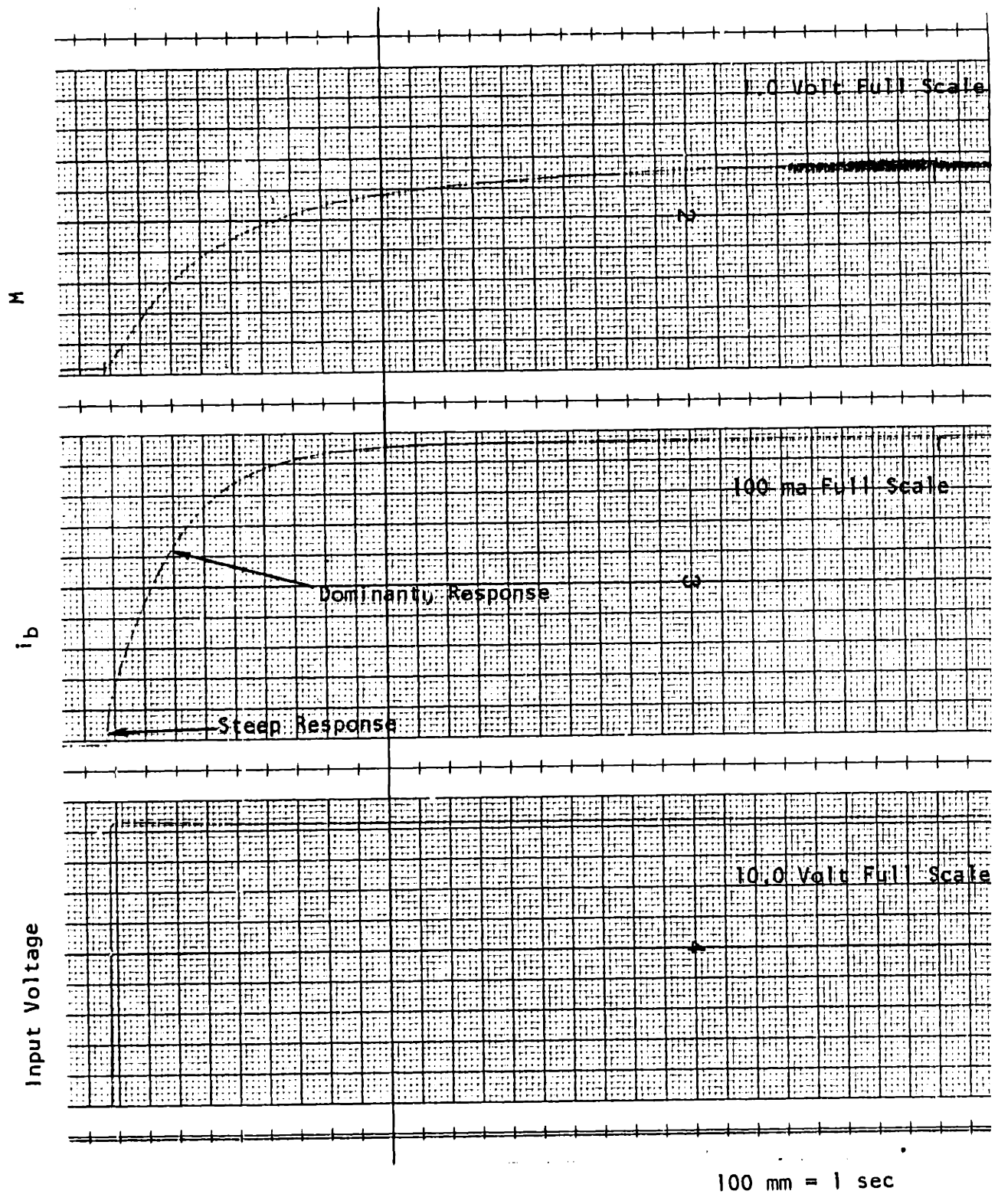


Figure 2-7 Response of M and i_b to a Step Input in Voltage

graphically from the initial slope of the response. The dominant response of i_b is a slower exponential rise with a 120 msec time constant, again determined graphically. Use of this time constant alone would be a good approximation of the response of i_b to step changes in voltage since the initial response is so short lived. Also shown in Figure 2-7 is the response of the torque to step changes in voltage applied to the brake. This torque is the voltage output, M , of the torque transducer and amplifier.

2.4.3 Current Stage

Use of a voltage controlled current source minimizes the effect of these electrical time constants. Hence, one of these sources was used to control the brake current. This circuit, shown in Figure 2-8, uses a high voltage op amp incorporating feedback to regulate the current through a power transistor in series with the brake. When switched on, this power transistor can apply up to 40 volts DC to the magnetic particle brake. With this voltage capacity, the direction and magnitude of i_b can be rapidly changed inspite of the inductive element in the brake. For a step input of 400 mV, i_b reaches 62% of its final value within 2.5 msec compared to the 120 msec observed without the current stage. Table 2-2 shows the time measured for i_b to reach its final value for a step change of 500mV as a function of the power transistor supply voltage. Figure 2-9 a,b,and c are polaroid photographs of these responses. Considerable time savings

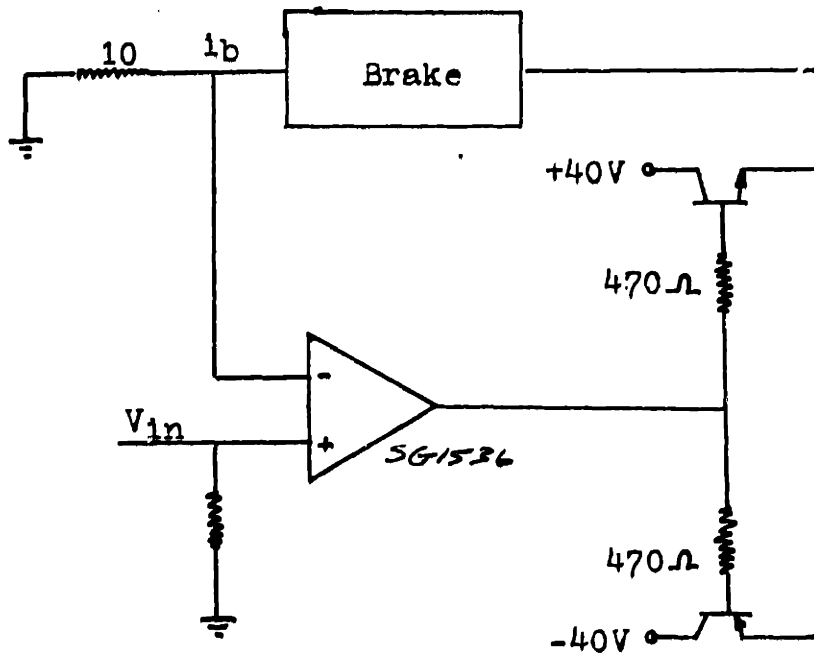


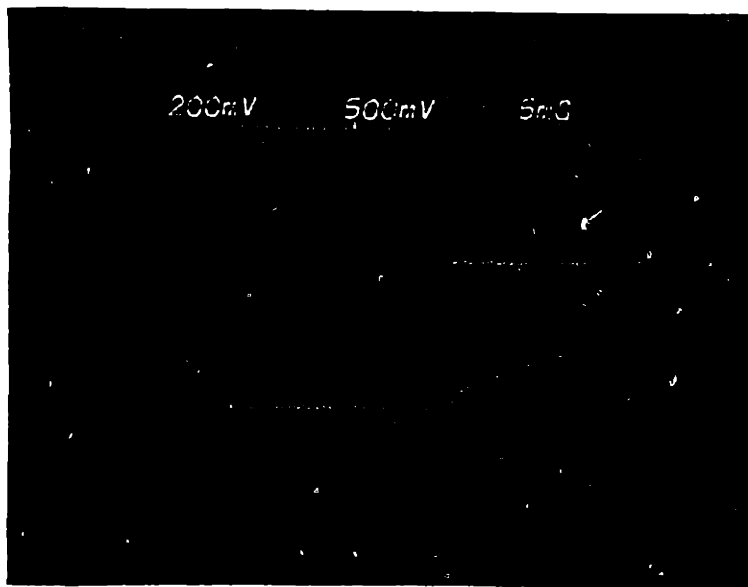
Figure 2-8 Current Stage

Table 2-2

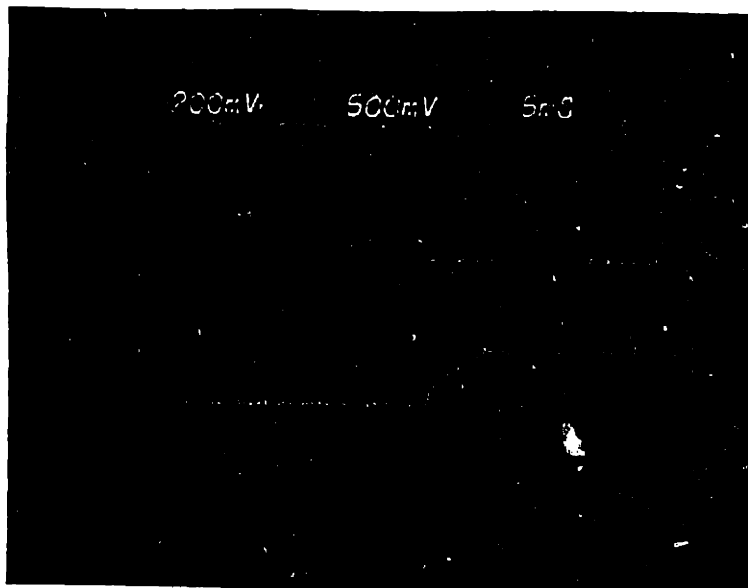
i_b Rise Time For Various Current
Stage Supply Voltages

<u>Supply Voltage (VDC)</u>	<u>Rise Time*(sec)</u>
<u>± 20</u>	11.0
<u>± 30</u>	6.0
<u>± 40</u>	3.5

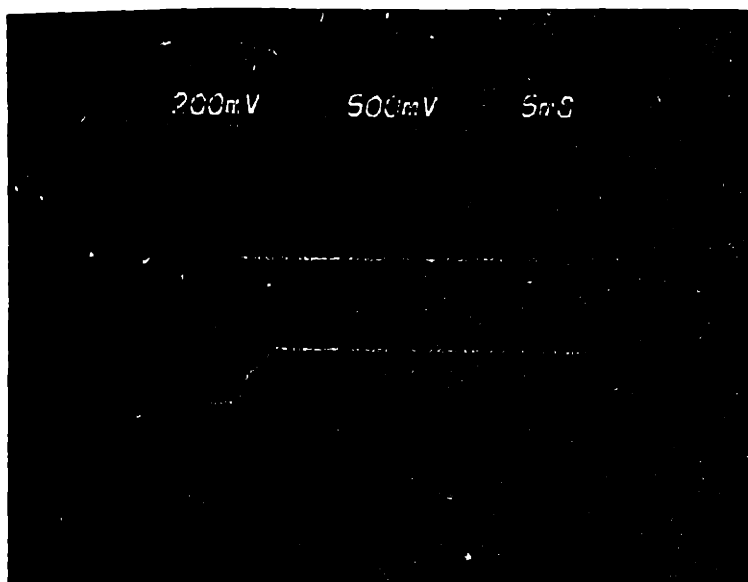
*Rise Time - The time it takes i_b to reach its final value with a step input to the current stage of 500 mV. See Figure 2-9.



a) $V_S = \pm 20 \text{ VDC}$



b) $V_S = \pm 30 \text{ VDC}$



c) $V_S = \pm 40 \text{ VDC}$

Figure 2-9 Effect of Power Transistor Supply Voltage, V_S , on i_b response time

are realized through the use of a 40 volt DC power supply.

The current stage with the brake as a load provides a precisely regulated i_b response to sinusoidal control voltages. For input voltages of ± 200 mV and ± 400 mV, no distortion, attenuation, or phase lag of i_b was measured at frequencies up to 30 Hz. These input levels correspond to i_b values of 20 and 40 mA respectively. For inputs of ± 600 mV (corresponding to $i_b = \pm 60$ mA) the current response becomes increasingly triangular for frequencies in excess of 20 Hz. For all frequencies and amplitudes encountered during actual trials with human subjects, this distortion is not significant.

2.4.4 Torque Transducer and Amplifier

A torque transducer was incorporated into the TLD to provide the capability of measuring the amount of torque applied to the handle. The design of the transducer was based on standard practices in which foil strain gages were mounted on a cylindrical section of the shaft connecting the brake and handle. BLH Electronics FAED-06B-12-S6 gages with a gain factor of $1.96 \pm 1\%$ were used. These gages are mounted 45° to the shaft axis, coincident with the 45° components of the combined normal and tangential stresses in the shaft resulting from applied torques. By applying two pairs of gages 180° apart on the shaft, a Wheatstone bridge with four active legs is fabricated. Consequently, the effects of temperature and forces or moments other than torques about

the shaft axis are nulled out.

The torque transducer amplification circuit is centered around a Burr Brown 3626AP instrumentation amplifier. This amplifier has a gain of 672 volts/volt, an offset output voltage of ± 0.4 mV, a temperature drift of ± 6.0 μ V/ $^{\circ}$ C, and an output noise level of 2.0 μ V peak to peak. The circuit diagram for this subsystem is shown Figure 2-10. The static or DC response of the combined torque transducer and amplification system is very linear, as shown in Figure 2-11. This subsystem has a total gain of 83.3 mV/in-lbf. This gain can be adjusted by modifying the gain control resistance in the instrumentation amplifier, which in this case equals 15 ohms.

2.4.5 Simple Brake Model

Ideally, the magnetic particle brake, with the torque transducer coupled to it, would produce a torque voltage, M , proportional to the velocity of the handle with no attenuation or lag. However, the time constant relating M to input steps of voltage applied to the brake in the absence of the current stage is 220 msec, as determined graphically from Figure 2-7.

This 220 msec time constant is reduced to approximately 100 msec when the current stage is incorporated in the system. Because the current stage nearly eliminates the lag of the electrical response, the major contributor to this remaining time constant must be the mechanical dynamic characteristics of the brake, coupling, and torque

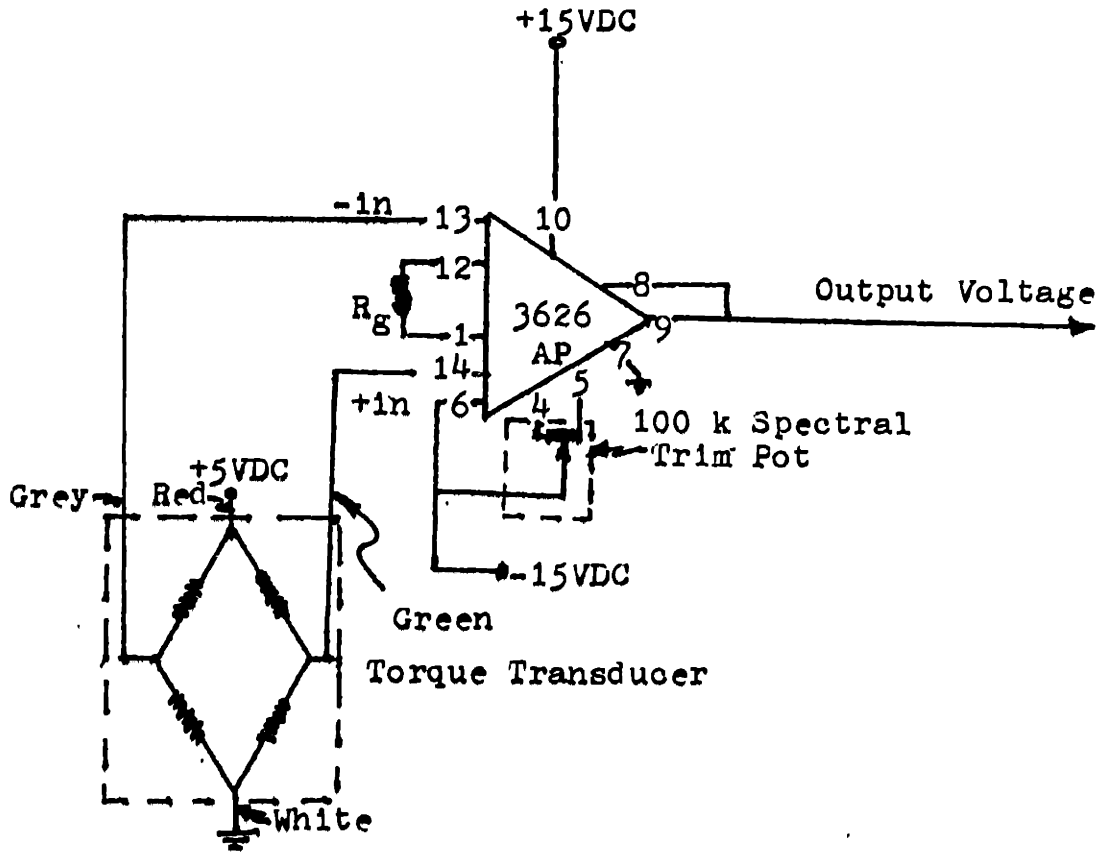


Figure 2-10 Torque Transducer Amplifier Circuit

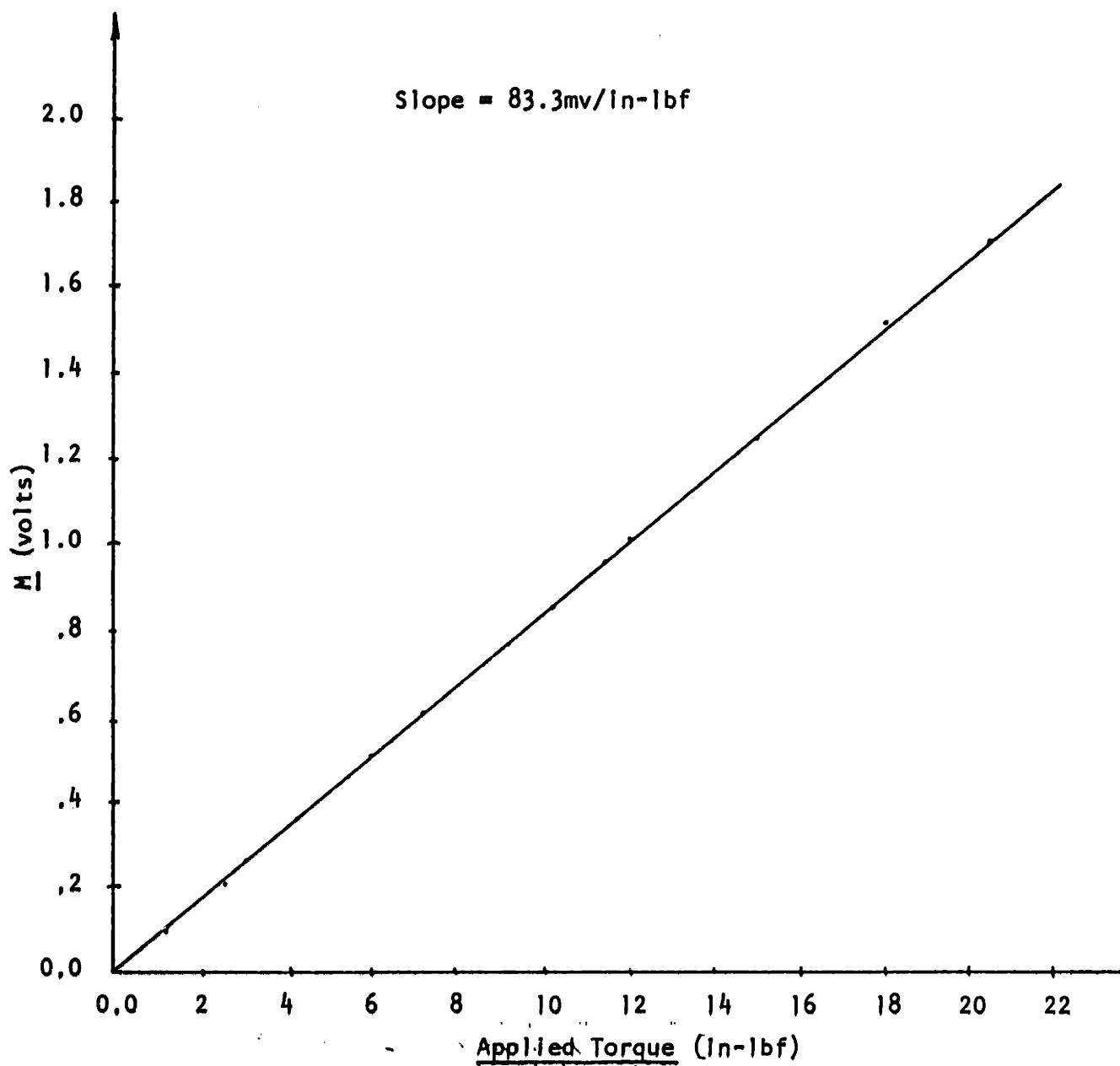
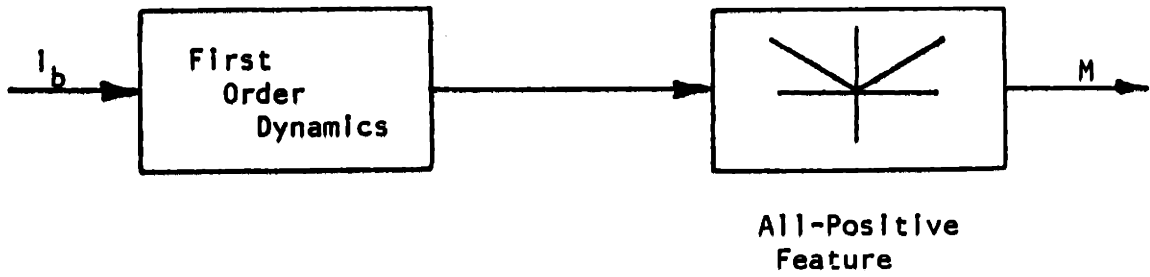


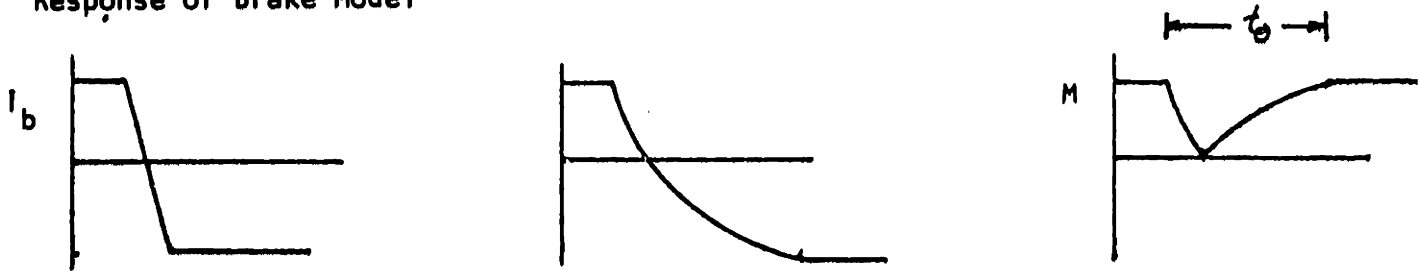
Figure 2-11 Instrumentation Amp Output, M, vs Applied Torque

transducer. These characteristics are functions of the amount of time required for the magnetic particles in the brake to alter their alignment in response to changes in i_b , and the "windup" of the coupling and torque transducer, (i.e. elastic deflection is required in these components to develop full rated torque). The "windup" of the coupling and torque transducer are 0.33° and 0.10° respectively, at 24 in-lbf torque. These correspond to torsional stiffnesses of 4300 in-lbf/rad for the coupling and 13,750 in-lbf/rad for the torque transducer.

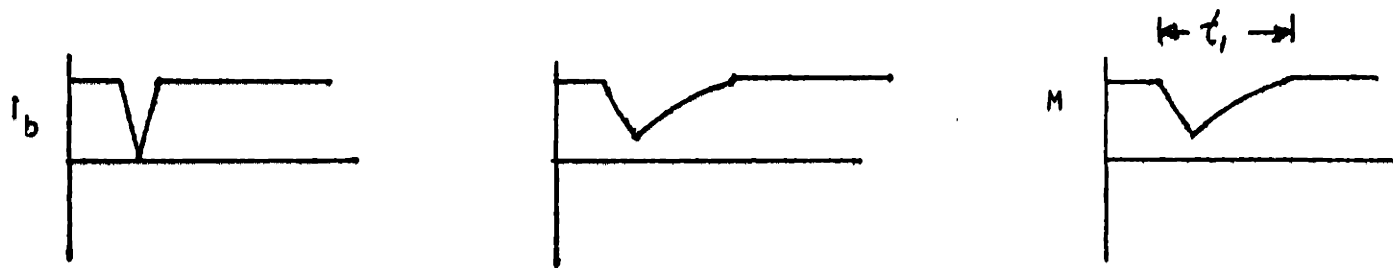
The magnetic particle brake produces M opposing rotation regardless of the direction of rotation. When this feature is combined with the above dynamics, a simple model of the brake can be developed. Shown in Figure 2-12, this model includes, as an approximation, first order dynamics followed by an all-positive nonlinearity. To study the response of this model, i_b will be decoupled from the shaft rotation; i.e. the changes in torque due to changes in i_b will be studied assuming shaft rotation is constant. During a rapid ramp change in the sign of i_b , made possible by the current stage, the output of the dynamics component, M' , would exponentially decay towards a new value of the opposite sign. However, the all-positive feature of the model inverts the negative portion of M' . The result seen in Figure 2-12 is an exponential decay in M to zero followed by an exponential rise to the original value of torque.



Response of Brake Model



Response of Brake Model with a Rectifier Added Before The First Order Dynamics



$$t_0 > t_1$$

Figure 2-12 Simple Magnetic Particle Brake Model and Its Response to Various Inputs i_b

This undesirable transient response can be shortened if the input current to the dynamic element were itself rectified. Rectifying the i_b causes it to drop to zero and rise back to a positive value during rapid sign changes of input. Following i_b , M' begins its decay as i_b drops to zero. However, i_b reverses direction before M' reaches zero. Consequently M' and hence M begins to rise towards its final value and reaches that final value sooner than for the model without input current rectification.

2.4.6 Rectifier

A rectifier hasⁱⁿ fact been incorporated into the TLD prior to the voltage controlled current source. This partially compensates for the time constants resulting from the mechanical dynamics. The design of the rectifier is based on a standard op amp circuit and is detailed in Figure 2-13. Although frequency response techniques cannot be directly applied to the description of this nonlinearity, the response of this component to unbiased sinusoidal inputs is to generate a full rectified sine wave with no attenuation for frequencies up to 40 Hz. In addition, this element does not introduce any delays.

2.4.7 Combined Current Stage, Brake, and Torque Transducer Response

The mechanical dynamics of the brake and transducer will attenuate responses above a relatively low frequency because the rectifier and current stage only partially compensate for the existing time constants. As shown in Figure 2-6, the i_b versus M static response exhibits a

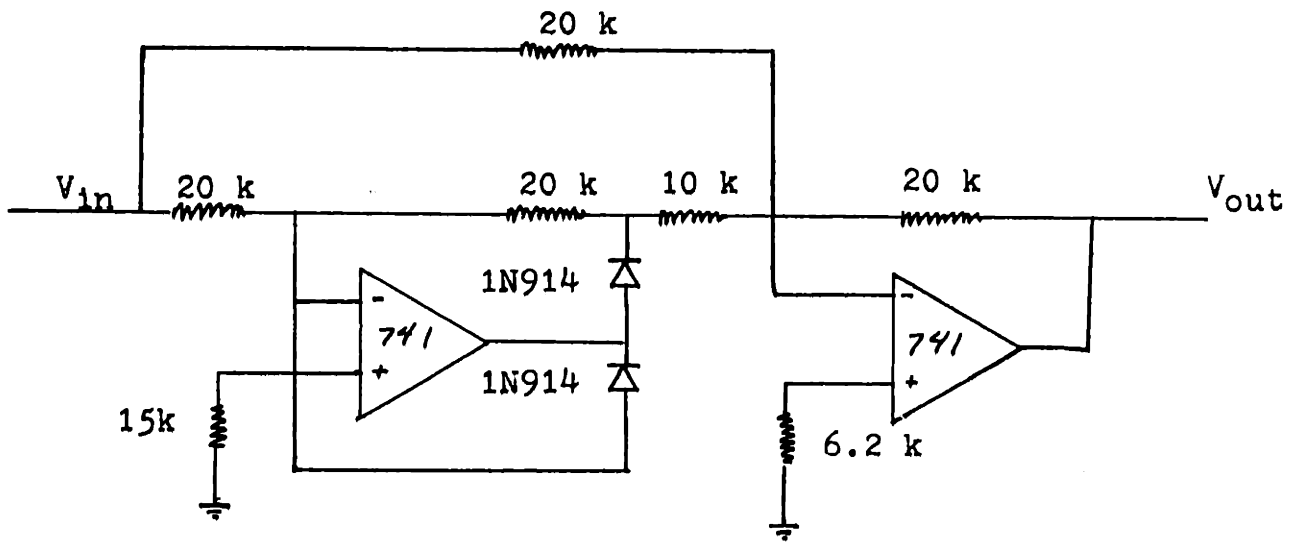


Figure 2-13 Full Wave Rectifier

square law relationship in the 0 to 50 mA region. Beyond this region, the DC torque is incrementally proportional to brake current with the exception of some small hysteresis. The M/i_b gain in this region is 15.8 mV/mA.

The input to the current^{stage} was DC biased to test the frequency response in the incrementally linear response region. Without such a bias, the system gain would be a function of the amplitude of the input and would vary over the course of a single cycle of an AC signal. The frequency response of the current stage, brake, and torque transducer in the region of proportionality is plotted in Figure 2-14. This plot shows the gain of this subsystem is relatively independent of frequency between 0.1 and 4.0 Hz. In this sector of the plot, the plot has a slope of $-\frac{1}{2}$ db/decade starting at a DC gain of zero db. The gains plotted in this figure have been normalized with respect to the DC gain for the given input. Between 0.1 and 4.0 Hz, the gain is down -3.0 to -5.0 db. The gain drops off to -6.5 db at 10.0 Hz and -8.2 db at 20 Hz. The phase plot shows nearly constant slope of -15° /decade. The lag is approximately 5° at 0.1 Hz, 32° at 4.0 Hz, and 43° at 20.0 Hz.

These response characteristics were obtained by moving the handle at a constant angular velocity with a large lever arm insensitive to varying torques applied by the brake. DC biased sinusoidal inputs were applied to the current stage by a function generator (Tektronix FG501).

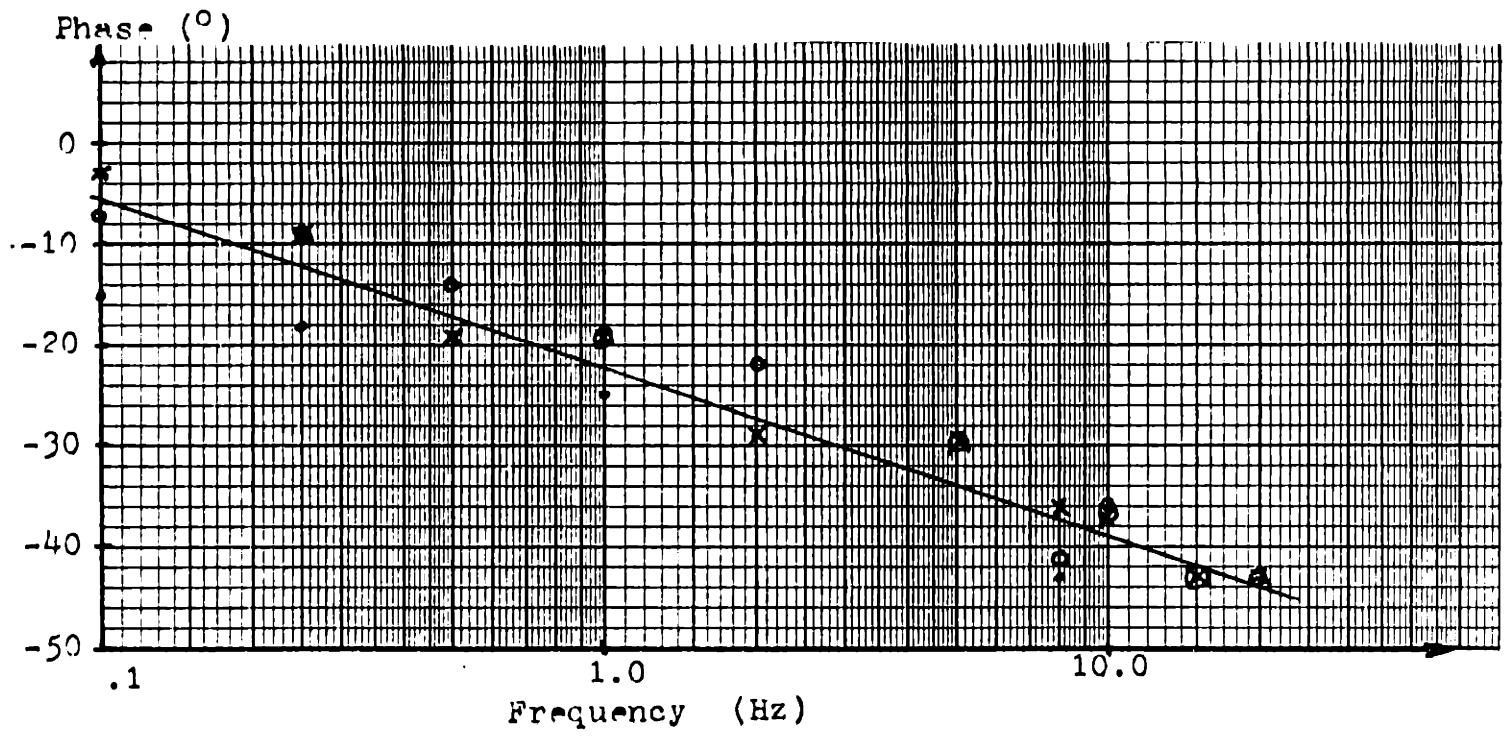
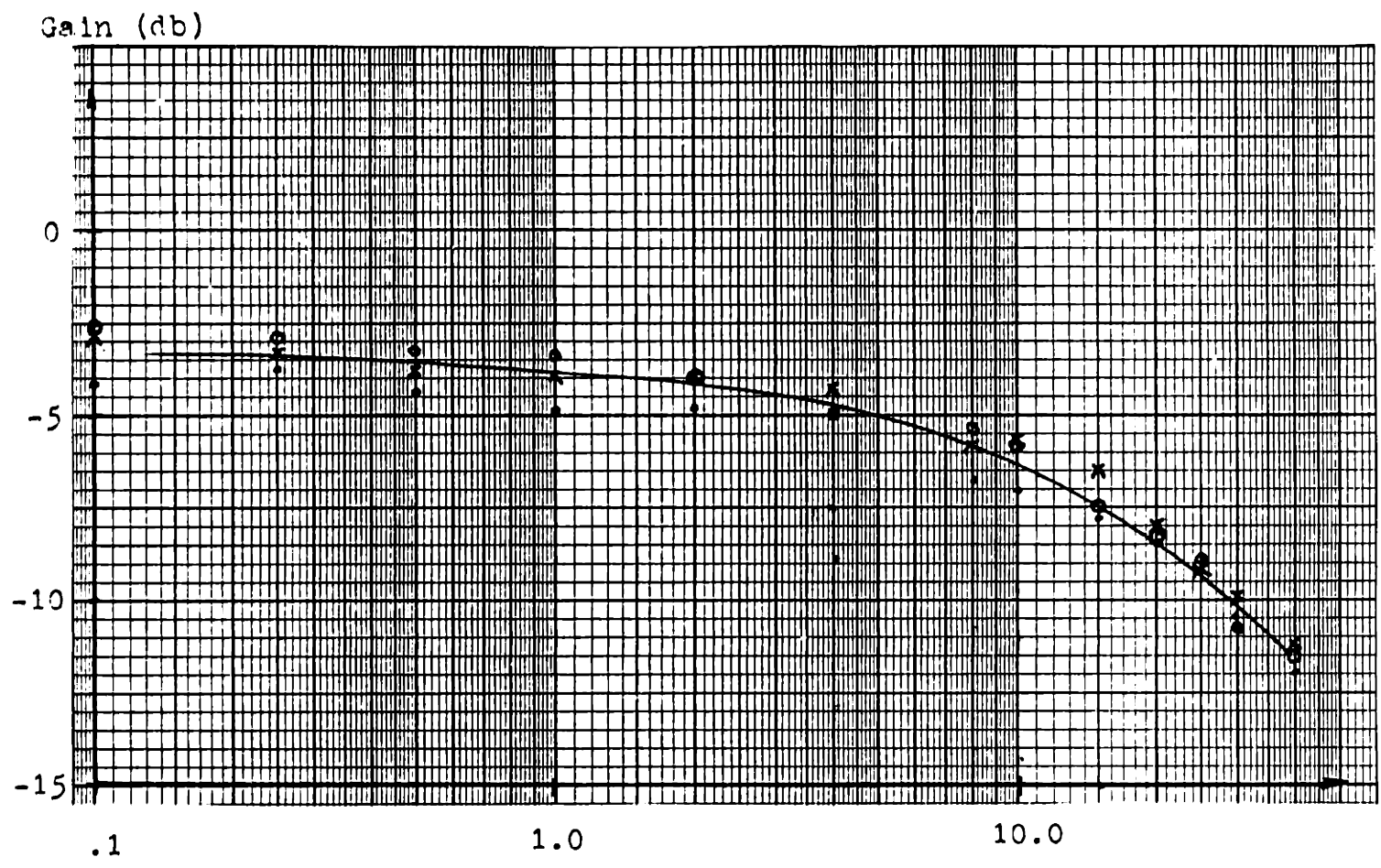


Figure 2-14 Frequency Response of Current Stage, Brake, and Torque Transducer

The input voltage and M were monitored on a Tektronix storage oscilloscope as the handle was moved through an arc.

It is obvious from this plot that this subsystem will act as a low pass filter. I believe this results from the spring-like response ("windup") of the torque transducer and brake to changing inputs. It would be worthwhile then to investigate the use of a smaller brake with a correspondingly smaller mechanical time constant, to stiffen the rotating elements, or to provide closed loop torque control.

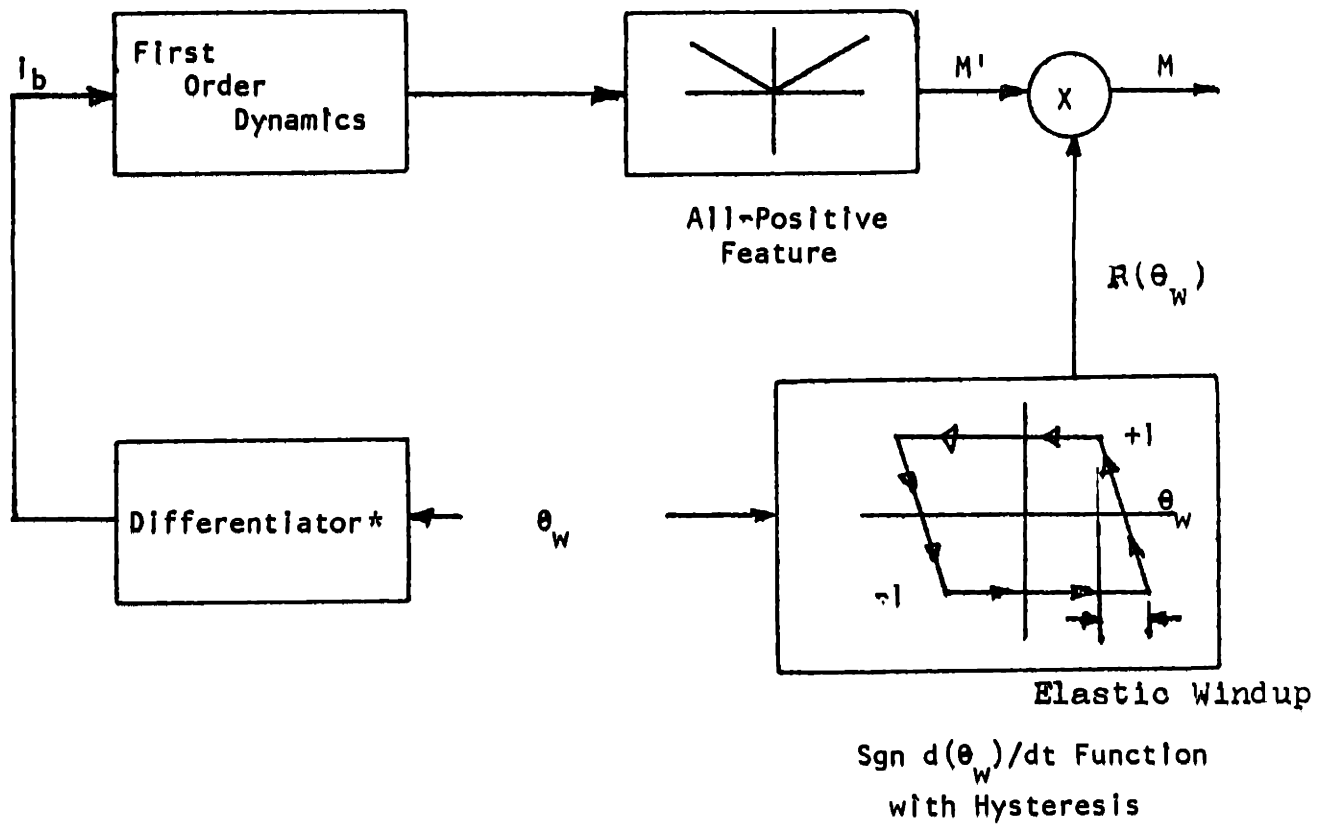
2.4.8 Brake Subsystem Model

In analyzing the magnetic particle brake response, it is worthwhile to develop a more sophisticated model of the brake subsystem than the one presented earlier. Such a model can give added insight into the features of this subsystem and how it could be expected to respond. The conceptual model developed for this purpose is shown in Figure 2-15. The model consists of the following components:

First order dynamics associated with the resistance and inductance of the brake and the mechanical dynamics of the brake and torque transducer.

An all positive nonlinearity which generates positive M' regardless of the sign of current.

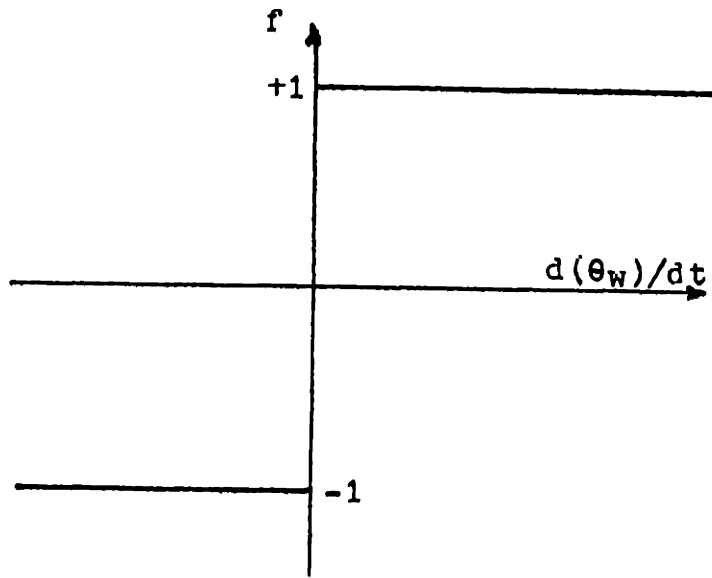
A hysteresis function $F(\theta_w)$ of magnitude 1 and sign opposite to the direction of rotation. See Figure 2-16.



*Differentiator is not included in the Brake model but is shown here to identify the relationship between I_b and θ_w .

Figure 2-15 Magnetic Particle Brake Model

$f = \text{Sgn}(d(\theta_w)/dt)$ can be graphed like this....



or this...

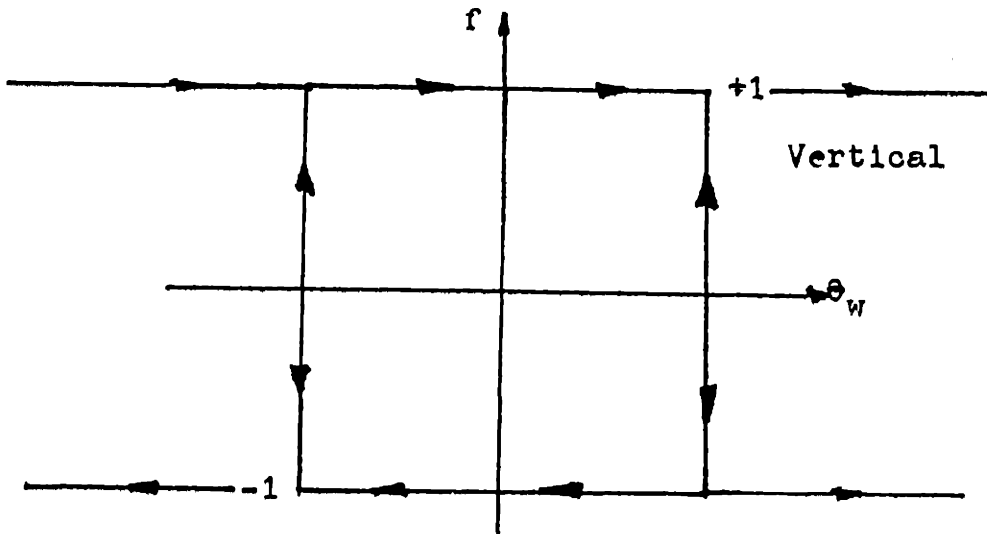


Figure 2-16 $\text{Sgn}(d(\theta_w)/dt)$ Function

The input to the first order dynamics is i_b which, in the assembled TLD, is proportional to the angular velocity of the handle (i.e. $i_b \propto d(\theta_w)/dt$). θ_w is the input to the hysteresis function as well. This hysteresis function multiplies M' by the necessary value to account for direction of rotation. Ideally, this would degenerate to $P(\theta_w) = -\text{Sgn } \dot{\theta}_w$ as in Figure 2-16, simply multiplying M' by ± 1.0 to generate M . However, due to the energy stored in the elastic windup of the brake, transducer, and coupling, the direction reversal lines of the hysteresis function are not vertical. The effect of this is shown in Figure 2-17.

As the shaft rotation changes direction, $d(\theta_w)/dt$ progresses through a rapid sign reversal as shown in Figure 2-17 a and b. During this time, the $-\text{Sgn } d(\theta_w)/dt$ function would ideally follow the dotted transition in Figure 2-17 c. However, due to energy storage in the various components, the $P(\theta_w(t))$ function follows the solid sloping line.

At the start of a direction reversal, M' would begin to decay towards a value of the opposite sign due to the first order dynamics. If the all positive feature did not exist, M' would continue through zero and follow the dotted response in Figure 2-17d. However, the all-positive feature inverts the negative portion of the response causing M' to follow the solid line in Figure 2-17d. The M' response is multiplied by the $P(\theta_w(t))$ function

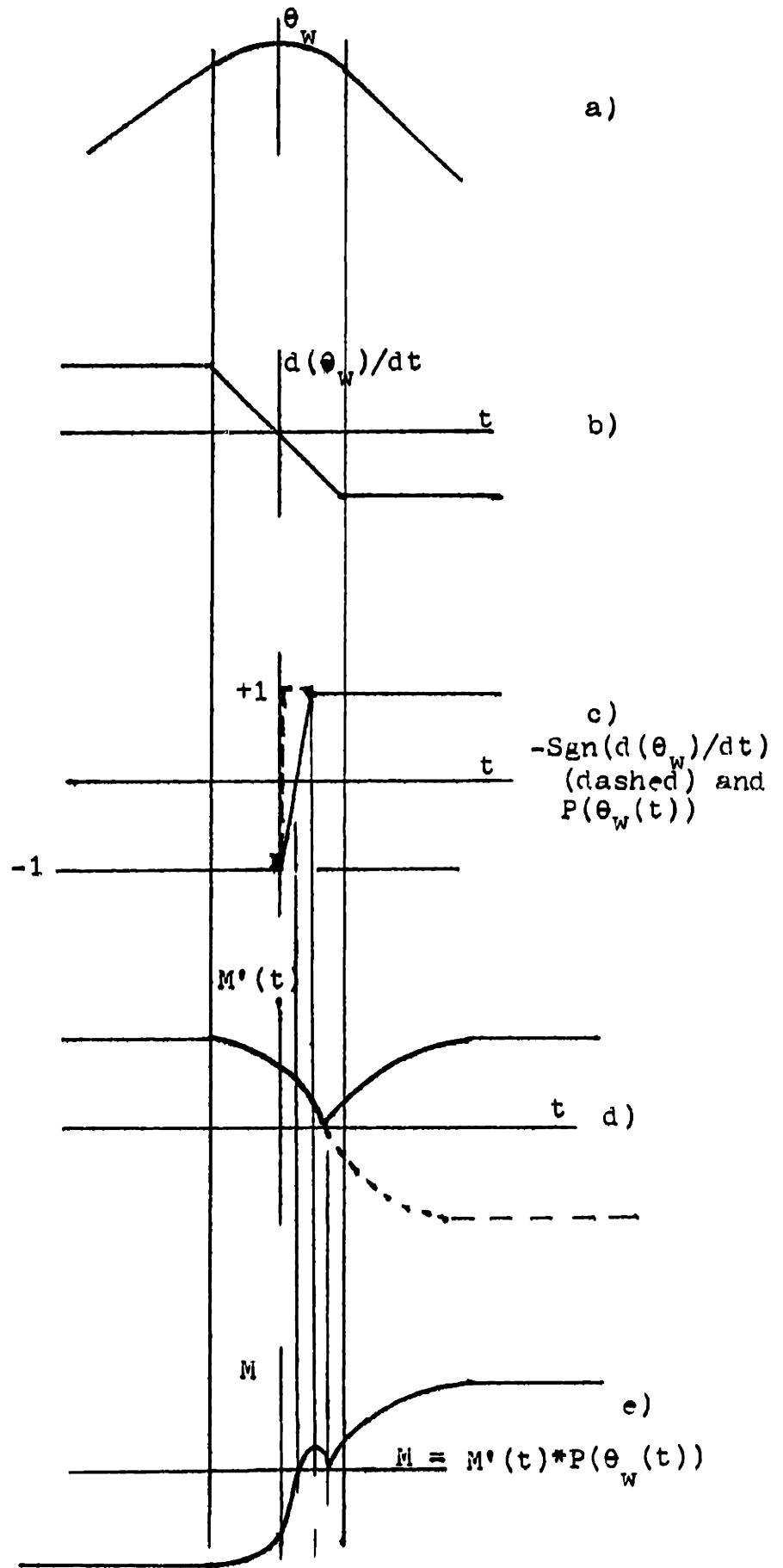


Figure 2-17 Magnetic Particle Brake Model Response

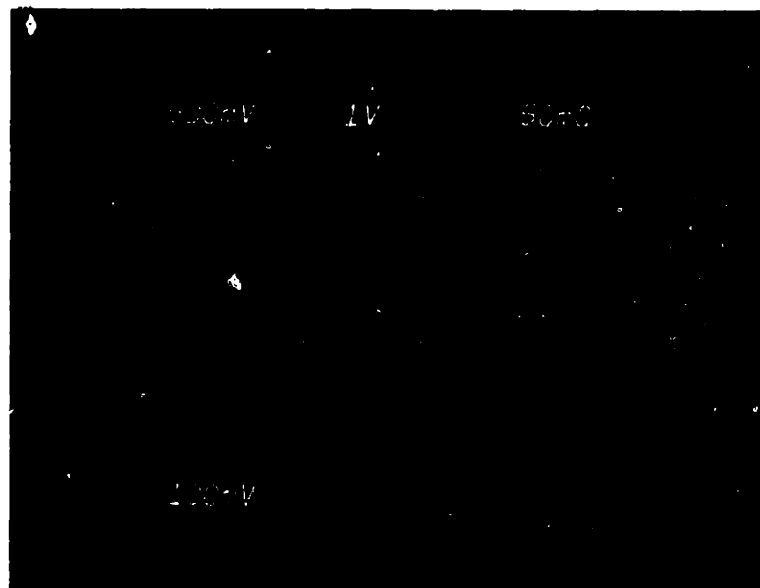


Figure 2-18 Observed Response of M
During Direction Reversals

Note: On left side of photograph;
Top trace is P (wrist angle voltage),
Middle trace is I_b (brake current),
Bottom trace is M (torque voltage).

and the resulting response M is obtained, as shown in Figure 2-17e. This response was in fact observed and a Polaroid photograph of it is shown in Figure 2-18. The significance of this observation is that the brake will briefly assist the motion of the handle after a rapid direction reversal. This assistance comes from the energy stored in the elastic deflection of the system components. This energy is released during direction reversals. More generally, note that the distortions of $d(\theta_w)/dt$ seen in $M(t)$ result from the combined effects of brake response time and elastic energy storage. If $M(t)$ was truly a rectified version of $d(\theta_w)/dt$ and F was simply $-\text{Sgn}(\theta_w)$, then $M(t)$ would be instantaneously proportional to $\theta_w(t)$.

2.4.9 TLD System Response

The TLD frequency response was determined for the completely assembled system by having a normal subject track sinusoidal targets of increasing frequency and ensemble averaging the recorded response and torque voltages. Good sinusoidal tracking could be maintained on average for frequencies up to 4.0 Hz. At each frequency, the response and torque voltages were ensemble averaged to give an averaged response magnitude \bar{R} and an averaged torque magnitude \bar{M} . $20 \log(\bar{M}/\bar{R})$ was used to calculate the system gain while phase information was obtained by measuring the shift between peaks of \bar{M} and \bar{R} .

The result of this effort is shown in Figure 2-19.

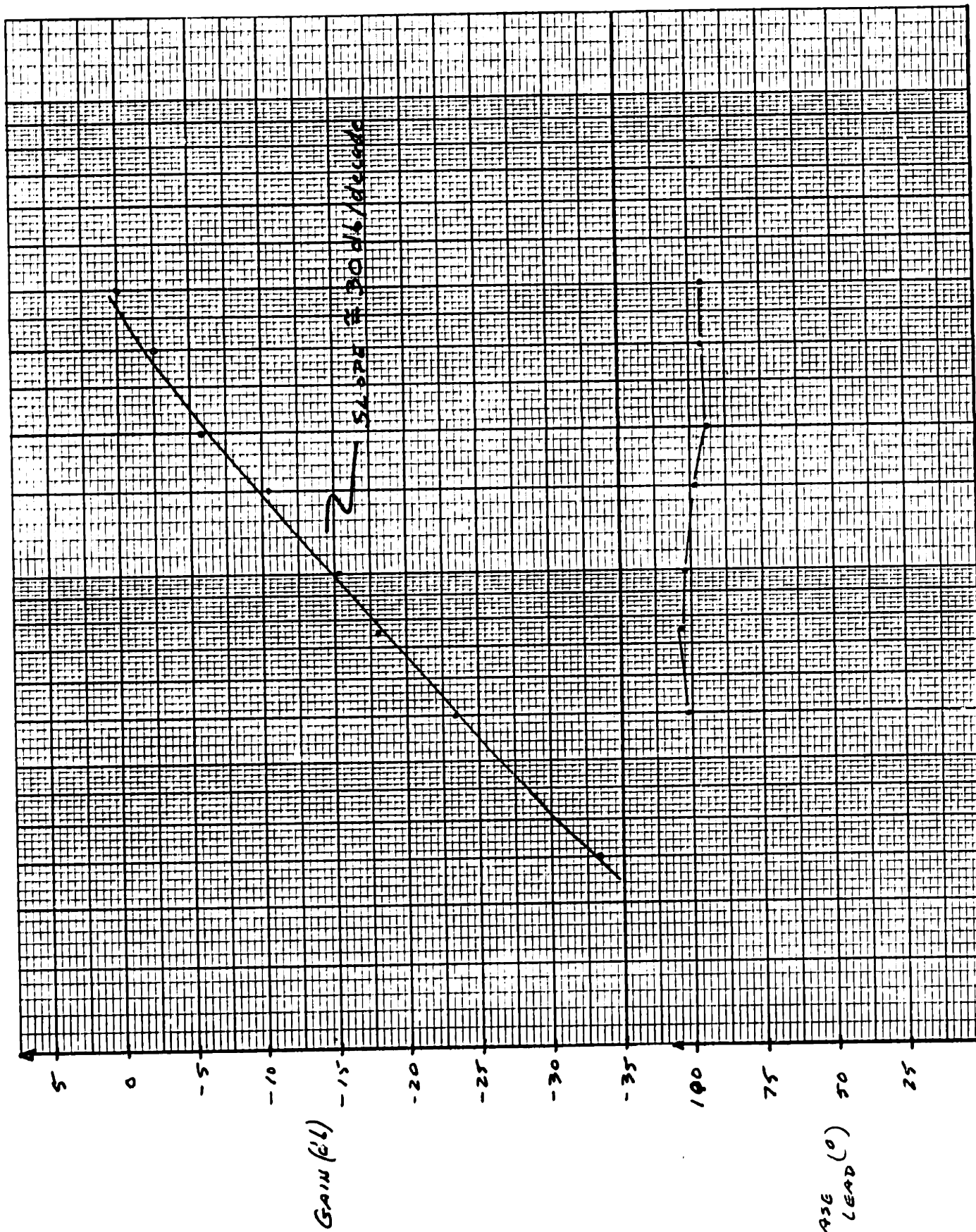


Figure 2-19 Frequency Response of TLD

Note: Gain = 20log(M/R)
D = 4

PHASE
(LEAD (°))

The slope of the gain curve is 30 db/decade in the $1/4$ to $3/4$ Hz range and tapers off to nearly 20 db/decade above 1.0 Hz. Ideally, this plot should have a constant slope of 20 db/decade, that of a pure viscous damper. The increase in gain more than proportional to frequency is caused by the increasing static gain (torque vs current in Figure 2-6) of the magnetic particle brake. For low frequencies, the input to the current is very small, resulting in low brake gain and hence low torque. As velocity of the handle increases, the brake current is driven higher resulting in an increase in the brake gain. This occurrence is evidenced in Figure 2-20 which is a Bode plot for the combined current stage, brake, and torque transducer. Unlike the previous plot for this subsystem (Figure 2-14), the input voltage here was not DC biased when this data was obtained. In fact, the input voltage to the current stage and the output voltage of the transducer stage were recorded while a normal subject was tracking at various frequencies. As a result, brake current was varying through the range of varying brake gain. Hence, when this plot is combined with the frequency response for the differentiator and gain stage (Figure 2-5), the plot in Figure 2-19 results. In other words, the nonlinear response of the brake is responsible for the additional 10 db/decade.

Finally, Figure 2-21 shows the equivalent damping constant B in in-lbf/(rad/sec) for the entire system.

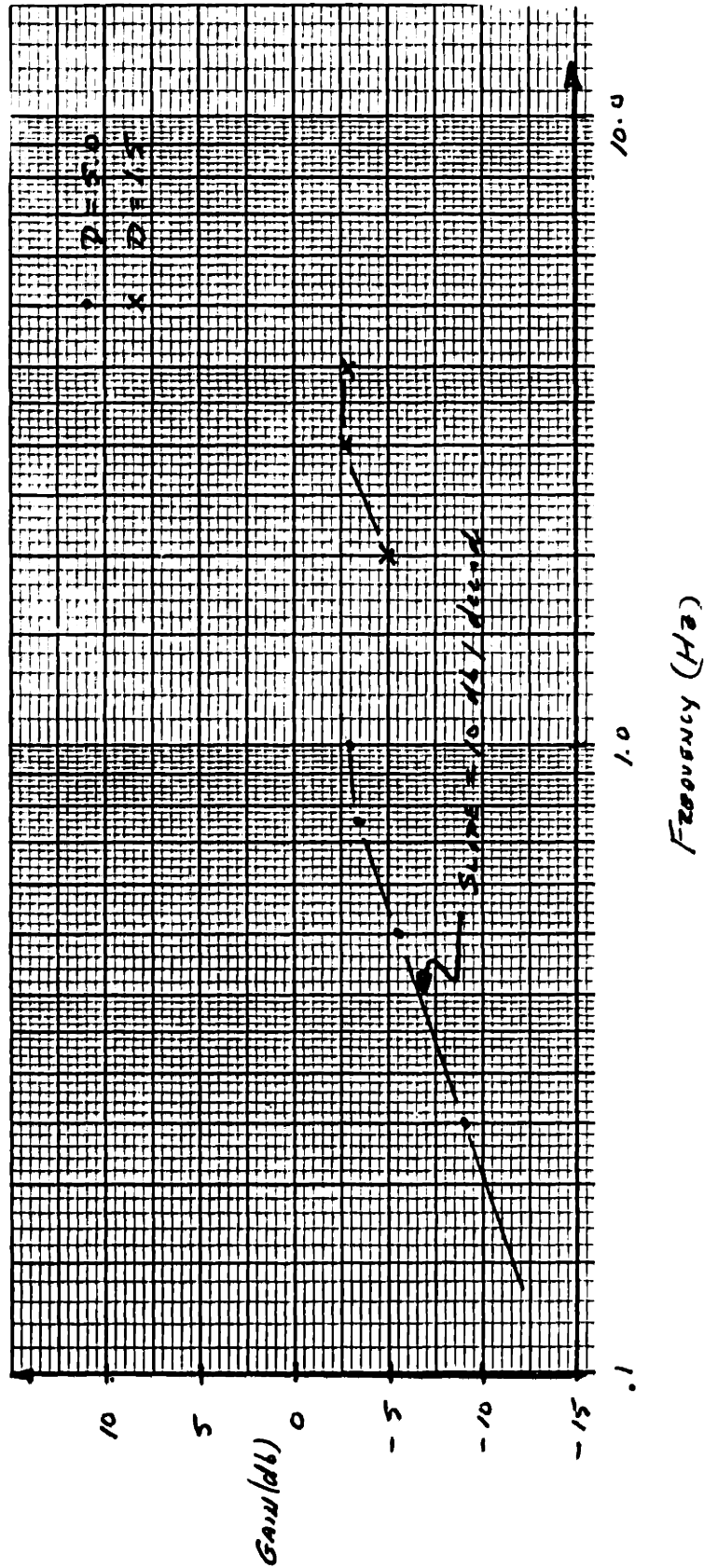


Figure 2-20 Current Stage, Brake, and Torque Transducer Frequency Response as Measured in Complete TLD System.

These values are plotted against the dial pot setting D (gain stage control) for various rotational velocities. It is obvious from the plot that B is dependent upon the rotational velocity of the handle as well as the value of D. This relationship complicates the description of the TLD since it becomes difficult to establish exactly what damping constant was used during a specified trial. This emphasizes the need to incorporate closed loop torque control into the TLD since this deficiency is the result of the changing gain of the magnetic particle brake. In addition to "closing the loop", it may prove worthwhile to use a smaller brake with a more constant gain in the region of interest. Only 50% of the rated capacity of the presently used brake is utilized and its time constants and changing gain are detrimental to the proper functioning of the TLD.

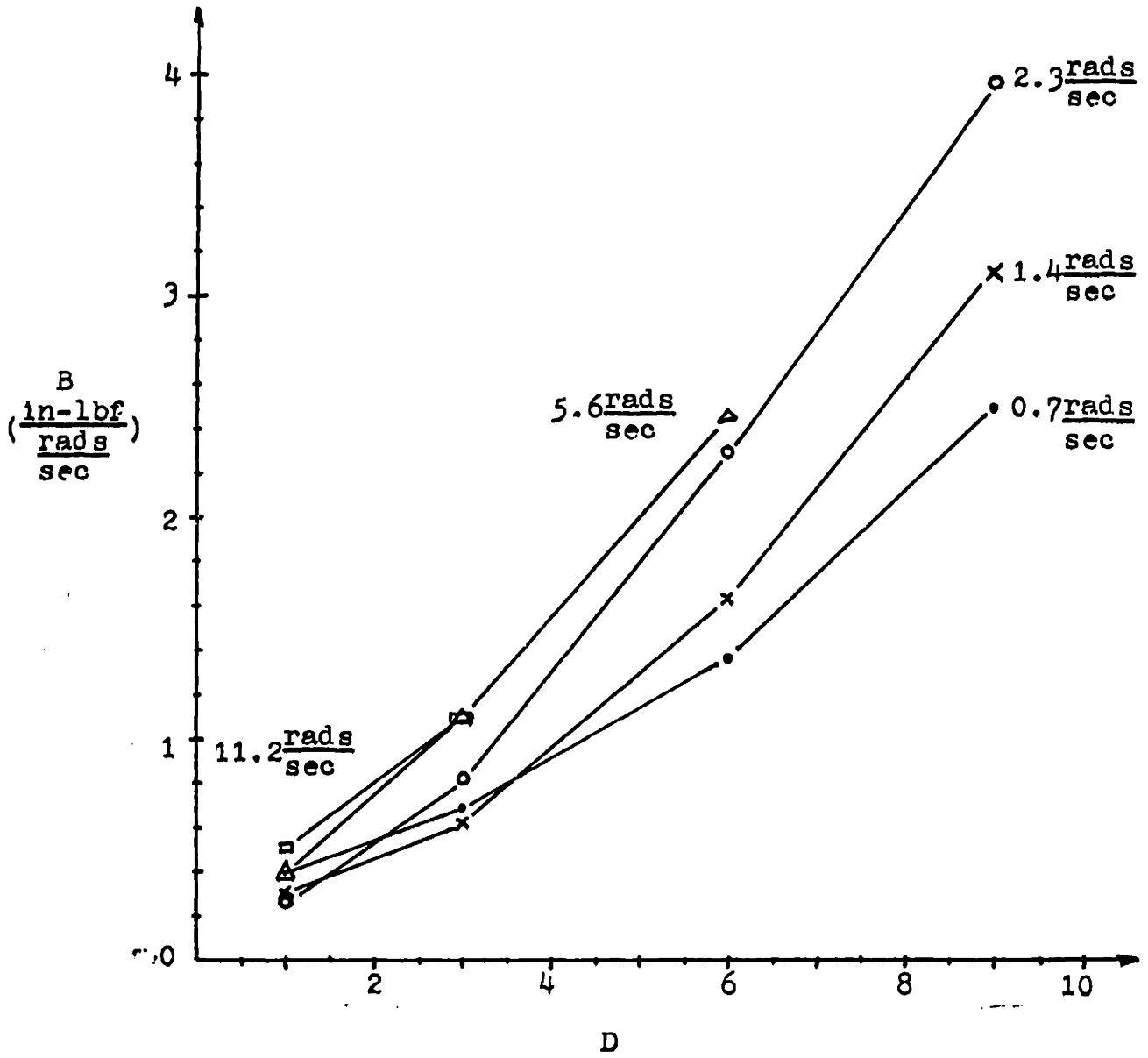


Figure 2-21 Equivalent Damping Constant (B) vs Pot Setting (D)

Note: Velocities are purely rotational velocities

CHAPTER 3

METHODS

3.1 Introduction

The driving force behind this thesis is the hypothesis that abnormal involuntary movement, particularly intention tremor, may be suppressed through the addition of an external damping element. Chapter 1 presents the theoretical justification for doing this and Chapter 2 discusses the apparatus used. This chapter treats the methods used to conduct the experiments and analyze the results.

3.2 Selection of Subjects

Contact with local neurologists was established early in the project for the purpose of locating suitable and willing subjects. Criteria for selecting subjects for the trials were: the obvious presence of action tremor at the wrist; sufficient strength to move the hand against a 3 to 4 in-lbf torque; visual acuity so the subject could observe the movements of the target and response lines on the oscilloscope screen; and mental competence so the subject could understand the intent, scope, and procedures of the trials. Prior to participating in the program, each subject was screened in light of these criteria, and received an oral and written explanation of the experiment. Subjects willing to participate were asked to sign an informed consent form. This form, listed in Appendix I, meets the requirements of the human subjects committees of MIT, Peter Bent Brigham Hospital, and the Brockton V.A. Hospital.

Three subjects were tested: subject JF, male age 54 with rubral intention tremor resulting from multiple sclerosis; subject FS, age approximately 70 years, female with idiopathic essential tremor; and subject ED, male age 26 with no abnormal movement. Subjects JF and FS had a long history of their diagnosed disorder prior to participating in the experiments. Hence their condition during the experiments was considered stable. Neither were receiving medication for their tremor at the time of the experiments. With both of these subjects, previous therapeutic treatments had had little or no effect on their tremor. A more detailed clinical description of these two subjects is contained in Appendix I - "SUBJECTS".

3.3 Experimental Procedures

The experimental trials were conducted ^{at} the subject's residences because of their inability to come to the Rehabilitation Engineering Center at MIT. The trials with JF were conducted at the Brocton Veterans Administration Hospital while FS was tested in her own home. Each subject's participation was limited to two or three experimental sessions, each session lasting approximately two hours. Frequent rest periods were given throughout the sessions to minimize the effects of boredom and fatigue. To the extent that it fit each subject's schedule, all experiments were conducted at the same time each day. FS, for example, commented that her tremor was worse in the morning than in the afternoon, and was attenuated after a glass of wine.

Hence, stanardization of this experimental procedure with each subject is important to avoid any obvious variations in levels of tremor experienced during daily activities.

Prior to conducting the experiments, a thermo-plastic cuff was fitted to each subject's forearm. In so doing, the forearm was positioned on a flat surface in oriented to match the its position in the TLD.

During each trial, the subject sat upright in a wheelchair or comfortable arm chair. The plywood TLD foundation with the TLD attached was fastened to the arms of the chair. With the subject seated a comfortable distance away from the oscilloscope (usually 4 to 5 feet), the subject's forearm was placed in the restraint and his hand fastened to the handle.

During the trials, two horizontal lines appeared on the oscilloscope screen in fornt of the subject. Each line was only as long as half of the screen width. The target line oscillated up and down sinusoidally while the other line was controlled by the position of the subject's hand. The subject's task was to keep the two lines aligned.

A sinusoidal tracking task was selected since it requires direction reversals as well as constant control of hand position. The sinusoidal tracking task represents a realistic task since direction reversals and limb position control are encountered in daily living activities. Also, direction reversals are known to aggrivate intention tremor. Thus the results of these trials would provide an accurate assessment of the clinical utility of this approach to tremor management.

Four experimental parameters could be varied during the trials. These parameters are, in order of increasing importance:

Display gain - The relationship between the angle of deflection of the hand and the trace displacement on the screen.

Target amplitude on the screen

Target frequency

Damping constant

Each parameter value used in the trials was assigned a single digit code number. These code numbers were then listed in the above order and the resulting four digit number could be used to identify a specific trial for a given subject.

Only the effects of target frequency and damping constant were studied in this work. The display gain, k_{wb} , was set so a 30° deflection of the handle corresponded to a 1.6 division excursion of the response line on the screen. This implies a value of k_{wb} equal to 3.84 and an overall gain of .053 cm excursion/degree of rotation. If k_{wb} equaled 8.69, corresponding to an overall gain of .121 cm/degree, the displacement of the handle along its arc (with a radius of 6.9 cm) would match the displacement of the response line on the screen. This latter value of gain may be interpreted as "normal" gain since there would be a one-to-one correlation between hand movement and line movement.

An overall gain of 0.053cm/degree was used in order to keep the response (including largeamplitude tremor peaks) on the display at all times while providing a tracking task that was comfortable and of reasonable amplitude. This

precedent was established for subject JF since his abnormal movements were large in amplitude. It remained unchanged throughout the remainder of trials documented herein. The target amplitude was maintained at a constant ± 1.5 divisions requiring $\pm 28^\circ$ of movement at the wrist.

For each subject several series of trials were conducted. In any given series, the display gain, target amplitude, and target frequency were held constant. The damping constant, adjusted through D, was changed for each trial within a series. This was done in a random fashion to minimize any trend recognition by the subject. Each series began and ended with a trial with zero damping.

During each trial, the target, response, and torque voltages were recorded on a 4 channel FM tape recorder. The input ranges for each of the channels, channel assignments, tape speed, date, and subject identification were verbally recorded on the tape prior to each series. Any appropriate information such as changes in input ranges, D values, tape counter reading, and subject comments were also recorded on the tape as well as in a lab notebook. It was especially important to record input range, D, and tape counter since these parameters are necessary for proper scaling of the data and for efficient data processing. Flutter compensation was used at all times to reduce tape noise resulting from fluctuations in tape speed. Levels of tape noise for a tape speed of 1 7/8 inches per second were reduced from 120 mV RMS to 25 mV RMS at 10 to 20 Hz through the use of flutter compensation. The

The sensitivity of the oscilloscope was set at 1.0 volts/division and remained fixed throughout these experiments.

The duration of each trial was long enough to include a minimum of 20 cycles of tracking. This was sufficient for the signal averaging program discussed in the next section. It is recommended that all future trials be run for the same amount of time, in addition to obtaining a minimum number of cycles since equal lengths of records facilitates spectral analysis of the data. Future tests should last at least 2.0 minutes so enough data can be obtained to produce power spectra with reasonable confidence limits. For example, if a record is divided into 15 overlapping segments of 512 samples each, a 102.4 second sample would be required, assuming the sampling frequency was 40 Hz. The power spectra for each segment could then be calculated and averaged with the spectra for the other segments. The resulting estimated average power spectra would have a confidence limit of 3 db at a 90% confidence level.¹⁵ In other words, by averaging 15 segments, you could be 90% sure that the resulting values were within 3 db of the actual spectral value you would obtain if you had an unlimited number of segments. Doubling the record length (increasing it to 204.8 seconds) would improve these limits. However, the cost of doing this in terms of computing time and the subject's attention span may render this approach impractical.

3.4 Data Analysis

Three effects of the viscous damping approach were

analyzed in this study. These included the effect on the intended response, the effect on the abnormal movement, and the effect on the frequency content of the subject's response. The procedures used to extract this information from the recorded analog signals are presented here.

3.4.1 Evaluating Intended Response

It is important to investigate the influence of viscous damping on the intended response. It is hypothesized that the additional damping introduced by the TLD will suppress the AIM while not significantly attenuating the intended response. If the TLD does suppress the intended response, then the utility of this approach to tremor management is open to question.

The gain and phase of the intended response relative to the target had to be determined in order to assess the impact of the TLD. To make this comparison, an average response was obtained by ensemble averaging a subject's response over a large number of tracking cycles. Only those components of the response which had a fixed temporal relationship with the target would remain after this averaging. Ideally, if many tracking cycles were available all tremor components of the response randomly related to the target would be averaged out. However, only a limited number of cycles were available for tracking and as a result not all of these random components could be averaged out.

Hence, to assist the process of averaging, the analog

response signal was low-pass filtered prior to averaging. This nearly eliminates all of the tremor components while the presumably lower frequency intended motion would be passed with much less attenuation. The target signal was filtered in an identical manner in order to maintain the original phase relationship between the target and response signals. An eighth order Butterworth filter (Krohnkite Filter Model 3343) with a corner frequency of 2.0 Hz was used for filtering both signals. This corner frequency was used since the frequency hand tremor, both normal and pathological, is in the 3 to 12 Hz range, and because the tracking frequencies used in these experiments were at or below $3/4$ Hz.

The subject's average response may have contained harmonics above the 2.0 Hz cut off frequency if the response was distinctly non-sinusoidal. These harmonics could have been attenuated by filtering since it is impossible to differentiate them from oscillatory components of tremor at the same frequency. To determine the upper limit of the frequency content of the intended response, the filter corner frequency was moved progressively up. Eventually a corner frequency was reached where the ensemble averaged response did not change shape when the corner frequency was raised further. For the two abnormal subjects tested, shifting the corner frequency above 2.0 Hz did not noticeably alter the ensemble averaged response providing there were at least 15 cycles available for averaging. Figure 3-1 is a Polaroid photograph of an

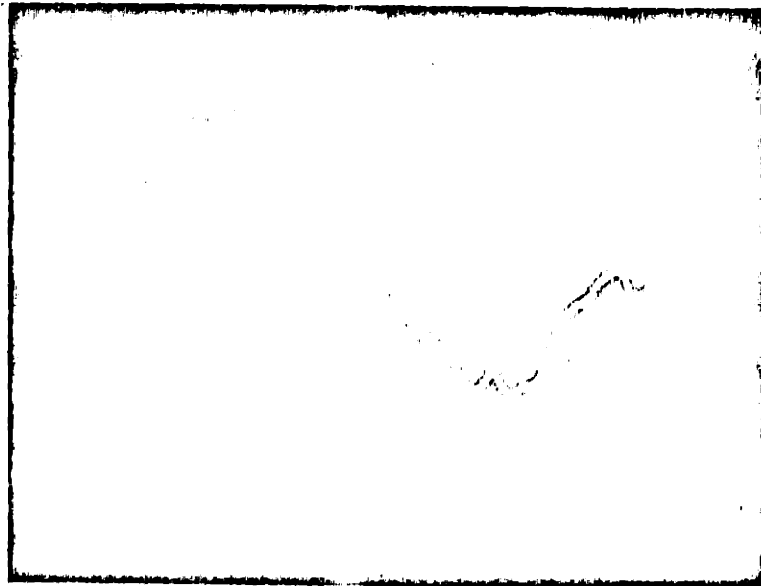


Figure 3-1 Unfiltered Ensemble Averaged
Response Target Frequency = $1/4$
Hz $D = 0$

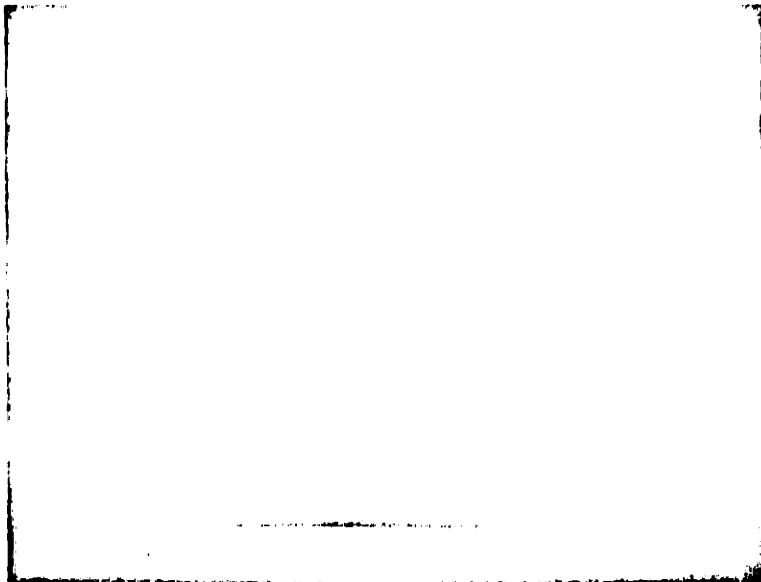


Figure 3-2 Filtered Ensemble Averaged response
Target Frequency = $1/4$ Hz $D = 0$
Corner Frequency = 2.0 Hz

unfiltered ensemble averaged response for subject JF where the target frequency was 1/4 Hz. Figure 3-2 shows the same ensemble averaged response but filtered at 2.0 Hz prior to averaging.

After filtering, the response signal was sampled at 25.0 Hz over at least 15 cycles. Each cycle was averaged with the rest to extract an average response. This averaging was accomplished using a BASIC signal averaging program developed by Drs. M.J.Rosen and D.Rowell and run on the Digital Equipment Corporation PDP8e computer available at the Rehabilitation Engineering Center. This program is listed in Appendix II - "COMPUTER PROGRAMS". The filtered target signal was also sampled at the same rate to provide an equal number of points for comparison. The sampled target signal, T, and the ensemble averaged response, \bar{R} , were stored on a Floppy disc for future processing.

For each trial, an \bar{R}/T amplitude ratio was calculated and normalized with respect to the $D = 0$ amplitude ratio for that series. Phase relationships were determined from the times of the respective peaks. These normalized amplitude ratios and phase relationships are plotted and discussed in Chapter 4.

3.4.2 Evaluating Abnormal Movement

The relationship between the amplitude of the abnormal component of motion and the damping applied is of primary importance in assessing the impact of the external damping element. This relationship is an objective measure of the

validity of the proposed hypothesis.

A measure of the abnormal motion was obtained by band pass filtering an error signal (target minus response), ensemble averaging that filtered response, then computing the RMS of the ensemble average. The set up used for this analog data processing is shown in Figure 3-3. To accomplish this, an analog error signal was computed by subtracting the response signal, P, from the target signal, T. This error signal was band pass filtered between 2.0 and 20.0 Hz using the same eighth order Butterworth filter mentioned in section 3.4.1 (two cascaded filters enabled signals to be band passed). This filtering eliminated 1 kHz tape hiss and any 60 cycle noise on the analog signals in addition to any portion of the intended response due to lags in the subject's response. The error signal was then gain adjusted and squared to obtain an all-positive signal. This squared error signal was then ensemble averaged over 15 cycles of tracking sampling at 100 Hertz. The mean of the averaged signal was then computed using the "MEAN" routine of the program. The mean value obtained was then scaled down according to the gains used in the processing, and the square root of that value was computed. This resulted in RMS (Root Mean Square) measure of the tremor in the subject's response. The RMS Tremor values for each subject were plotted against D. These plots are shown in Chapter 4.

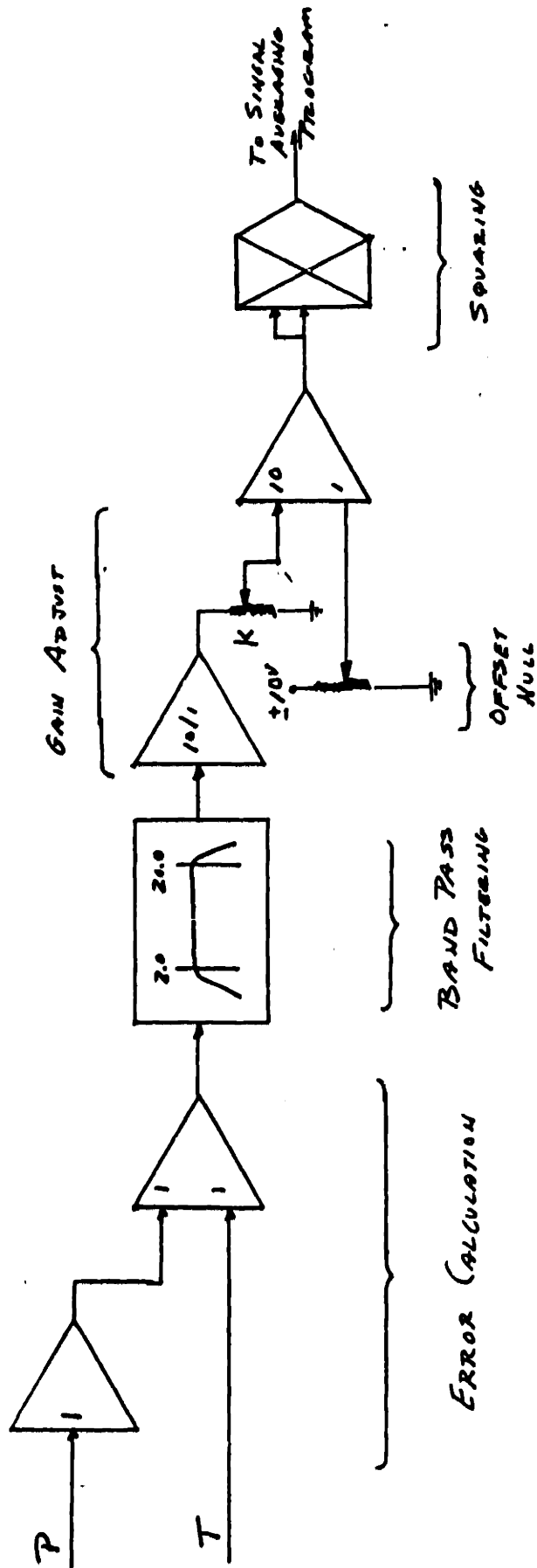


Figure 3-3 Analog Data Processing Setup For Determining Tremor

3.4.3 Spectral Analysis of Responses

Spectral analysis work done by Stiles et al has helped to identify the frequency content of normal and parkinsonian hand tremor. These researchers have used these procedures to quantitatively assess the impact of added mass, for example, on the amplitude and frequency content of hand tremor. It is obvious from Stile's work that spectral analysis capabilities can be a valuable asset to this kind of research. Consequently, a spectral analysis program was written and implemented on the Joint ME/CE Computing Facilities Interdata MBO computer. This program will be helpful in assessing the impact of the TLD with its viscous damping on the frequency content of hand tremor.

In computing the power spectra of the subject's responses, it was assumed that their AIM was random and stationary. The approach used in the developed program was to sample a time record and divide this record into a number of discrete segments of equal length. The DFT (Discrete Fourier Transform) for each segment was computed, squared, averaged with the other segments and then scaled to give an estimate of the actual power spectra.¹⁵ The flow chart, listing, and operating instructions for the program are found in Appendix II - "COMPUTER PROGRAMS".

Prior to sampling, the analog response signal, R , was band pass filtered between 2.0 and 20.0 Hz. This eliminated any DC component of the response, any response components

related to the target (i.e. intended response), and any high frequency noise existing on the recorded analog signals. The output of the filter (two cascaded eighth order Butterworth filters) was then patched to an A/D (analog to digital) converter.

The analog signal was effectively sampled at 50.0 Hz to prevent aliasing in the computed DFT. (To expedite the sampling process, the tape recorder was actually played back at twice the original recording speed of 1 7/8 inches per second. At the same time, the filter frequencies were doubled to 4.0 and 40.0 Hz as was the sampling rate doubled to 100.0 Hz resulting in a real time sampling rate of 50.0 Hz.) 4096 samples of the analog signal were taken resulting in a sampling time of 82 seconds. The 4096 sample record was divided into seven overlapping segments of 1024 samples each. Hence each segment is approximately 20 seconds long resulting in the power spectral estimates having bandwidths of 0.05 Hz.

In this method of power spectral estimation, the confidence limits for the estimates are a function of the number of discrete segments averaged together. In this case, seven segments were used so the spectral estimate for a given frequency band will with a probability of 0.9 fall within a 6 db interval around the actual spectral value for that frequency band. The units of the power spectral estimates generated by this program were $(\text{volts})^2/\text{bandwidth}$. The volts here represent the

output of the position sensing potentiometer. By gain adjusting the digitized record in the software prior to computing the DFT, the units could be in (degrees)²/bandwidth. The estimates for each segment were smoothed by impressing a Hanning data window over each digitized segment. This window minimizes leakage effects when calculating the DFT of the segment.

Two slight modifications to the methods used in this power spectra estimating would help to further refine the results. The output of the Tandberg FM tape recorder ranges between ± 5.0 Volts DC. The dynamic range of the A/D converters used on the analog computer is ± 10.0 volts DC. Hence, only 50 % of the dynamic range of the A/Dconverters could be utilized. In future runs, it would be worthwhile to gain adjust the filtered output to utilize a greater portion of the dynamic range of the converters. This could be easily implemented through the use of the operational amplifiers available on the analog computer. Secondly, a larger number of samples should be taken to help improve the confidence limits on the spectral estimates. Only additional blocks of 1024 samples are needed, the number added depending on the confidence limits desired and the capabilities of the subjects to track for longer periods.

CHAPTER 4

RESULTS4.1 Introduction

After all is said and done, the significance of this thesis rests in the results of the experiments conducted using the equipment and procedures discussed in the previous chapters. Does the TLD with its viscous damping filter out the AIM while allowing the intended response to pass unattenuated? The answer to this and other questions are presented in the following chapter, fortunately in a positive sense. First, the effect of viscous damping on the magnitude and phase of the intended response and the magnitude of the abnormal movements is reviewed for the two subjects with intention tremor. Following this, the frequency content of JF's response is presented to show the usefulness of the spectral analysis program.

4.2 Intended Responses

Using the techniques described in 3.4.1, a plot of the normalized average intended response amplitude ratio \bar{R}/T versus the damping pot setting was developed for each of the subjects tested. These plots are shown in Figures 4-1, 2, and 3. Again, these plots show the ratio of the amplitude of the subject's ensemble averaged response, \bar{R} , to the target amplitude, T . The closer this ratio is to 1.0 the better the subject is tracking.

For 1/8 and 1/4 Hz target frequencies, both abnormal

Subject JF

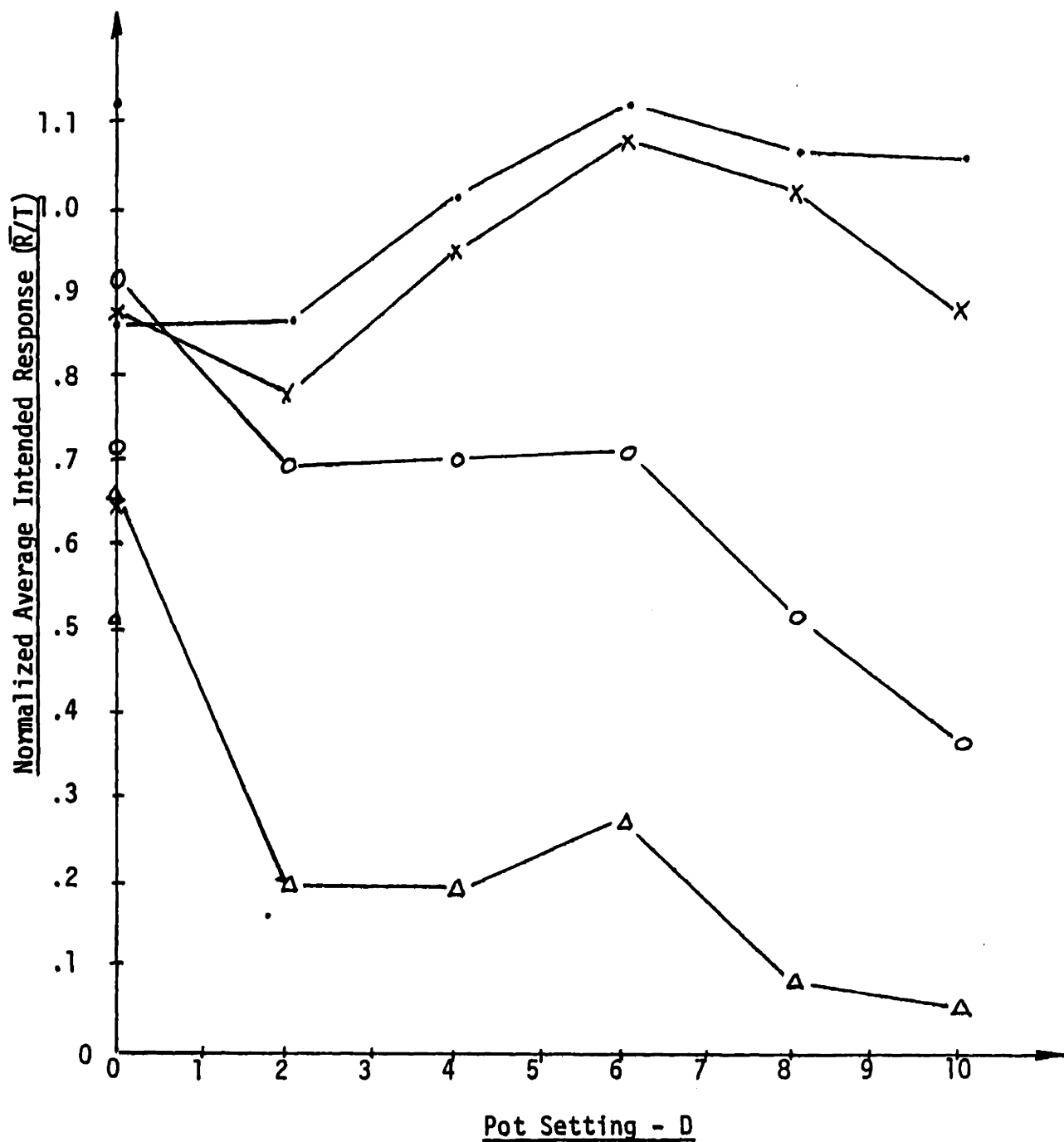


Figure 4-1 Normalized Average Intended Response \bar{R}/T
vs Pot Setting D

Note: \bar{R}/T is plotted for the following Target frequencies;

• 1/8 Hz, x 1/4 Hz, ○ 1/2 Hz, △ 3/4 Hz.

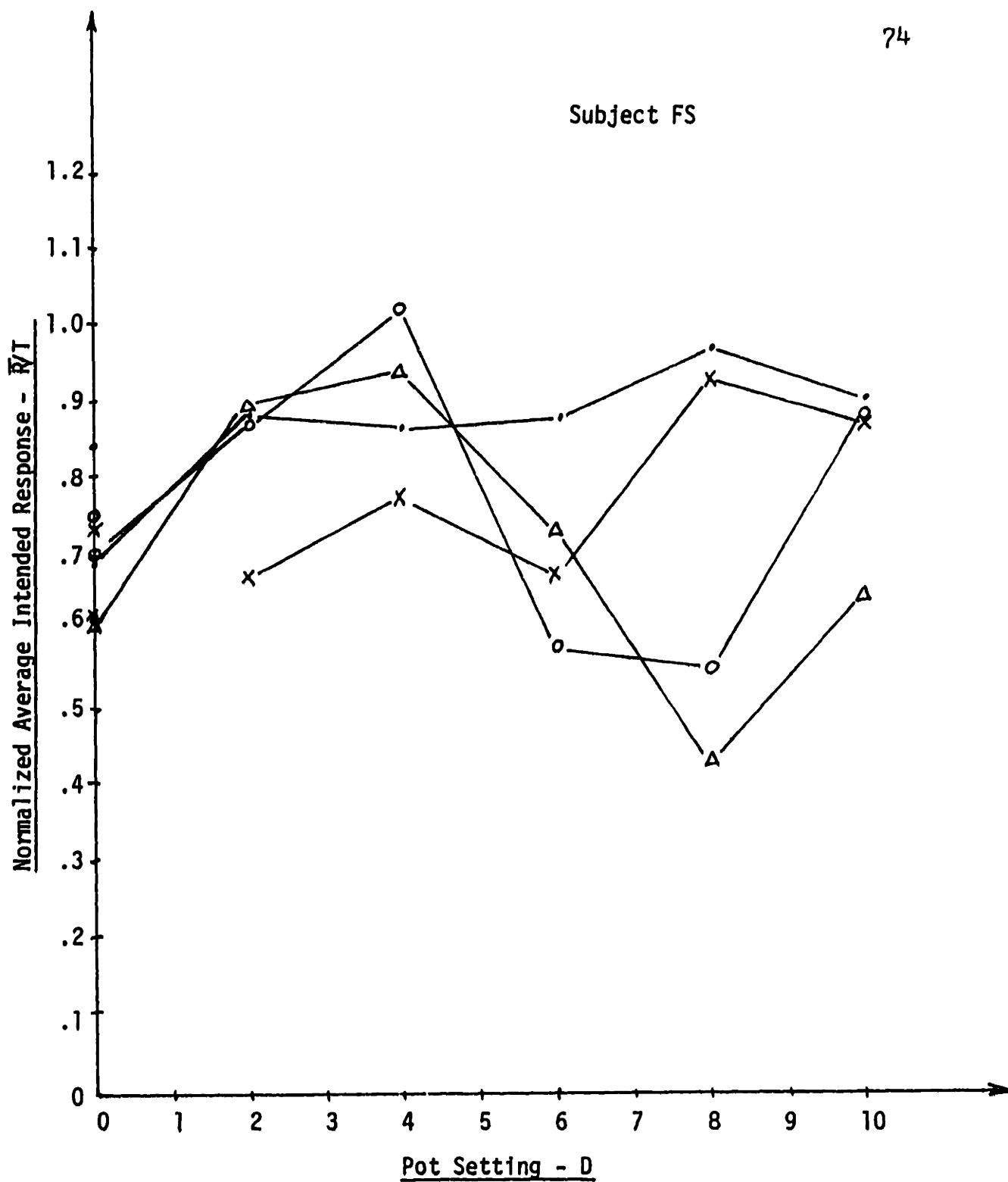


Figure 4-2 Normalized Average Intended Response - \bar{R}/T
vs Pot Setting - D

Note: \bar{R}/T is plotted for the following target frequencies;
• 1/8 Hz, x 1/4 Hz, ○ 1/2 Hz, Δ 3/4 Hz.

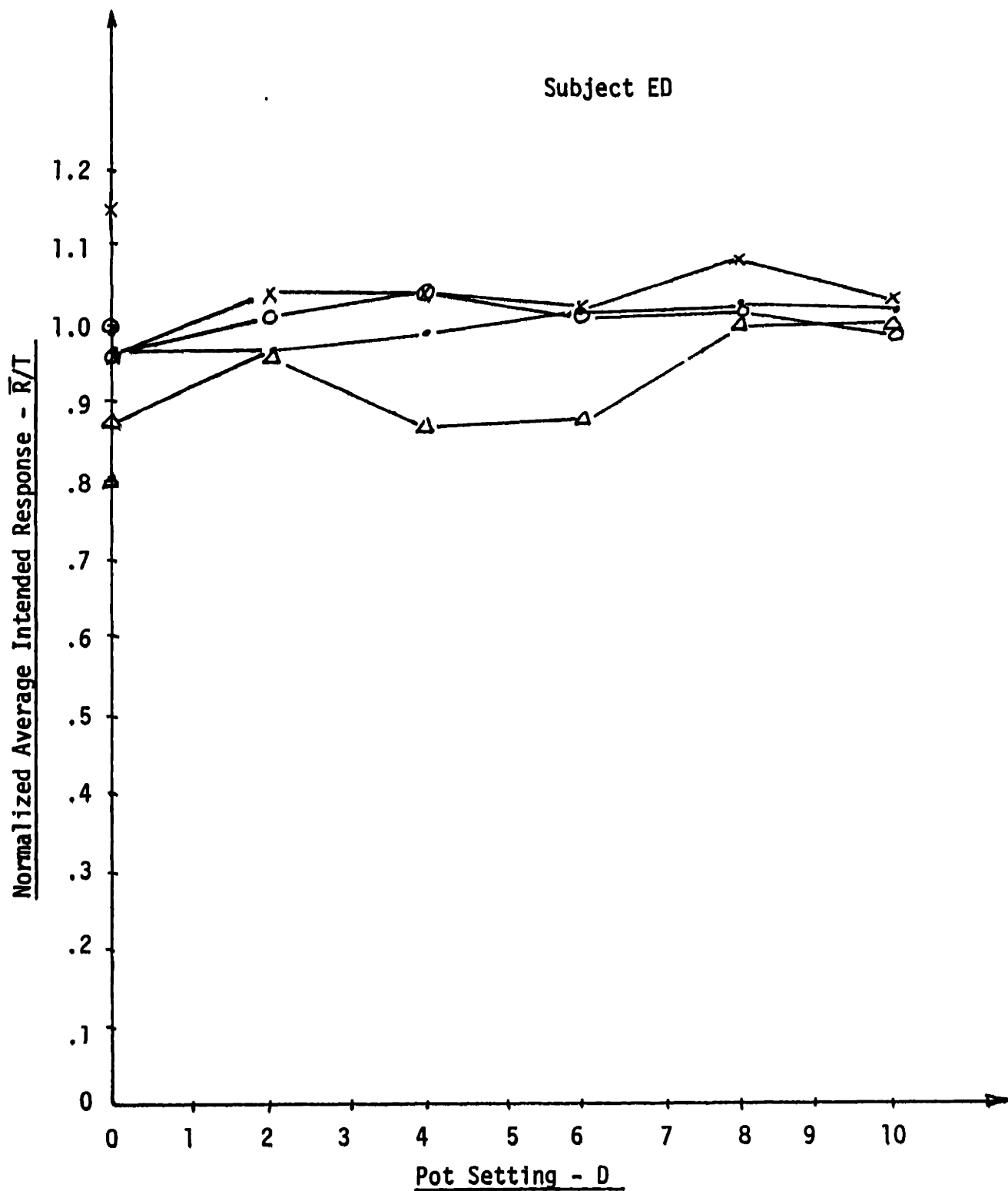


Figure 4-3 Normalized Average Intended Response - \bar{R}/T
vs Pot Setting - D

Note: \bar{R}/T is plotted for the following target frequencies;
• 1/8 Hz, x 1/4 Hz, ◦ 1/2 Hz, Δ 3/4 Hz.

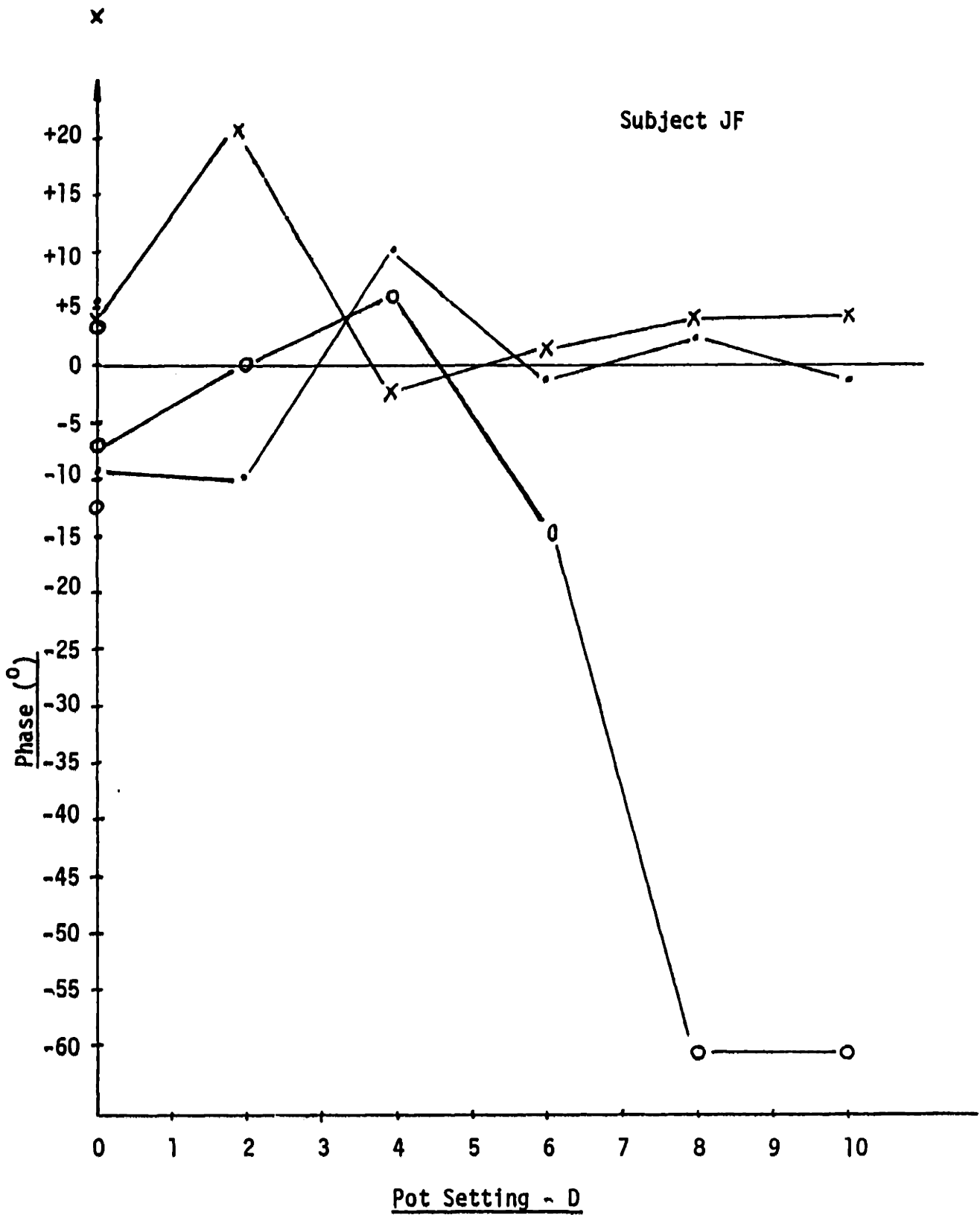


Figure 4-4 Phase Lag or Lead of Intended Response vs Pot Setting - D

Note: Phase is plotted for the following target frequencies;
 • 1/8 Hz, x 1/4 Hz, o 1/2 Hz, Δ 3/4 Hz.

Subject FS

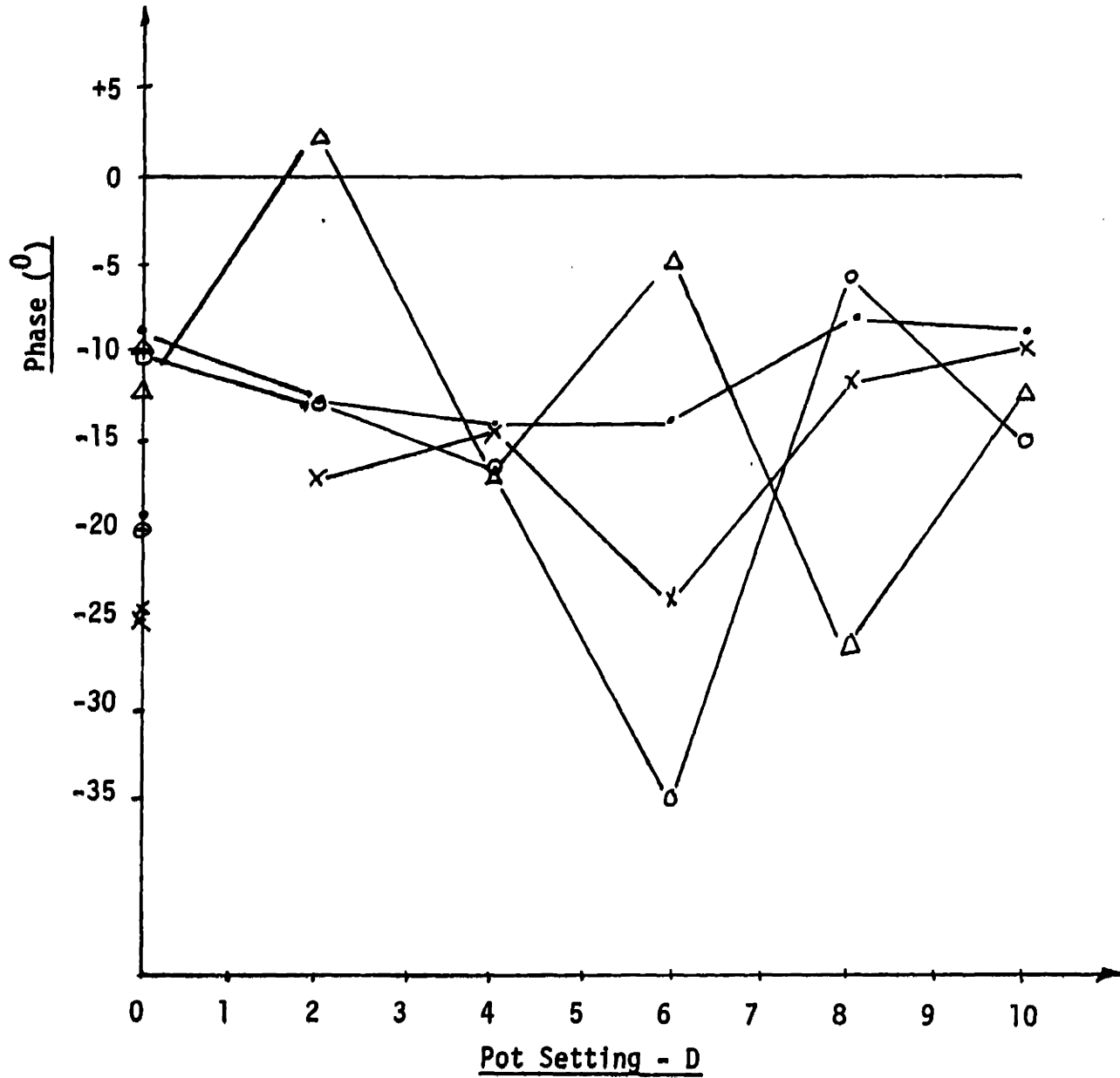


Figure 4-5 Phase of Average Intended Response (\bar{R}) vs Pot Setting -

Note: Phase is plotted for the following target frequencies;
 • 1/8 Hz, × 1/4 Hz, ○ 1/2 Hz, △ 3/4 Hz.

Subject ED

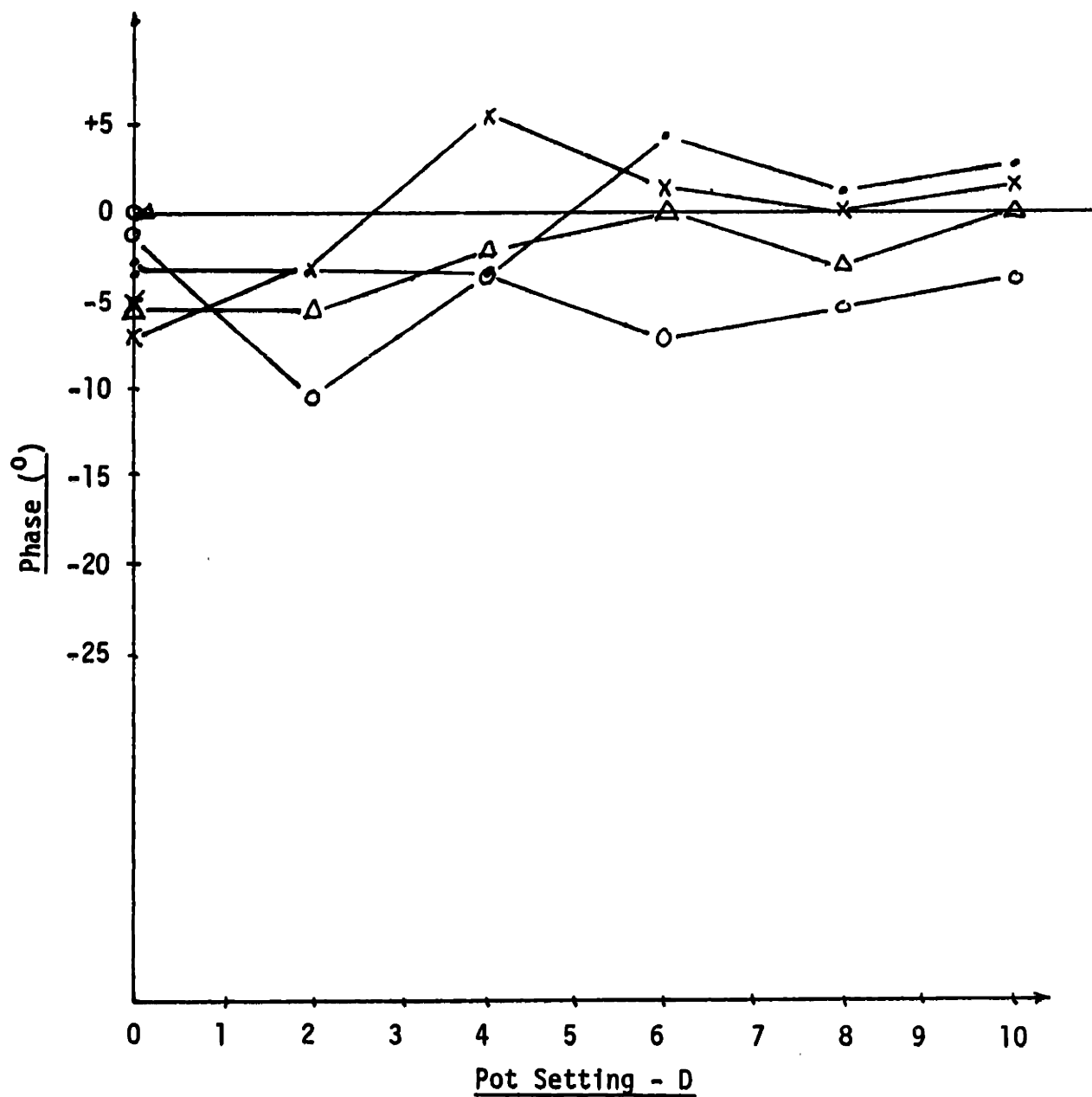


Figure 4-6 Phase of Average Intended Response (\bar{R}) vs Pot Setting -

Note: Phase plotted for the following target frequencies;
 • 1/8 Hz, × 1/4 Hz, ○ 1/2 Hz, △ 3/4 Hz.

subjects JF and FS and the normal ED showed improvements in tracking with increasing values of D. JF improved from an average of .86 to an average of .97 while FS increased her responses from averages of .71 to .88. ED's intended response ratios improved only slightly from .97 to 1.01. These overall improvements in tracking are consistent with the results observed by Rosen and Gesink.

Increasing the target frequency to $1/2$ and $3/4$ Hz provided increasingly difficult tasks for JF because of the severity of his intention tremor. This increasing difficulty was compounded by the application of damping. As Figure 4-1 shows, JF's average response at these frequencies diminished with increasing damping, indicating that his response was becoming increasingly random. This reflects JF's inability to track the target in a sine-like fashion at these frequencies. His response in these faster trials could be described as a summation of random step-like responses of varying magnitude applied in an attempt to keep up with the target.

At $1/2$ and $3/4$ Hz, FS's tracking improved when low levels of damping ($D = 2$ and 4) were applied. Higher levels of damping did not effect her response in a consistent manner. ED's response at these frequencies did not appear to have been significantly effected by the addition of damping.

All of these plots show two points for $D = 0$. Those points connected to the rest of the data points for that series represent the first trial in that series. The second point represents the $D = 0$ trial that was run at the end of each

series. No statistically significant trend relating the initial $D = 0$ trial to the final $D = 0$ trial could be found.

It is also important to know the phase of the subjects' responses relative to the target. At the 1/8 and 1/4 Hz target frequencies with $D = 6$ or better, damping appeared to stabilize the phase of JF's responses. The result was a decrease in the range of the phase lag of his responses from between -10° (lag) and $+20^\circ$ (lead) to between -1° and $+3^\circ$. In all series except the 3/4 Hz series, JF's phase in the final $D = 0$ trial was ahead of his initial $D = 0$ trial by 10 to 30° .

Damping did not seem to consistently modify the phase of FS's responses as seen in Figure 4-5. FS seemed to lag an average of -15° behind the target in the majority of her trials. In ED's trials, an initial lag of -5° was reduced to zero through the application of damping.

4.3 Tremor Attenuation

It is most interesting to review the reduction in RMS tremor brought about by the application of viscous damping. Figures 4-7, 8, and 9 show the tremor attenuation resulting from damping. With JF, the higher values of D in the 1/2 and 3/4 Hz trial are shown in figure 4-7 even though his response in these trials was so random that no meaningful intended response existed.

The reductions in levels of RMS tremor are quite pronounced in the case of JF. In all four of his series, JF's RMS tremor

Subject JF

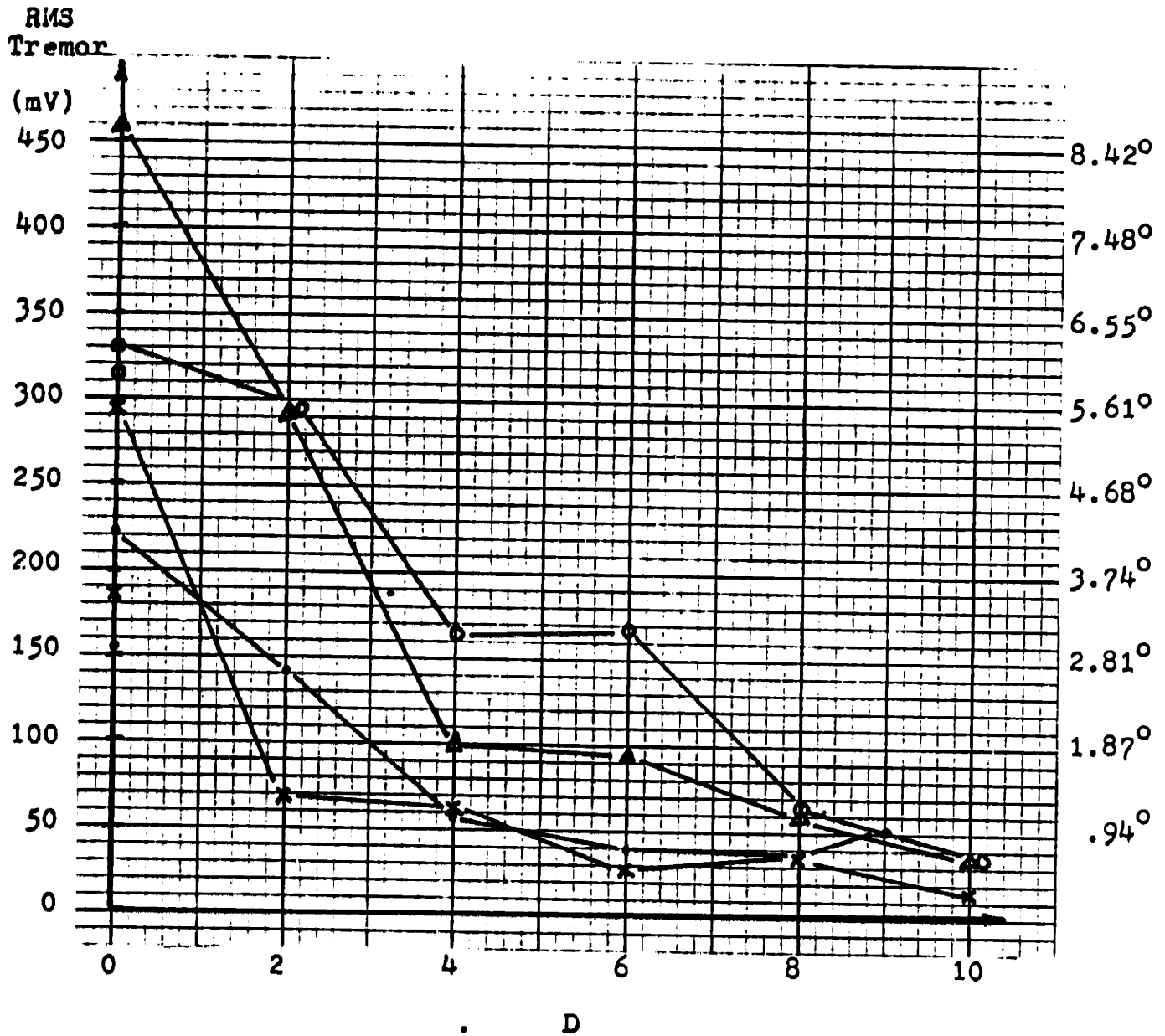


Figure 4-7 Rms Tremor vs Pot Setting, D

• 1/8 Hz, x 1/4 Hz, ○ 1/2 Hz, ▲ 3/4 Hz

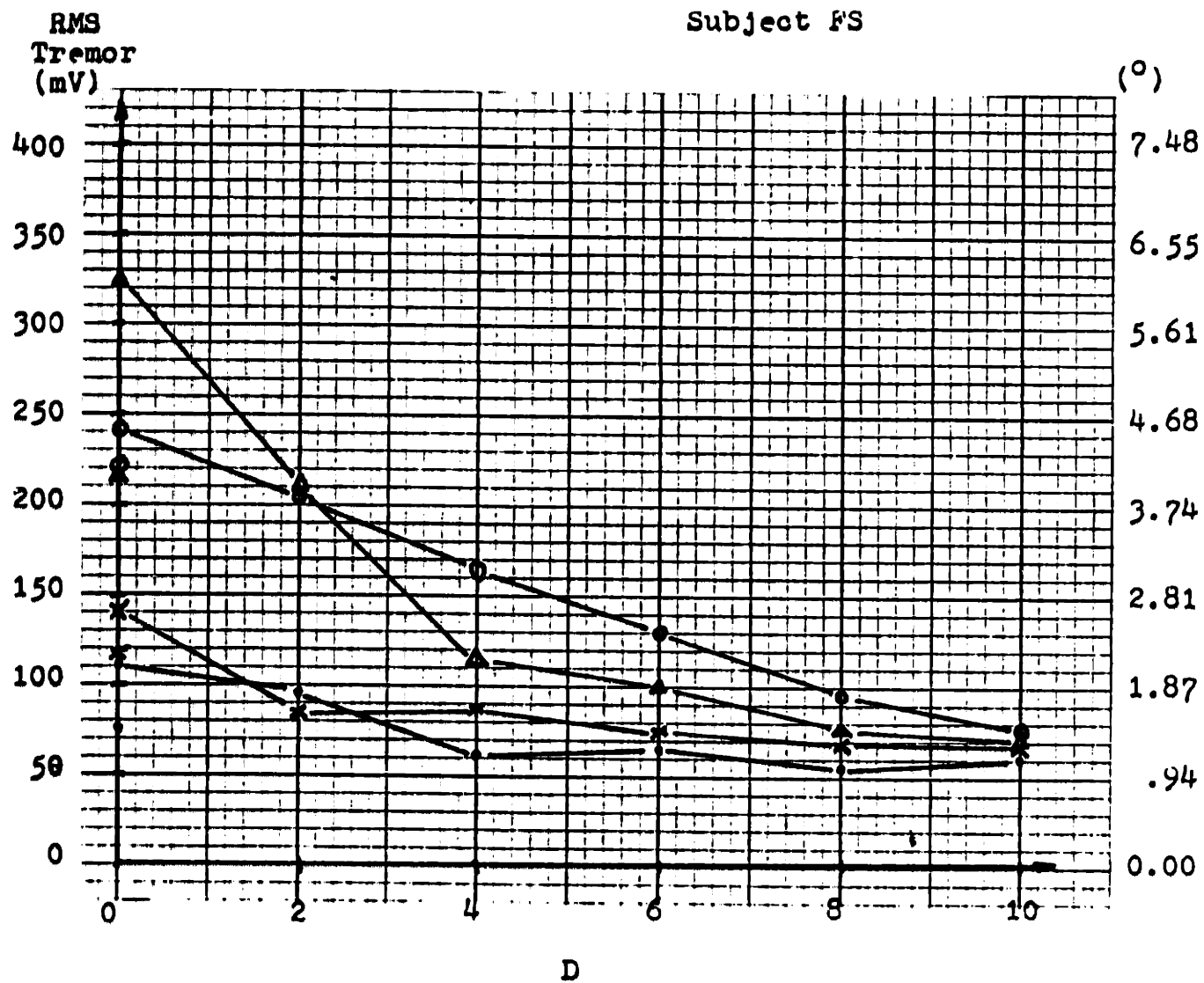


Figure 4-8 RMS Tremor vs Pot Setting, D

• 1/8 Hz, * 1/4 Hz, ○ 1/2 Hz, △ 3/4 Hz

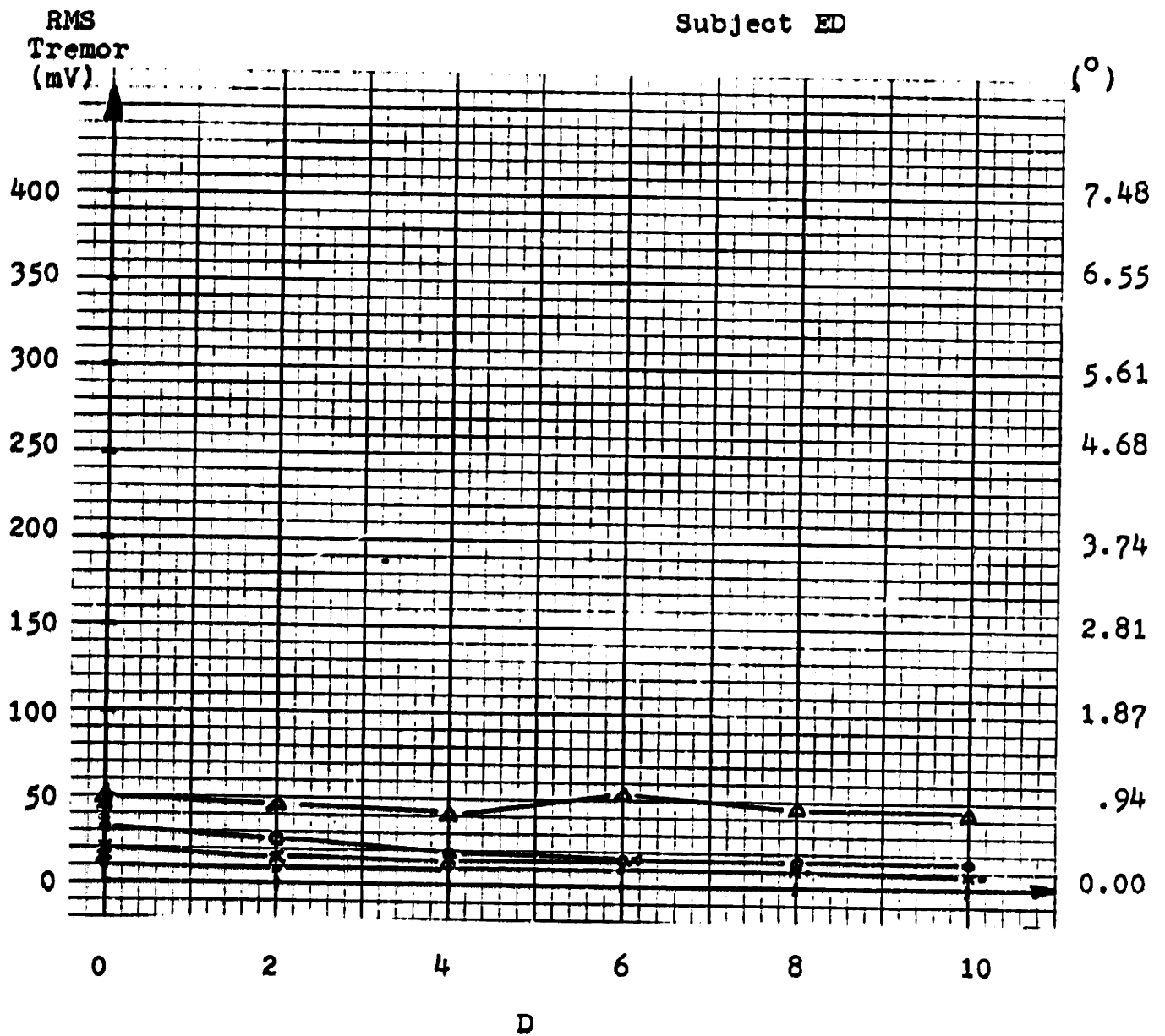


Figure 4-9 RMS Tremor vs Pot Setting, D

• 1/8 Hz, * 1/4 Hz, ○ 1/2 Hz, △ 3/4 Hz

was reduced by a factor of 10 when the maximum level of damping was applied. In the undamped trials, JF's RMS tremor ranged between 4.2° and 8.4° , increasing in this range as the target frequency increased from $1/8$ to $3/4$ Hz. With maximum damping, his RMS tremor ranged between $.28^{\circ}$ and $.94^{\circ}$. This corresponds closely to the $.15^{\circ}$ to $.80^{\circ}$ tremor observed in the normal. The greatest percentage reductions in tremor were brought about with the first two applications of damping. With $D = 2$ reductions of 12 to 77% were observed while with $D = 4$, reductions of 50 to 79% were observed.

The reductions in RMS tremor was not quite as dramatic for FS, particularly in the $1/8$ and $1/4$ Hz series. In these series, her tremor was reduced only by a factor of 2.0 from typical values of 2.1° to 1.15° . In the $1/2$ and $3/4$ Hz trials the reduction was somewhat greater. At $1/2$ Hz, FS's tremor was reduced from 4.1° with $D = 0$ to 1.4° with $D = 10$ in nearly a straight line reduction. At $3/4$ Hz, her tremor was reduced from 6.1° with $D = 0$ to 1.4° with $D = 10$.

The RMS tremor of the normal ED was decreased only slightly from 0.2° to 0.15° in the $1/8$ Hz series. The most extreme tremor observed with this subject was in the $3/4$ Hz series where it remained close to $.84^{\circ}$, regardless of the damping applied by the TLD.

A paired Student's t test was used to determine the statistical significance of the observed reductions in tremor. The results of this analysis are shown in Table 4-1. Each value of RMS tremor, listed in Table 4-3, was compared to

Table 4-1
Statistical Significance of
 Reduction in Abnormal Population RMS Tremor

<u>D</u>	<u>Significance Level</u>
2	.05
4	.01
6	.01
8	.01
10	.05
0	.Not Significant

Table 4-2
Statistical Significance of
 The Difference in RMS Tremor Between
 Abnormal Subjects With Damping And
 Undamped Normal

<u>D</u>	<u>Significance Level</u>
2	.05
4	.05
6	} .Not Significant
8	
10	.05

Table 4-3

RMS Tremor Data(mV)

<u>Subject</u>	<u>Target Frequency</u>	<u>Value of D</u>						
		<u>0</u>	<u>2</u>	<u>4</u>	<u>6</u>	<u>8</u>	<u>10</u>	<u>0</u>
JF	1/8	221	142	59	42	34	-	154
	1/4	296	68	61	27	37	15	186
	1/2	331	293	163	164	-	-	314
	3/4	-	-	-	-	-	-	-
FS	1/8	112	96	62	65	55	59	75
	1/4	116	83	85	75	69	61	142
	1/2	220	206	165	131	94	76	238
	3/4	327	211	114	98	72	70	213

Statistical Parameters

\bar{B}	74.9	130	146	155	158	43
s	71.1	77.7	82.5	85.6	96.7	59.4
n	7	7	7	6	5	7
$\hat{\sigma}$	76.9	83.9	89.1	93.8	108.1	65
t	2.45	4.1	4.34	4.05	3.27	1.62

$B = \text{RMS Tremor at } D - \text{RMS Tremor at } D = 0 \text{ (initial)}$

$$s^2 = \sum \frac{B^2}{n} - \bar{B}^2$$

$$\hat{\sigma} = s \sqrt{\frac{n}{n-1}}$$

$$t = \frac{\bar{B}\sqrt{n}}{\hat{\sigma}}$$

the value of RMS Tremor for the initial $D = 0$ trial. The reductions observed are significant at better than the levels shown in the table.

With all values of D used in the trials, reductions significant at better than the .05 level were observed, with values of $D = 4, 6, \text{ and } 8$ giving reductions significant at better than the .01 level. In addition, in 6 out of 8 trials reductions in RMS Tremor were recorded in the final $D = 0$ trial of each series. These reductions however, were not significant.

Finally, it is important to know from a clinical utility viewpoint whether or not the reduced levels of tremor existing in the damped abnormal trials are significantly different from the tremor in normals with no damping. If a statistical difference is found then additional clinical evaluation may be required to determine if the damped level of tremor is low enough in displacement to allow the individual to regain the functional usefulness of the afflicted limb.

Table 4-2 shows the statistical significance of the difference in RMS Tremor between the abnormals with damping and the undamped normal. A Student's t test was used to determine if the difference was significant. As the table shows, the difference is significant at the .05 level for values of $D = 2, 4, \text{ and } 10$. For $D = 6 \text{ and } 8$, the difference was not significant. In other words, no significant difference between damped tremor in our abnormals and normal tremor could be demonstrated at $D = 6 \text{ and } 8$.

As a point for comparison, Figure 4-10 shows the difference in undamped RMS Tremor for various target frequencies between the abnormals and the normals. As can be seen, abnormal undamped tremor ranges between 6 and 10 times that of the undamped normal tremor.

4.4 Frequency Content

The spectral analysis program was developed to provide a means of studying the impact of viscous damping on the power spectrum (and hence frequency content) of the subjects' responses. After debugging the program, one series of test data was analyzed to show the capabilities of the program. JF's response for the 1/4 Hz series was selected for this purpose. Chart recordings of his response for $D = 0, 4,$ and 8 are shown in Figure 4-16. The corresponding power spectra are shown in Figures 4-11, 12, and 13 for values of $D = 0, 4,$ and 8 respectively. As can be observed, the total area under these curves decreases with increasing damping. The most dramatic reductions result when going from $D = 0$ to $D = 4$ rather than from $D = 4$ to $D = 8$. This is consistent with the RMS Tremor attenuation evident in Figure 4-7 which shows that most of the tremor reduction occurs with the first two values of D (2 and 4).

Unfortunately, the signals being digitized were rather low level signals, and, as a result, these signals were contaminated by various sources of noise in the processing setup. The frequency content of this noise is shown in

Figure 4-14. This was obtained by holding the handle in a fixed position, taking a record of the unchanging position voltage, then determining the spectra of that record.

If the power spectra of this processing noise is subtracted from the undamped power spectra, as shown in Figure 4-15, two spectral peaks are evident; one at 2.5 Hz and the other at 5.0 Hz. The magnitudes of these peaks, as well as the rest of the spectral values, were reduced through the application of damping. However, no obvious shifts in the frequency of these peaks was observed when damping was applied.

4.5 Discussion

These results demonstrate with statistical significance the ability of the TLD to selectively attenuate involuntary components of our subject's response. This reduction, with the accompanying improvement in tracking, suggests the use of viscous damping will prove to be an effective means of returning function to individuals with intention tremor. Subject JF, for example, found it very frustrating and fatiguing to track with no damping because of the severity of his tremor. At the lower target frequencies however, he noted from time to time the damping enabled him to just "glide along" and gave him "support". It was obvious that he was considerably more relaxed during trials with damping than in those without.

Damping does reduce tremor in these subjects then, and this reduction may be due in part to the more relaxed state of

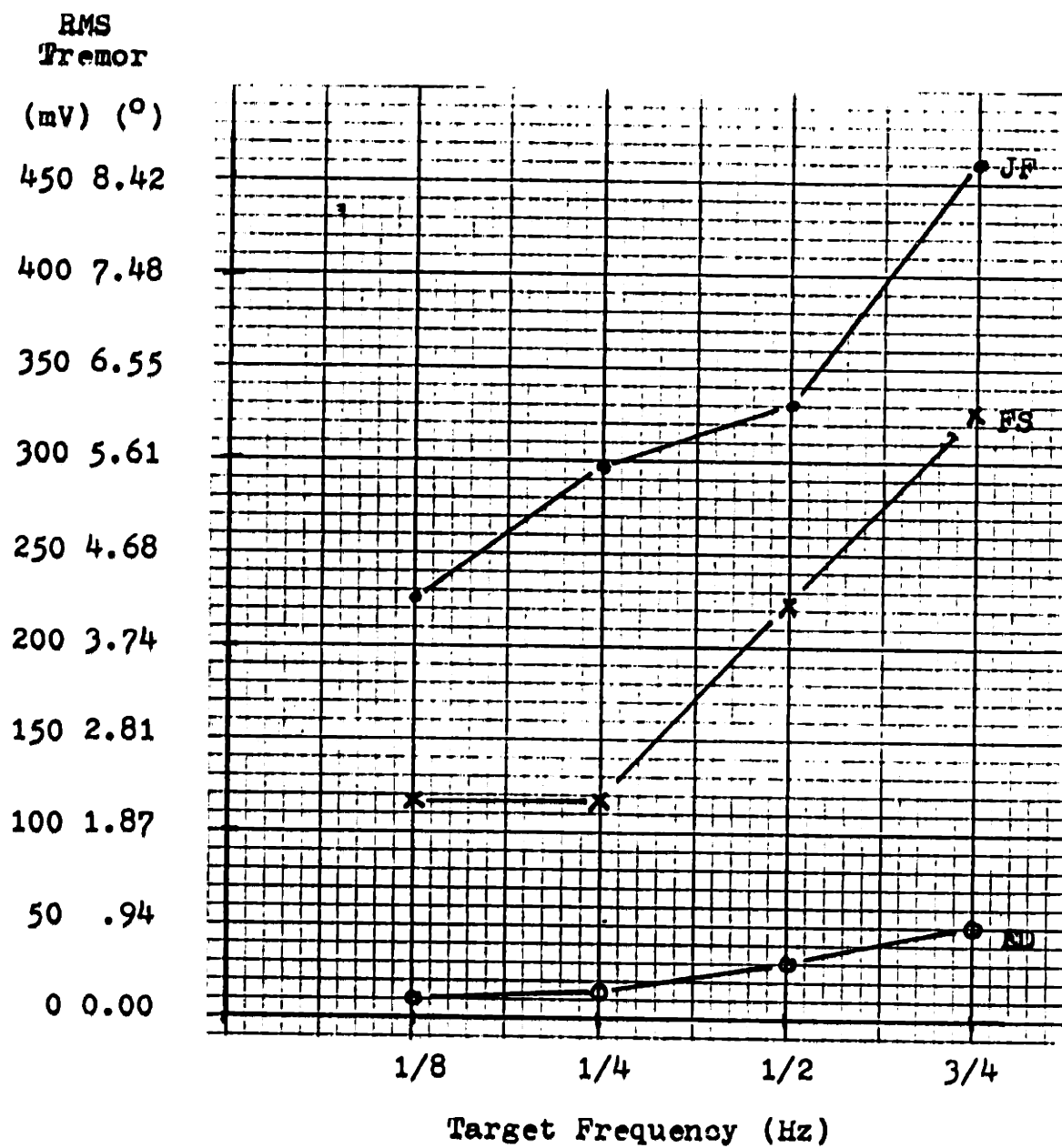


Figure 4-10 RMS Tremor vs Target Frequency for All Subjects Tested With No Damping

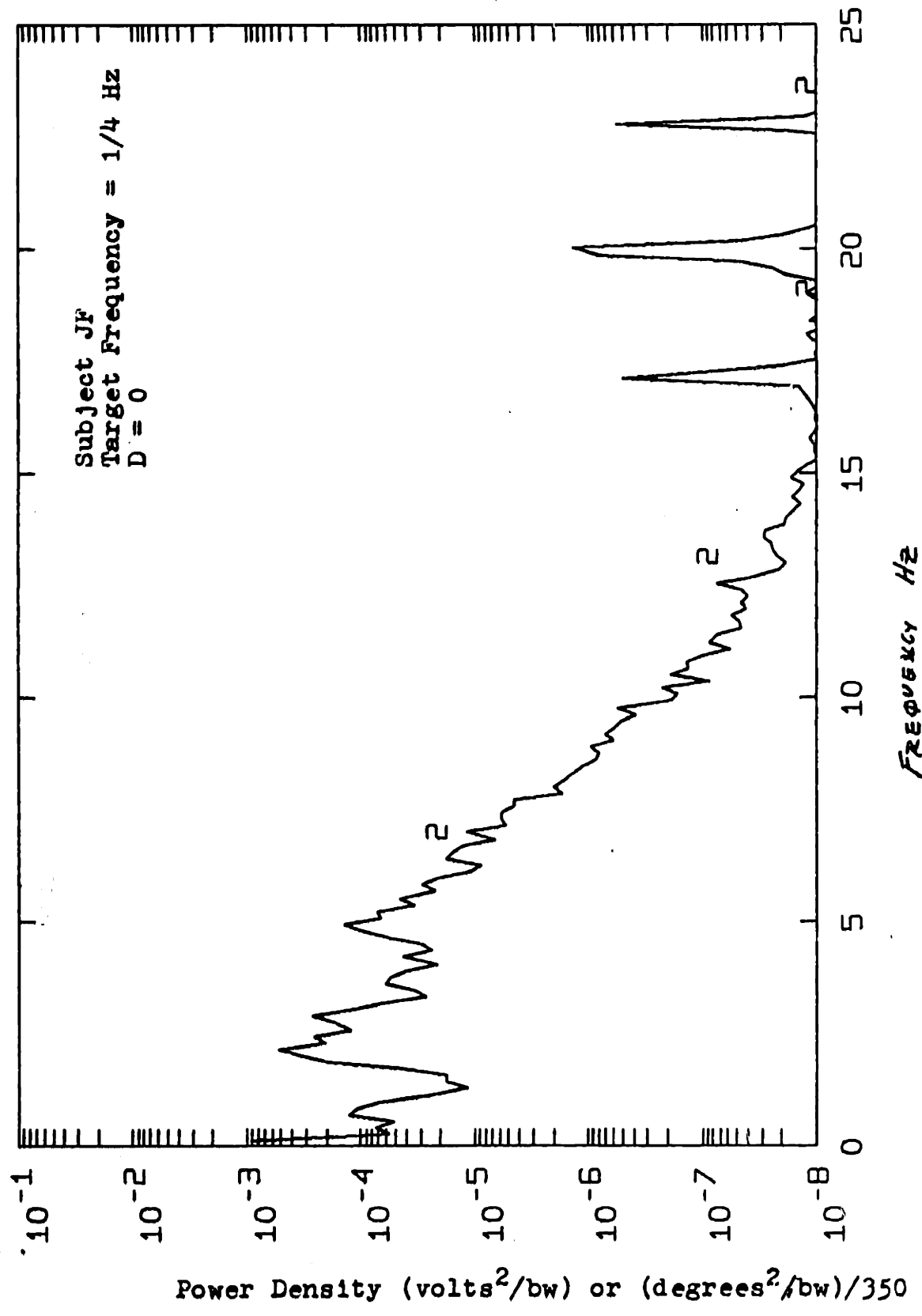


Figure 4-11 Response Power Spectra

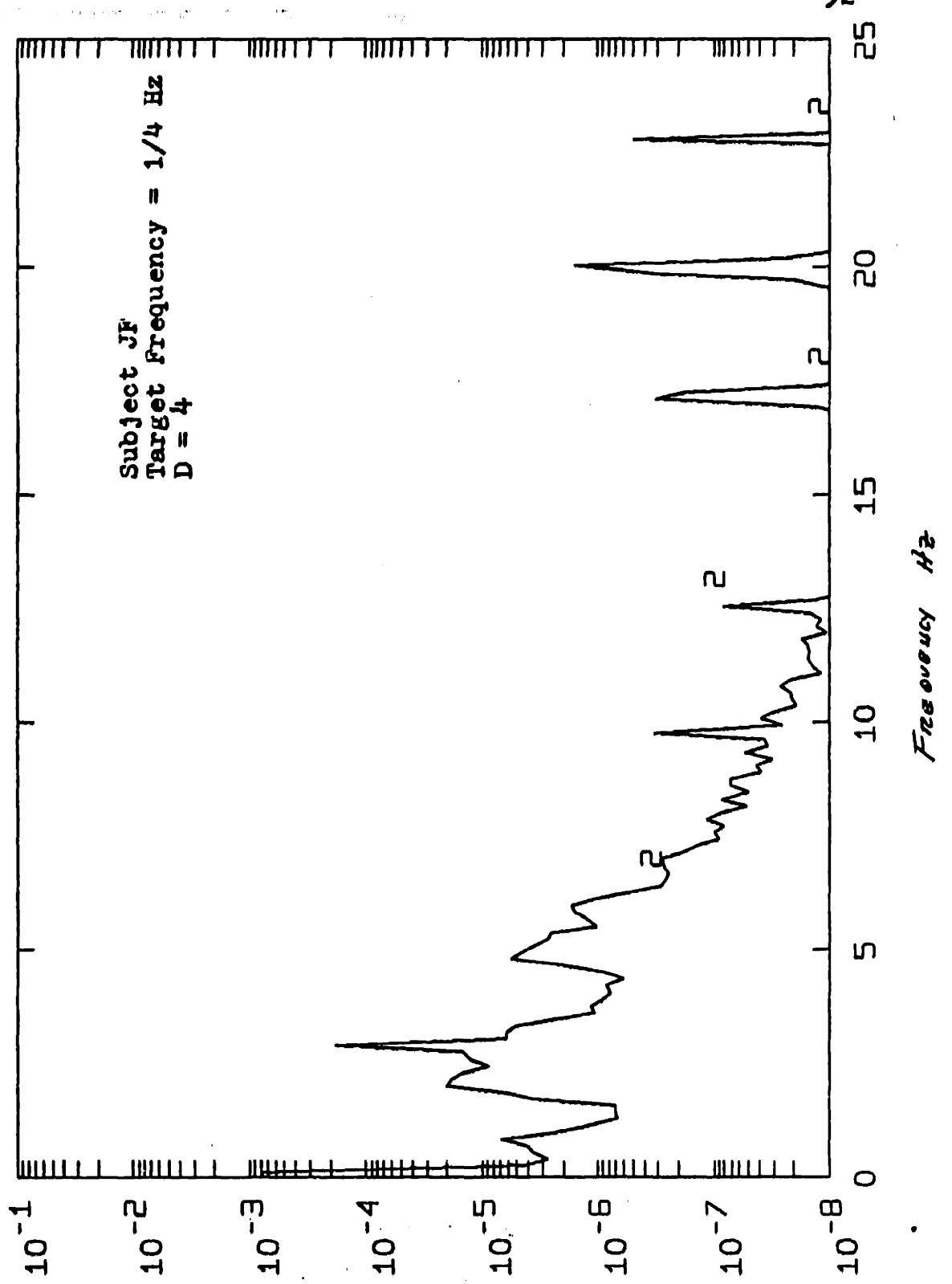


Figure 4-12 Power Spectra of Response

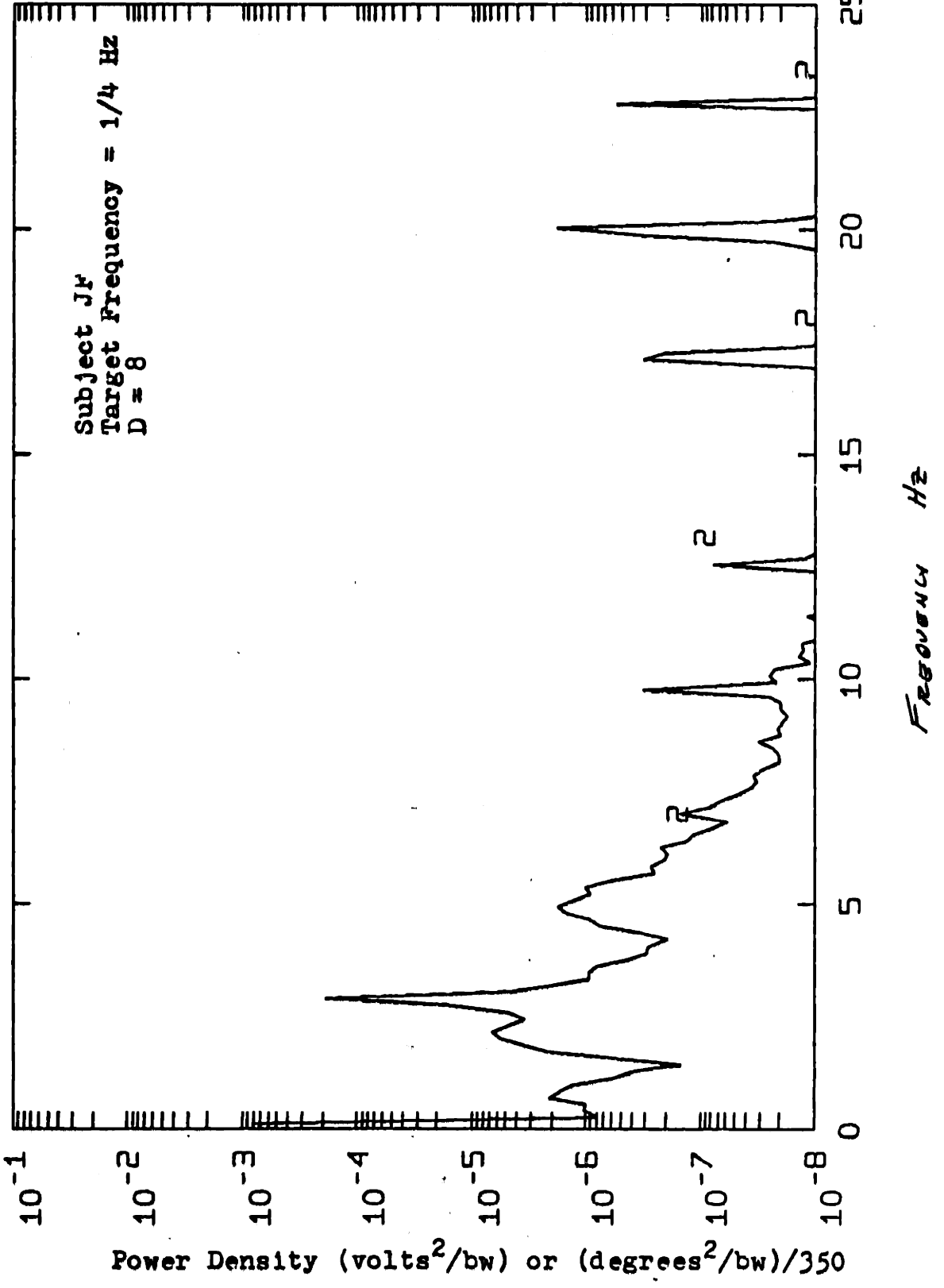


Figure 4-13 Response Power Spectra

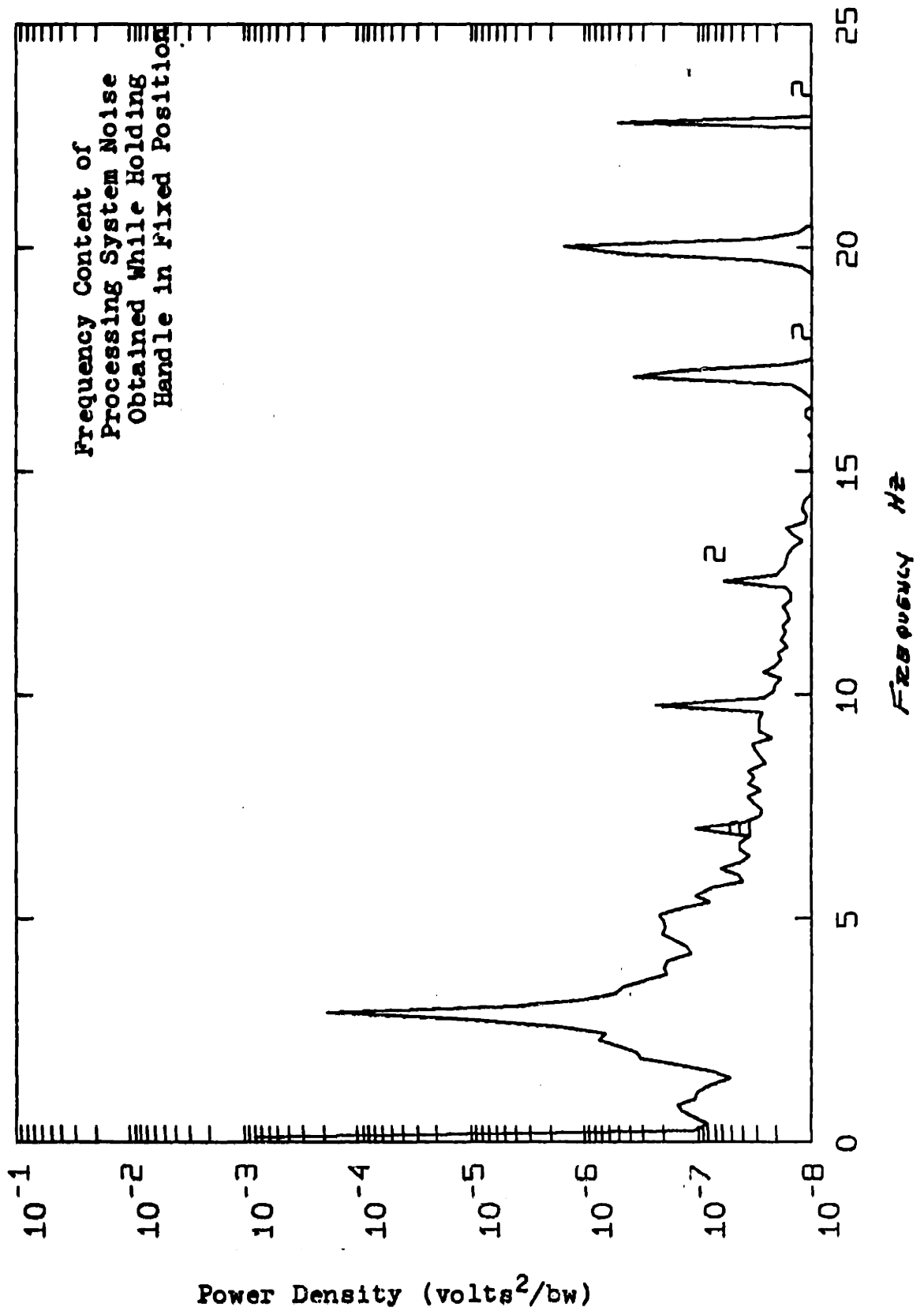
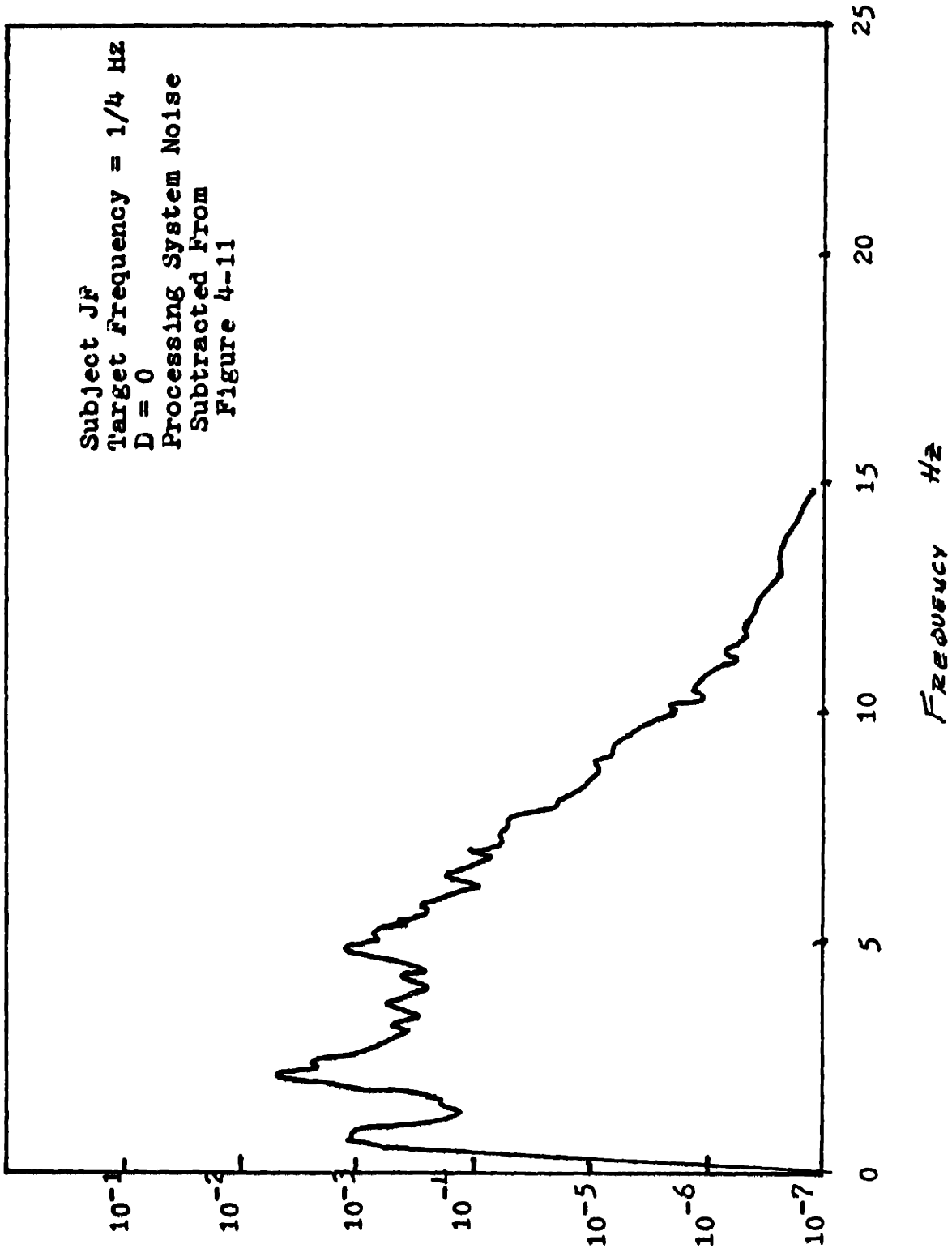


Figure 4-14 Power Spectra of Processing System Noise



Power Density (volts²/bw) or (degrees²/bw)/350

Figure 4-15 Power Spectra of Response Minus Contribution of Processing Noise

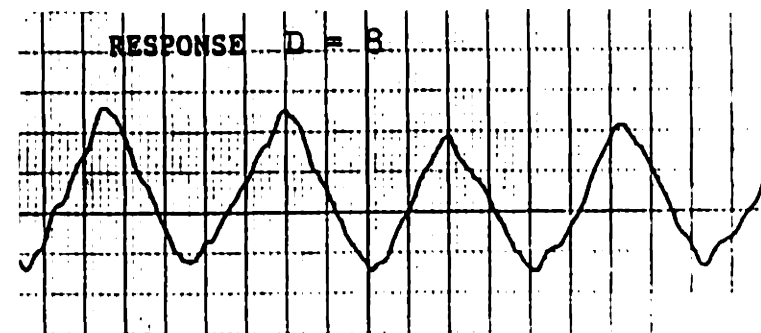
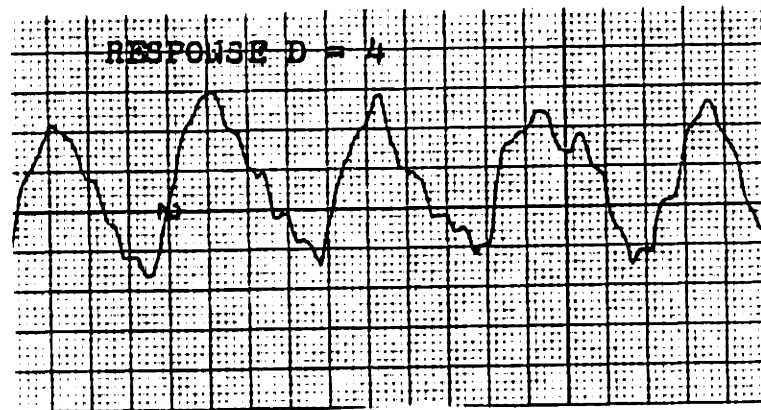
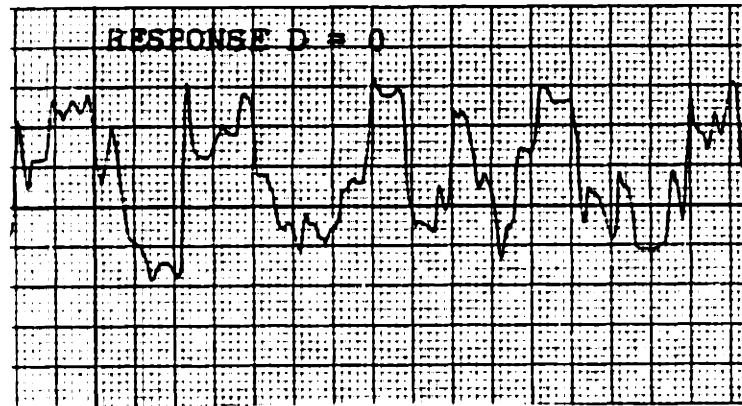
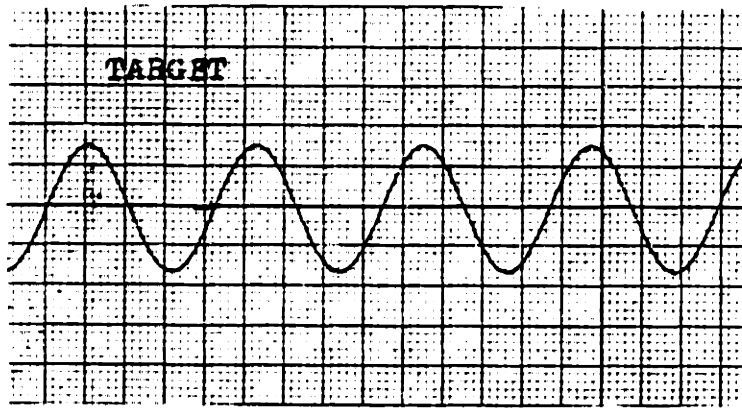


Figure 4-16 Response of Subject JF for Target
Frequency = $1/4$ Hz

mind the subject is in when he or she is tracking well as a result of the attenuation (mechanical or physiological) of their tremor. Hence, the total reduction in tremor may be the sum of the reductions due to the damping effects on the muscle/load system and the improved voluntary hand control resulting from the more relaxed state of mind. It is possible that the reduced tremor observed in the final $D=0$ trial of each series may have been the result of a carry over from this relaxed state. In any event, the key is that the application of viscous damping has modified the muscle/load dynamics in such a manner as to attenuate the involuntary motions while maintaining or improving the average intended response.

CHAPTER 5

CONCLUSIONS

The application of viscous damping through the TLD has resulted in statistically significant reductions in the AIM of the subjects tested. One subject's tremor was reduced by a factor of 10, approaching the levels of tremor observed in normal, when the highest level of damping was applied. For the other subject tested, the reductions were not as dramatic but, nevertheless, the reductions observed in the sample population were statistically significant at better than the .05 level, for all levels of damping. The tracking of the target was also maintained or improved as a result of the viscous damping. The application of viscous damping also attenuated the frequency content of a subject's AIM but did not shift the peaks of the power spectra.

Future work on this project should be directed towards improving the response of the TLD and acquiring additional subject data. Because of the significant attenuation observed in the trials documented herein, additional subjects should be tested to provide a larger sample population and hence a higher level of confidence in the data. Prior to additional testing however, more accurate control of the damping constant of the TLD should be implemented. Closed loop torque control is probably the most effective means of accomplishing this. In addition, trials of uniform length should be conducted in future tests regardless of the tracking

frequencies used. This will facilitate spectral analysis and will lead to improved confidence limits on the power spectral estimates.

All in all, the results of this work are quite encouraging. It is obvious that viscous damping does suppress the abnormal involuntary movements while maintaining or improving the average tracking of the subjects tested. Based on this data, a possible therapeutic technique for tremor management has been identified and, it is hoped that the application of viscous damping may assist people with AIM gain functional independence.

Appendix I - SUBJECTS

This appendix includes:

- a) Informed Consent Form
- b) Clinical Description of Subject JF'

PREPARED: _____

PROJECT TITLE: SUPPRESSION OF ABNORMAL INVOLUNTARY MOVEMENTS BY APPLICATION OF MECHANICAL LOADS AND BIOFEEDBACK

Investigator(s): M. Rosen, Ph.D.; M. Hallett, M.D.; P. Drinker, Ph.D.

IDENTIFYING NUMBER(s) _____

WITNESS/PATIENT NAME: _____
(not imprinted above)

APPROVED FOR USE OF THE PETER BENT BRIGLIAM HOSPITAL HUMAN SUBJECTS COMMITTEE ON: _____

SIGNED BY: _____
Secretary, Human Subjects Committee

DOCKET NUMBER: _____

EXPIRATION DATE: _____

Description and Explanation of Procedures: We are interested in testing new methods of suppressing tremors and other abnormal movements in people who could use their arms more effectively if it weren't for these movements. We hope to determine whether such movements may be reduced by (1) providing a brace for the afflicted limb which resists the muscles' "attempts" to move it in an undesirable way and (2) training the patient to control his/her tremor by conscious effort. You may be a subject in one or both of these studies.

You will be asked to view a screen somewhat like a small television. Two lines will appear on the screen. The right line will move up or down as the arm we are testing moves. The left line will be under our control and may or may not move. The limb will be fitted to an apparatus which measures its position. In some experiments it is used to apply a force to the limb which opposes the tremor. You will be asked to try to move the limb being tested in such a way as to make the right line on the screen keep up with the left one. The force, when applied, may make it easier for you to perform this task.

The line-matching task will be performed repeatedly for about five minutes at a time. Between trials, you may rest as long and as frequently as necessary for your comfort. An experimental session will last at least an hour - counting breaks - but beyond that point their length and scheduling will be suited to your capacity and convenience.

During each session a tape recorder will be kept running to store our comments, your comments and other data. The tapes and the information obtained from them will be kept in a confidential file. If this information is used for education or published reports, your name will be withheld. Short sequences of moving picture or video tape may be taken for our records, but this material will not be used for education or publication if you request that it be kept confidential.

Risks or Discomforts to be Expected: The measuring and loading device which will be attached to the limb being tested will be cushioned and fitted to suit you and produce no discomfort. Although much of the equipment we will use is electronic in nature, you will be in contact with none of this and no shock hazard is present. You may withdraw from participation in this study at any time. You are encouraged to ask questions and make comments or suggestions at any time. The success of these experiments depends to some extent on your willingness to do so.

Benefits to be Expected: The intention of these studies is limited. We will test only one joint of one limb. We will not construct a practical tremor-suppressing device for you to use in normal activities. If these experiments are successful on you and other subjects, the need for such a device will have been demonstrated. Its ultimate availability to you should, however, be thought of as a potential, indirect, long-range outcome of these studies.

If your participation in these studies involves attempts to reduce your abnormal movement by conscious effort on your part, and if your attempts are successful, it is conceivable that this ability may carry over into your daily use of the affected limbs. This would, of course, be of direct benefit to you. No such ability has been demonstrated in the past, however.

Alternative Procedures: There are, at present, more conventional methods of treatment which might be appropriate for your movement disorder. It has not yet been demonstrated that the techniques to be tried in these experiments are useful alternatives to present methods of treatment.

I have fully explained to _____ the above procedures, identifying those which are investigational, and have explained their purpose. I have asked whether or not any questions have arisen regarding the procedures and have answered these questions to the best of my ability.

Investigator's Signature

The above procedures have been satisfactorily explained to me, and I agree to become a participant in the study as described. I understand that I am free to withdraw my consent and discontinue participation at any time, without prejudice of any kind. I understand, also, that if I have any questions at any time they will be answered.

In the event that I should later feel I have not been adequately informed of the risks, benefits, and alternative procedures, or feel under any pressure to continue this treatment against my wishes, I understand I may ask for a representative from the Committee on the Protection of Patients to be available to speak with me.

Signature of Patient (Parent or Guardian)
or patient's Legal Representative when
appropriate

Subject JF

The subject is a 53 year old male with a degenerative neurological illness that has evolved over the past 30 years or more. The subject is confined to a wheelchair and bed. The by-products of this illness are severe incoordination, ataxia (both appendicular and truncal), and tremor most reminiscent of rubral tremor. Anatomically, these symptoms result from degeneration of cerebellar efferent dentate nucleus and pyramidal tracts. It is speculated that the subject suffers from a multiple system degeneration involving dentato-rubral pathways.

Appendix II - COMPUTER PROGRAMS

This Appendix includes:

- a) A Listing of the Signal Averaging Program**
- b) A Flowchart, Listing, and Discussion of the Spectral Analysis Program**

BASIC Signal Averaging Program

```

10 DIM A(1000),C(1000)
11 DIM B(10),N(10),T1(10),T2(10),N$(100,3),CS(100,3)
12 DEF AVG(D,E,F,G),DIS(F),GET(N),PUT(Y,K)
13 GO TO 100
14 PRINT "A/D CHANNEL";
15 INPUT D
16 PRINT "SAMPLING INTERVAL";
17 INPUT E
18 PRINT "NUMBER OF SAMPLES";
19 INPUT F
20 PRINT "NUMBER OF SWEEPS";
21 INPUT G
22 Y=AVG(D,E,F,G)
23 PRINT "NUMBER OF SWEEPS WAS ";X
24 PRINT/PRINT "WHAT NOW";
25 INPUT AS
26 IF AS="START" THEN 41
27 IF AS="DIS" THEN 277
28 IF AS="PRINT" THEN 300
29 IF AS="NO" THEN 400
30 IF AS="MI" THEN 300
31 IF AS="NNSA" THEN 600
32 IF AS="NNSV" THEN 700
33 IF AS="CALC" THEN 700
34 IF AS="MEAN" THEN 700
35 IF AS="SDEV" THEN 700
36 IF AS="PDEV" THEN 700
37 IF AS="WRITE" THEN 2000
38 IF AS="PROCESS" THEN 100
39 IF AS="AVG" THEN 100
40 IF AS="READ" THEN 100/IF AS="FILEDIE" THEN 100
41 PRINT "EOF";
42 GO TO 110
43 PRINT "WANT TO SAVE OLD CONTENTS FIRST";
44 INPUT BS
45 IF BS="YES" THEN 120
46 IF AS="AVG" THEN 50
47 IF AS="READ" THEN 3000/IF AS="FILEDIE" THEN 4000
48 IF AS="PROCESS" THEN 1000
49 Z=DIS(F)
50 GOTO 120
51 FOR I=1 TO F STEP 5
52 PRINT GET(I),GET(I+1),GET(I+2),GET(I+3),GET(I+4)
53 NEXT I
54 GOTO 100
55 INPUT I
56 GOTO 120
57 INPUT E
58 GOTO 120
59 INPUT F
60 GOTO 120
61 INPUT G
62 GOTO 120
63 CS=AS

```

```

782 PRINT "SAMPLING INTERVAL WAS" I
783 PRINT "NUMBER OF SAMPLES PER SWEEP WAS" F
792 PRINT "NUMBER OF SWEEPS WAS" I3
792 IF C$="NONE" THEN 8292
793 IF A$="FILEDIE" THEN 8172
802 FOR I=1 TO F
803 LET A=((I-1)*I+GET(I))/I
812 NEXT I
812 IF C$="SDEV" THEN 825
813 IF C$="PDEV" THEN 825
814 IF A$="WRITE" THEN 2022
815 PRINT "MEAN FROM 1 TO F =" ; A
822 IF C$="CALC" THEN 823
821 IF A$="PROCESS" THEN 8292
822 GO TO 122
823 LET S=2
824 FOR J=1 TO 5
827 LET P(J)=0
828 N(J)=0
829 T1(J)=0
830 T2(J)=0
831 NEXT J
835 FOR I=1 TO F
842 LET G1=GET(I)-A
843 LET S=G1*G1/F+S
846 IF C$="SDEV" THEN 972
847 IF G1<0 THEN 872
852 FOR J=5 TO 1 STEP -1
855 IF ABS(G1)<P(J) THEN 866
862 LET P(J+1)=P(J)
861 LET T1(J+1)=T1(J)
862 NEXT J
863 LET P(1)=ABS(G1)
864 T1(1)=I*I*2.2721
865 GO TO 972
866 LET P(J+1)=ABS(G1)
867 T1(J+1)=I*I*2.2221
868 GO TO 872
872 FOR J=5 TO 1 STEP -1
875 IF ABS(G1)<L(J) THEN 813
882 N(J+1)=N(J)
885 T2(J+1)=T2(J)
886 NEXT J
895 N(1)=ABS(G1)
892 T2(1)=I*I*2.2221
893 GO TO 972
912 N(J+1)=ABS(G1)
915 T2(J+1)=I*I*2.2221
972 NEXT I
973 R=SCR(S)
982 IF C$="PDEV" THEN 1002
983 PRINT "STANDARD DEVIATION FROM 1 TO F =" ; R
992 IF C$="CALC" THEN 1002
991 IF A$="PROCESS" THEN 8292
992 GO TO 122

```

```

1200 F=(P(1)+P(2)+P(3)+P(4)+P(5))/5
1202 N=(N(1)+N(2)+N(3)+N(4)+N(5))/5
1205 PRINT "MAXIMUM POSITIVE DEVIATION FROM MEAN FROM 1 TO F =";P
1206 PRINT "MAXIMUM NEGATIVE DEVIATION FROM MEAN FROM 1 TO F =";N
1207 PRINT "PEAK POS VALUES OCCUR AT T =";
1208 PRINT T1(1);T1(2);T1(3);T1(4);T1(5);"SEC"
1209 PRINT "PEAK NEG VALUES OCCUR AT T =";
1210 PRINT T2(1);T2(2);T2(3);T2(4);T2(5);"SEC"
1215 PRINT "APROX TIME OF POS PEAK =";
1216 PRINT (T1(1)+T1(2)+T1(3)+T1(4)+T1(5))/5;"SEC"
1218 PRINT "APROX TIME OF NEG PEAK =";
1219 PRINT (T2(1)+T2(2)+T2(3)+T2(4)+T2(5))/5;"SEC"
1220 IF A$="PROCESS" THEN 3090
1221 GO TO 122
1302 M=1
1305 PRINT "FILENAME";
1310 INPUT M$(M)
1311 PRINT "WHAT CALCULATION";
1312 INPUT C$(M)
1313 IF C$(M)="NONE" THEN 1519\IF C$(M)="MEAN" THEN 1519
1314 IF C$(M)="SDEV" THEN 1519
1315 IF C$(M)="PDEV" THEN 1519
1316 IF C$(M)="CALC" THEN 1519
1317 PRINT "HUE";
1318 GO TO 1512
1319 PRINT "ANOTHER?";
1322 INPUT F$
1325 IF F$="NC" THEN 3212
1330 M=M+1
1335 GO TO 1305
3200 PRINT "FILENAME";
3210 INPUT M$
3211 FOR I=1 TO F
3212 C(I)=GET(I)
3213 NEXT I
3215 GO TO 302
3220 FILEN #1:M$
3230 PRINT #1:A,I,F,X
3240 FOR I=1 TO F
3250 PRINT #1:C(I)
3260 NEXT I
3270 CLOSE #1
3280 GO TO 120
3300 PRINT "FILENAME";
3310 INPUT N$(1)
3311 M=1
3313 FOR K=1 TO M
3320 FILEN #1:N$(K)
3330 INPUT #1:E,I,F,G
3340 FOR I=1 TO F
3350 INPUT #1:C(I)
3360 NEXT I

```

```

3272 CLOSE #1
3273 FOR I=1 TO F
3274 Z=PUT(I,C(I))
3275 NEXT I
3276 IF A$="REAL" THEN 202
3277 C$=C$(Z)
3278 PRINT
3279 PRINT "FILE ";N$(Z);":"
3280 GO TO 782
3281 NEXT Z
3282 GO TO 120
4000 PRINT "FIRST FILE";
4001 INPUT Y$
4002 PRINT "SECOND FILE";
4003 INPUT Z$
4004 FILE# #1:Y$
4005 INPUT #1:A1,E,F,G
4006 FOR I=1 TO F
4007 INPUT #1:C(I)
4008 NEXT I
4009 CLOSE #1
4010 PRINT "ELIMINATE DC SHIFT";
4011 INPUT X$
4012 FILE# #1:Z$
4013 INPUT #1:A2,E,F,G
4014 S=0
4015 IF X$="YES" THEN 4152
4016 FOR I=1 TO F
4017 INPUT#1:V
4018 C(I)=(C(I)-V)^2
4019 S=S+C(I)
4020 NEXT I
4021 GO TO 4150
4022 FOR I=1 TO F
4023 INPUT#1:V
4024 C(I)=(C(I)-A1-V+A2)^2
4025 S=S+C(I)
4026 NEXT I
4027 CLOSE #1
4028 GO TO 782
4029 PRINT "RMS DIFFERENCE =";SOR(S/F)
4030 GO TO 100
5000 END

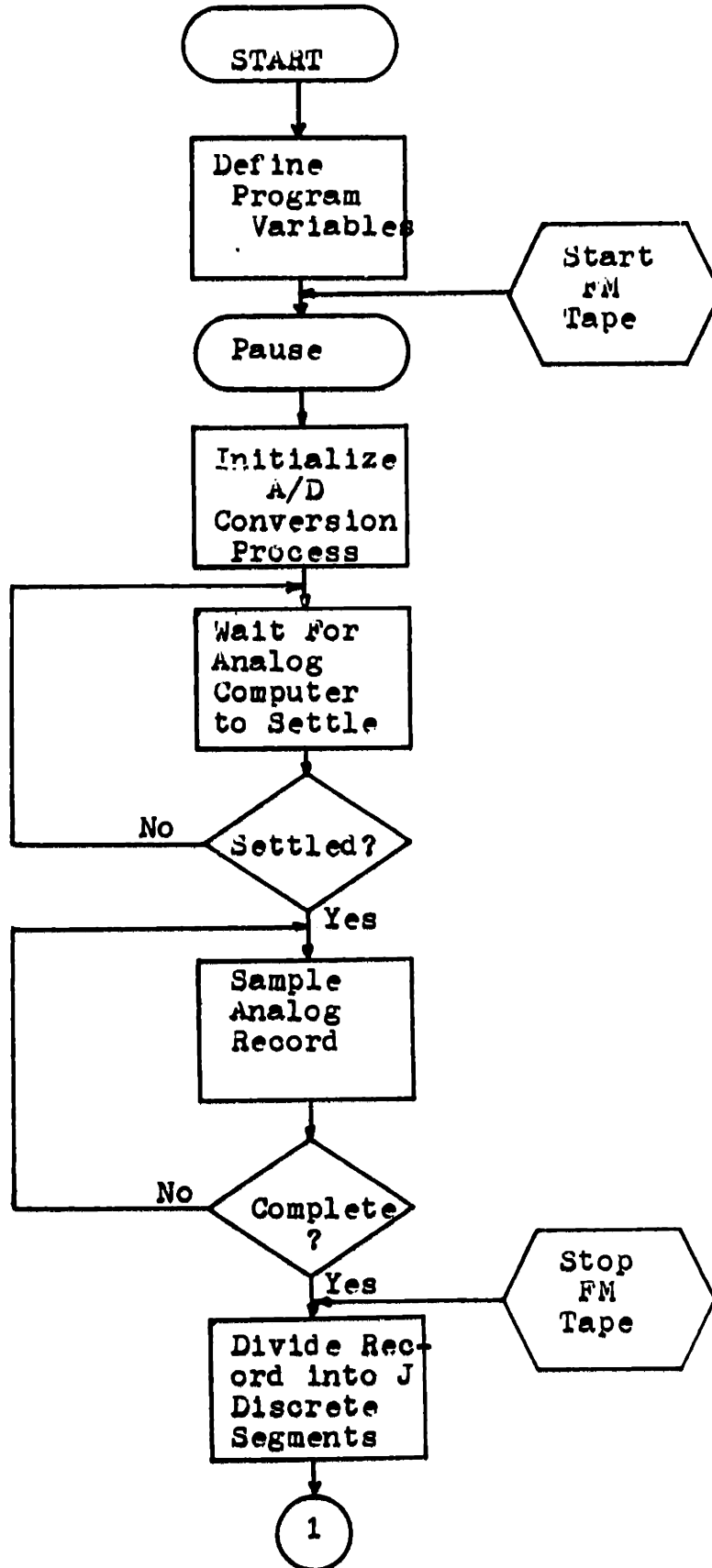
```

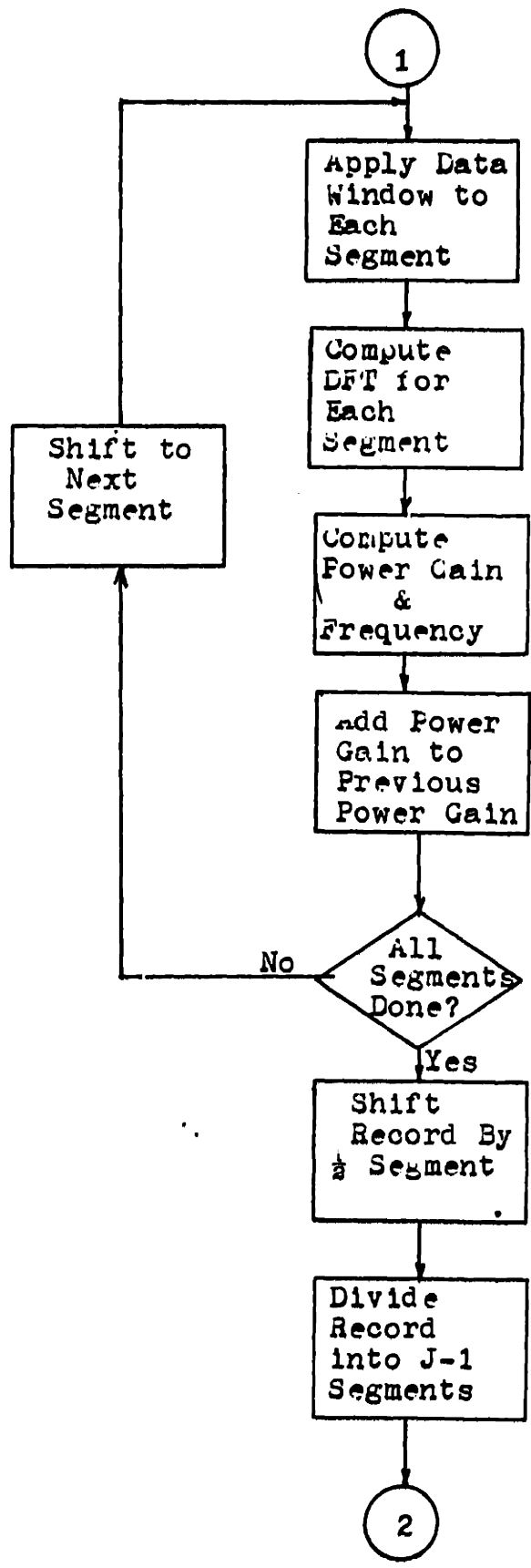
SPECTRAL ANALYSIS PROGRAM

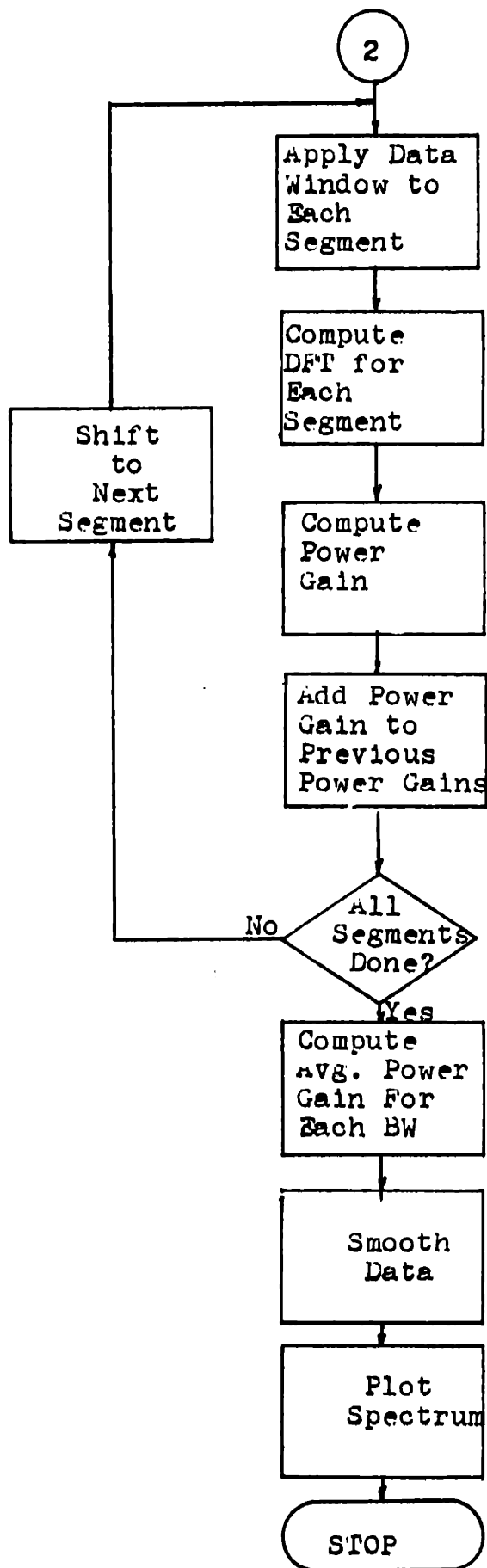
The following documented FORTRAN program computes an estimate of the power spectra of an analog voltage signal assumed to be random with zero mean. The signal used in this case is the response signal, band pass filtered between 2.0 and 20.0 Hz. The filtered signal was patched to an A/D converter on the analog computer in the Joint ME/CE Computing Facility at MIT. Upon loading the FORTRAN program into the Interdata M80, the computer would pause, under command from the program. At this time, the FM tape recorder is started, and then the computer is given the go ahead by pressing the space bar then "CR". This activates the sampling process and ceases any program interrupts. Upon completion of sampling, the program computes the power spectra using the techniques discussed in the text of this thesis and plots the power spectra.

Spectral Analysis Program
Flowchart

100
III







SEPTEMBER, 1978

THIS PROGRAM CALCULATES THE POWER SPECTRA OF AN ANALOG SIGNAL BY SAMPLING THE SIGNAL THEN DIVIDING THAT SAMPLE RECORD INTO A NUMBER OF OVERLAPPING SEGMENTS. THE POWER SPECTRA FOR EACH SEGMENT IS CALCULATED THEN AVERAGED WITH THE SPECTRA OF THE OTHER SEGMENTS TO RESULT IN AN AVERAGED POWER SPECTRA WHICH IS AN ESTIMATE OF THE ACTUAL POWER SPECTRA. THE CONFIDENCE LIMITS FOR THE ESTIMATED POWER SPECTRA ARE A FUNCTION OF THE NUMBER OF SEGMENTS TO BE AVERAGED. THIS IN TURN IS A FUNCTION OF THE LENGTH OF TIME RECORD AVAILABLE. SEE R.A. STARNES "DIGITAL SIGNAL ANALYSIS", CHAPTERS 13 AND 14 FOR FURTHER DETAILS.

```

DIMENSION XSC(4)
DIMENSION SAM(4096)
DIMENSION AME(2,1024)
COMPLEX CXPX
COMPLEX INPUT(1024)
COMPLEX WPAR(512)
REAL*8 FR

```

```

C
C* ****DEFINE THE NUMBER OF SAMPLES AND THE SAMPLING FREQUENCY
C SAMFRQ = TWICE THE REQUIRED SAMPLING FREQUENCY SINCE THE
C TAPE IS PLAYED BACK AT TWICE THE ORIGINAL RECORDING SPEED.
C

```

```

DATA XSC/0.,25.,1.0E-3,.1/
DATA S/4096/
DATA NSPS/1024/
CALL HINT
SAMFRQ=100.0
DT=1./SAMFRQ
PAUSE

```

```

C
C* ****INITIALIZE EVERYTHING
C

```

```

CALL CVIO(0)
CALL CISTPR(DT)
CALL IC
DO 5 I=1,20
CALL CSYNCH(LDST)
CONTINUE
CALL CSTART(DT)
CALL DP

```

```

C
C* ****SAMPLE TIME RECORD
C

```

```

DO 50 I=1,N

```

```

CALL CSYNCH(LOST)
SIN(I)=AD(0)
50 CONTINUE
AMP(2,1)=0.0
CALL CVD(1)
I=M/NSPS

C
C* *** DIVIDE RECORD INTO J SEGMENTS AND APPLY A HANNING WINDOW TO DATA
C
DO 200 I=1, J
DO 75 L=1, NSPS
M=I*NSPS-NSPS+L
WINFAC=1.0
RO=WINFAC*SIN(M)
INPUT(L)=CMPLX(RO,0.0)
75 CONTINUE

C
C* *** CALCULATE THE DFT OF THE SEGMENT
C
CALL FFT(INPUT,10,1,NEAR,1)

C
C* *** COMPUTE THE POWER GAIN AND ADD TO PREVIOUS POWER GAINS.
C ALSO COMPUTE THE ASSOCIATED FREQUENCY.
C
NSPS2=NSPS/2
DO 100 L=1, NSPS2
AMAG=CABS(INPUT(L))
AMIN=.00035
IF(AMAG.GT.AMIN) GO TO 20
AMAG=.00035
80 AMP(2,L)=AMP(2,L)+AMAG**2
AMP(1,L)=FLOAT(L)/(2.0*PI*FLOAT(NSPS))
100 CONTINUE
200 CONTINUE

C
C* *** SHIFT AND DIVIDE THE RECORD INTO K=J-1 SEGMENTS
C
K=J-1
DO 300 I=1, K
DO 250 L=1, NSPS
M1=I*NSPS-NSPS2+L
WINFAC=.5*(1.0-COS(360.0*FLOAT(L)/FLOAT(NSPS)))
RO=SIN(M1)*WINFAC
INPUT(L)=CMPLX(RO,0.0)
250 CONTINUE

C
C* *** CALCULATE THE DFT OF THE SEGMENTS
C
CALL FFT(INPUT,10,1,NEAR,1)

C
C
C COMPUTE THE POWER GAIN AND ADD TO THE PREVIOUS POWER GAINS.
C
DO 275 L=1, NSPS2

```

```

      AMAG=CLASS(INPUT(L))
      AMIN=.00035
      IF(AMAG.GT.AMIN) GO TO 260
      AMAG=.00035
260   AMP(2,L)=AMP(2,L)+(AMAG**2)
275   CONTINUE
300   CONTINUE
C
C*****COMPUTE THE AVERAGE POWER GAIN FOR EACH BANDWIDTH
C
      K1=J+K
      DO 350 L=1,NSPS2
      AMP(2,L)=AMP(2,L)*DT+2.0/(2.0*FLOAT(NSPS2)*FLOAT(K1)*0.375)
350   CONTINUE
      DO 300 I=3,NSPS2,3
      J=I-1
      M=I-2
      I2=I/3
      AMP(1,I2)=AMP(1,J)
      AMP(2,I2)=(AMP(2,I)+AMP(2,J)+AMP(2,M))/3.0
800   CONTINUE
      NF=NSPS2/3
      CALL QPCTR(AMP,2,NF,QY(2),QY(1),QISCL(12),QYSCL(YSC1))
      STOP
      END

```

BIBLIOGRAPHY

- 1 Brittan, Gilbert H.: Force and Torque. Instrumentation Society of America Transducer Compendium, 2nd Edition, Part 2, pp.29-37, 1970.
- 2 Chase, R.A., Cullen, J.K., Sullivan, S.A., and Ommaya, A.K.: Modification of Intention Tremor in Man. Nature 206; 485-487, 1965.
- 3 Contini, Renato: Body Segment Parameters Part II. Artificial Limbs No. 1, pp.1-19, Spring 1972.
- 4 Cooper, I.S.: Involuntary Movement Disorders. Hoeber Medical Division, Harper and Row Publishers, N.Y. 1969
- 5 Joyce, G.C., Rack, P.M.H.: The Effects of Load and Force on Tremor at the Normal Elbow Joint. J. of Physiology 240; 375-396, 1974.
- 6 Lampe, D.W.: Design of a Magnetic Particle Brake Above-Knee Prosthesis Simulator System. S.M. Thesis, Dept. of Mechanical Engineering, Massachusetts Institute of Technology, February, 1976.
- 7 Morgan, M.H., Hewer, R.L., Cooper, R.: Application of an Objective Method of Assessing Intention Tremor - A Further Study on the Use of Weights to Reduce Intention Tremor. J. of Neurology, Neurosurgery, and Psychiatry 38; 259-264, 1975.
- 8 Moroney, M.J.: Facts From Figures. Penguin Books, Baltimore Maryland; 216-237, 1974.
- 9 Ogata, K.: Modern Control Engineering. Prentice Hall Inc. Englewood Cliffs, N.J.; 1970.
- 10 Cguztoreli, M.N., and Stien, R.B.: Tremor and Other Oscillations in Neuromuscular Systems. Biological Cybernetics 22; 147-157, 1976.
- 11 Rietz, R.H., Stiles, R.N.: A Viscoelastic-Mass Mechanism as a Basis for Normal Postural Tremor. J. of Applied Physiology 37; 852-860, 1974.
- 12 Rosen, M.J., Gesink, J.W., and Rowell, D.: Suppression of Intention Tremor by Application of Viscous Damping. Proc. 4th Annual New England Bioengineering Conf, Saha (ed.), Pergamon Press, New York; 1976.

- 13 Rosen, M.J.:Suppression of Abnormal Involuntary Movements by Application of Mechanical Loads and Biofeedback. Research Proposal 1976.
- 14 Simoes,N., Barber,L., Waylett, J., and Peterson,A.: Evaluation and Evolution of a Damper Brace. In house report from Rancho Los Amigos Hospital.
- 15 Stearns, R.A.:Digital Signal Analysis. Hayden Book Company, Rochelle Park, N.J., pp.223-257, 1975.
- 16 Stiles,R.N.:Frequency and Displacement Amplitude Relations for Normal Hand Tremor. J. of Applied Physiology 40; 44-54, 1976.
- 17 Stiles, R.N., Pozos,R.S.: A Mechanical-Reflex Oscillator Hypothesis For Parkinsonian Hand Tremor, J. of Applied Physiology 37; 852-860, 1974.
- 18 Stiles, R.N., and Randall, J.E.: Mechanical Factors in Human Tremor Frequency. J. of Applied Physiology 23; 324-330, 1967.